

Journal: ESSD

Title: Improved estimate of global gross primary production for reproducing its long-term variation, 1982–2017

MS No.: essd-2019-126

MS Type: Data description paper

Dear editor and reviewers,

We are very grateful to your great efforts and constructive comments on our manuscript “Improved estimate of global gross primary production for reproducing its long-term variation, 1982–2017” (**MS No.:** essd-2019-126). The comments have helped improve the paper quite tremendously. We have carefully studied these comments and substantially revised our manuscript accordingly.

Here are our detailed responses to the comments point by point. Please note that the comments from the reviewer are in **bold** followed by our responses in regular text. The changes in our manuscript are underlined with red.

Please contact us if further materials or information are required. We deeply appreciate your consideration of our manuscript.

Sincerely,

Yi Zheng, Wenping Yuan, on behalf of all co-authors

School of Atmospheric Sciences,

Sun Yat-sen University, Zhuhai 519082, Guangdong, China

Email: yuanwpcn@126.com

Response to Reviewer #1:

1. LUE model is an important empirical model for estimating GPP. The authors added the impacts of CO₂ concentration, diffuse/direct PAR, and VPD to the traditional LUE model, which showed improvement.

Response: Thanks for your positive comments. We have revised the manuscript according to your comments point by point below.

2. Line 18-35 In the abstract section, it is necessary to present some quantitative results that can directly prove the improvement of the revised EC-LUE model over other currently popular models.

Response: As your suggestion, we adjusted and added more quantitative results to show the improvement of the revised EC-LUE model in the abstract section. The following is the revised abstract and the newly added sentences are underlined with red.

“Abstract. Satellite-based models have been widely used to simulate vegetation gross primary production (GPP) at the site, regional, or global scales in recent years. However, accurately reproducing the interannual variations in GPP remains a major challenge, and the long-term changes in GPP remain highly uncertain. In this study, we generated a long-term global GPP dataset at 0.05 ° latitude by 0.05 ° longitude and 8-day interval by revising a light use efficiency model (i.e. EC-LUE model). In the revised EC-LUE model, we integrated the regulations of several major environmental variables: atmospheric CO₂ concentration, radiation components, and atmospheric vapor pressure deficit (VPD). These environmental variables showed substantial long-term changes, which could greatly impact the global vegetation productivity. Eddy covariance (EC) measurements at 95 towers from the FLUXNET2015 dataset, covering nine major ecosystem types around the globe, were used to calibrate and validate the model. In general, the revised EC-LUE model could effectively reproduce the spatial, seasonal, and annual variations in the tower estimated GPP at most sites. The revised EC-LUE model could explain 71% of the spatial variations in annual GPP over 95 sites. At more than 95% of the sites, the correlation coefficients (R²) of seasonal changes between tower estimated and model simulated GPP are larger than 0.5. Particularly, the revised EC-LUE model improved the model performance in reproducing the interannual variations in GPP, and the averaged R² between annual mean tower estimated and model simulated GPP is 0.44 over all 55 sites with observations longer than 5-years, which is significantly higher than those of original EC-LUE model (R² = 0.36) and other LUE models (R² ranged from 0.06 to 0.30 with an average value of 0.16). At the global scale, GPP derived from light use efficiency models, machine learning models, and process-based biophysical models exist substantial differences in magnitude and interannual variations. The revised EC-LUE model quantified the mean global GPP from 1982 to 2017 as 106.2 ± 2.9 Pg C yr⁻¹ with the trend 0.15 Pg C yr⁻¹. Sensitivity analysis indicated that GPP simulated by the revised EC-LUE model was sensitive to VPD, radiation, and CO₂ concentration. Over the period of 1982–2017, the CO₂ fertilization effect on the global GPP (0.14 ± 0.001 Pg C yr⁻¹) could be offset by the effect of increased VPD (−0.16 ± 0.02 Pg C yr⁻¹). The long-term changes in the environmental variables could be well reflected in global GPP. Overall, the revised EC-LUE model is able to provide a reliable long-term estimate of global GPP. The GPP dataset is available at <https://doi.org/10.6084/m9.figshare.8942336> (Zheng et al., 2019).” (Line 18-40 in the revised manuscript)

3. Line 31-32 “The global GPP derived from different datasets exist substantial uncertainty in magnitude and interannual variations.” Which datasets and which models were used here? Do the

authors mean different datasets used to drive the revised EC-LUE model? Or other models?

Response: We mean different GPP datasets simulated by other models in different studies. We modified the sentence as follow:

“At the global scale, GPP derived from light use efficiency models, machine learning models, and process-based biophysical models exist substantial differences in magnitude and interannual variations.” (Line 33-34 in the revised manuscript)

4. Line 48 Do the authors mean process based ecosystem models by biophysical models? And empirical or data-driven models by satellite-based models?

Line 48: Similarly, a model comparison showed that none of the examined 16 biophysical models nor the 3 satellite-based models could consistently reproduce the observed interannual variations in carbon exchange at 11 forest sites in North America (Keenan et al., 2012).

Response: This sentence cited the results of Keenan et al., 2012, which includes 16 process-based biophysical models (i.e., BEPS, BIOME-BGC, Can-IBIS, CNCLASS, DLEM, ECOSYS, ED2, EDCM, ISAM, LoTEC-DA, LPJml, ORCHIDEE, SiB, SiB-CASA, SSiB2, and TECO) and 3 satellite-based model dataset (i.e., BESS, MODIS C5, and MODIS C5.1). BESS (Breathing Earth System Simulator) is a process-based model, and uses satellite-based leaf area index as driver. MODIS C5 and MODIS C5.1 indicate two MODIS-GPP products, and are based on MODIS-GPP algorithm which is satellite-based light use efficiency model. We changed the original sentences to make it clear:

“Similarly, a model comparison showed that none of the examined 16 process-based biophysical models or the 3 remote sensing products (BESS, MODIS C5, and MODIS C5.1) could consistently reproduce the observed interannual variations in GPP at 11 forest sites in North America (Keenan et al., 2012).” (Line 51-53 in the revised manuscript)

5. Line 50 The starting and ending years could be given while reporting a trend.

Line 50: Seven LUE models simulated the long-term trends of global GPP varied -0.15 to 1.09 Pg C yr⁻¹ (Cai et al., 2014).

Response: Thanks for your advice. We added starting and ending years as follow:

“Seven LUE models simulated the long-term trends of global GPP varied from -0.15 to 1.09 Pg C yr⁻¹ over the period 2000–2010 (Cai et al., 2014).” (Line 53-54 in the revised manuscript)

6. Line 70-90 (Major concern) The ratio of diffuse PAR is of course an important regulator of LUE for dense canopy. However, the amount of total PAR should not be ignored. LUE could rapidly decrease with the amount of total PAR because in clear sky the incident PAR could easily exceed light saturation point.

Response: Thanks for your deep thoughts. It is indeed that light saturation is an important response of GPP to varying PAR. The instantaneous LUE decreases rapidly when PAR exceed light saturation point. This is an instantaneous phenomenon which is obvious and nonnegligible at the hourly scale. The revised EC-LUE model was developed at the 8-day scale, and the light saturation can hardly be observed for the accumulation of GPP from hourly to 8-day temporal scale.

As an example, we examined the relation between GPP and PAR at hourly and 8-day scale at US-Ha1 site, respectively (Fig. R1). At hourly scale, there are obvious light saturation phenomenon when PAR exceeds 200 W m⁻² (Fig. R1a). However, at 8-day scale, the “ratio between GPP and LAI” (named GPP/LAI hereafter) keep increasing when PAR around its maximum value at 120 W m⁻² (Fig. R1b).

Some low GPP/LAI values may be introduced by unfavorable climate conditions (e.g., low temperature or high VPD) or the uncertainty/error of the EC measurements. So we did not integrate the light saturation phenomenon in our current model.

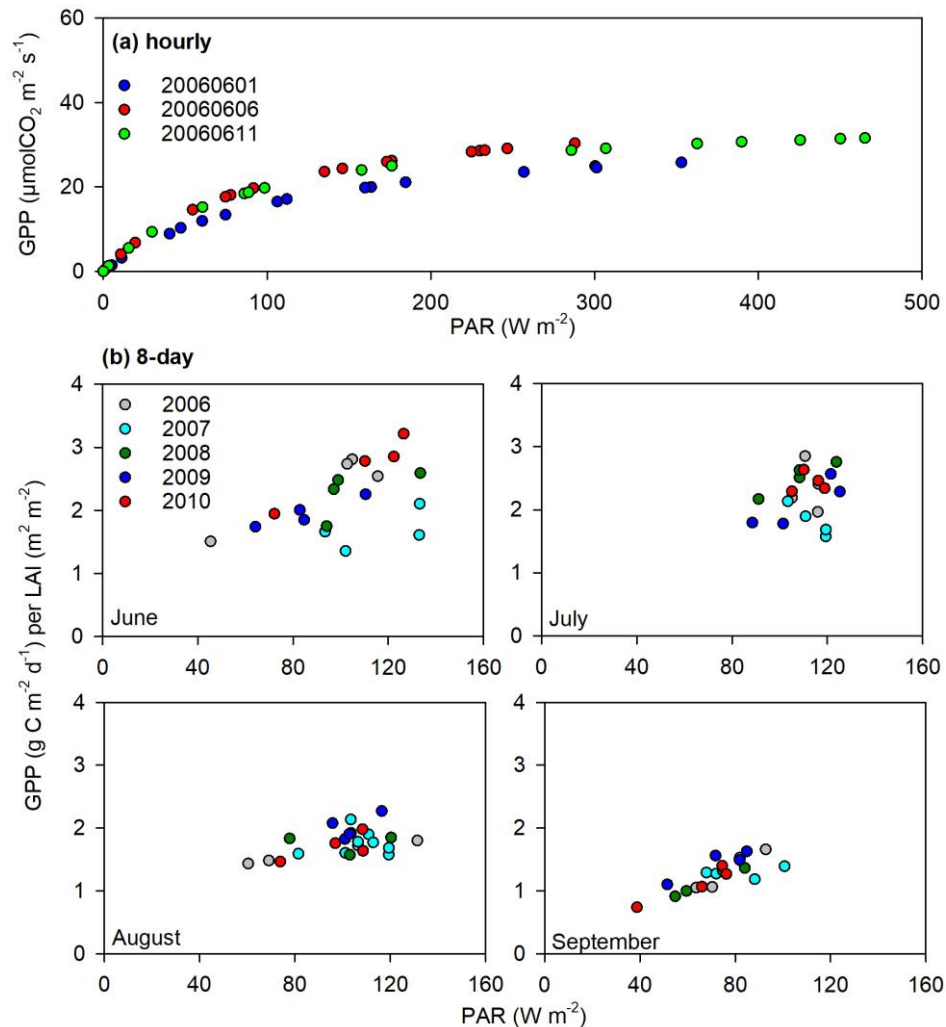


Figure R1: Correlations of GPP and PAR at hourly and 8-day scale, taking US-Ha1 site as an example. At 8-day scale, we used the ratio between GPP and LAI to eliminate the influence of season patterns of LAI on GPP.

7. Section 2.1 At which temporal and spatial resolutions were the model run? And some the variables in the equations were not explained, e.g. epsilon in eq 4. Line 113 intercellular [CO₂]? Line 114 add concentration after the second CO₂. How was 356.51 in eq 5 determined?

Line 113-123: where φ is the CO₂ compensation point in the absence of dark respiration (ppm); C_i is the leaf internal CO₂ concentration; C_a is the atmospheric CO₂ concentration; χ is the ratio of leaf internal to atmospheric CO₂ which can be estimated as follows (Prentice et al., 2014; Keenan et al., 2016):

$$\chi = \frac{\varepsilon}{\varepsilon + \sqrt{VPD}} \quad (4)$$

$$\varepsilon = \sqrt{\frac{356.51K}{1.6\eta^*}} \quad (5)$$

$$K = K_c \left(1 + \frac{P_0}{K_0}\right) \quad (6)$$

$$K_c = 39.97 \times e^{\frac{79.43 \times (T-298.15)}{298.15RT}} \quad (7)$$

$$K_o = 27480 \times e^{\frac{36.38 \times (T-298.15)}{298.15RT}} \quad (8)$$

where K_c and K_o are the Michaelis–Menten constants for CO₂ and O₂; P_o is the partial pressure of O₂; T_a is air temperature (K); η^* is the viscosity of water relative to its value at 25 °C depending on the air temperature (Korson et al., 1969); R is the molar gas constant (8.314 J mol⁻¹ K⁻¹).

Response: The model was run at 8-day temporal resolution and 0.05 °×0.05 °spatial resolution. We added the information in the method section 2.4 (in the revised manuscript):

“Using the averaged value of the optimized parameters (Table 3), a global GPP dataset at 0.05 ° × 0.05 °spatial resolution and 8-day temporal resolution over 1982-2017 was produced.” (Line 207-208 in the revised manuscript)

About the Eqs. (4)-(8) (in the original manuscript), we referred from Prentice et al. (2014) and Keenan et al. (2016). ε in Eq (4) is a parameter related to the ‘carbon cost of water’, which means the sensitivity of VPD to χ . We added the explanation of ε in the revised manuscript.

The 356.51 in Eq. (5) can be estimated using Eq (4)-(8) assuming the value of ε at 25°C as 0.8 (T=298.15 K; VPD=1 kPa) described in Keenan et al. (2016), and we cited this paper.

In line 113 (in the original manuscript), we think the “leaf internal CO₂” and “intercellular CO₂” have a same meaning, so both are OK.

According to the response above, we modified this part as following:

“The effect of atmospheric CO₂ concentration on GPP is determined by the following equations (Farquhar et al., 1980; Collatz et al., 1991):

$$C_s = \frac{C_i - \varphi}{C_i + 2\varphi} \quad (5)$$

$$C_i = C_a \times \chi \quad (6)$$

where φ is the CO₂ compensation point in the absence of dark respiration (ppm); C_i is the leaf internal CO₂ concentration; C_a is the atmospheric CO₂ concentration; χ is the ratio of leaf internal to atmospheric CO₂ concentration which can be estimated as follows (Prentice et al., 2014; Keenan et al., 2016):

$$\chi = \frac{\varepsilon}{\varepsilon + \sqrt{VPD}} \quad (7)$$

$$\varepsilon = \sqrt{\frac{356.51K}{1.6\eta^*}} \quad (8)$$

where ε is a parameter related to the ‘carbon cost of water’, which means the sensitivity of VPD to χ ; K is the Michaelis–Menten coefficient of Rubisco; η^* is the viscosity of water relative to its value at 25 °C (Korson et al., 1969).

$$K = K_c \left(1 + \frac{P_o}{K_o}\right) \quad (9)$$

where P_o is the partial pressure of O₂; K_c and K_o are the Michaelis–Menten constants for CO₂ and O₂ (Keenan et al., 2016):

$$K_c = 39.97 \times e^{\frac{79.43 \times (T_a - 298.15)}{298.15 \times R \times T_a}} \quad (10)$$

$$K_o = 27480 \times e^{\frac{36.38 \times (T_a - 298.15)}{298.15 \times R \times T_a}} \quad (11)$$

where T_a is air temperature (unit: K); R is the molar gas constant ($8.314 \text{ J mol}^{-1} \text{ K}^{-1}$).” (Line 155-170 in the revised manuscript)

8. Line 145-155 The fluxnet GPP contains many datasets of GPP according to the reference CO₂ profile between sensor and canopy. Which dataset was used? And what is the temporal resolution of GPP, 30-min, daily, or 8-day?

Response: In the FLUXNET2015 dataset, GPP was calculated considering flux partitioning methods and friction velocity (USTAR) threshold. In our manuscript, we used the GPP variable GPP_NT_VUT_REF at daily temporal resolution in the FLUXNET2015 dataset. And, to match the temporal resolution of the remotely sensed LAI, we aggregated the daily GPP to 8-day temporal resolution. We modified the corresponding part to:

“The FLUXNET2015 dataset (<http://www.fluxdata.org>) includes over 200 variables of carbon fluxes, energy fluxes, and meteorological variables collected and processed at sites by the FLUXNET community. In our study, ninety-five EC sites in FLUXNET2015 dataset were utilized to optimize the parameters and evaluate the performance of the revised EC-LUE model, including nine major terrestrial ecosystem vegetation types (Table 1): evergreen broadleaf forests (EBF), evergreen needleleaf forests (ENF), deciduous broadleaf forests (DBF), mixed forests (MF), grasslands (GRA), savannas (SAV), shrubland (SHR), wetlands (WET), and croplands (CRO). More information about the characteristics of these sites can be referred to the FLUXNET website. For each site, the daily GPP, PAR, air temperature (T_a), and VPD were used in our study. The GPP variable (GPP_NT_VUT_REF) used in this study was estimated from night-time partitioning method. The corresponding net ecosystem exchange (NEE) was generated using friction velocity (USTAR) threshold for each year (VUT), in which 40 versions of NEE were created by using different percentiles of USTAR thresholds. The model efficiency between each version and the others 39 versions were calculated to test their similarities and the reference (REF) NEE was selected as the one with higher model efficiency sum (the most similar to the others 39). The daily meteorological variables were gap-filled or downscaled from the ERA-interim reanalysis dataset in both space and time (Vuichard and Papale, 2015). The gap-filled technique of the carbon flux measurements and meteorological variables is the marginal distribution sampling (MDS) method described in Reichstein et al. (2005). For each variable, we aggregated the daily values to 8-day time step. Only the 8-day measurements with more than 5-day valid values were used” (Line 108-123 in the revised manuscript)

9. Line 164 Daily mean air temperature?

Line164-165: In our study, we obtained the daily air temperature (T_a , °C), dew point temperature (T_d , °C), direct PAR, and diffuse PAR at 0.625° in longitude by 0.5° in latitude from 1982 to 2017.

Response: Yes, modified.

“In our study, we obtained the daily mean air temperature (T_a , °C), mean dew point temperature (T_d , °C), total PAR (PAR_{dr} , $\text{MJ m}^{-2} \text{ d}^{-1}$), and total diffuse PAR (PAR_{df} , $\text{MJ m}^{-2} \text{ d}^{-1}$) at 0.625° in longitude by 0.5° in latitude from 1982 to 2017.” (Line130-132 in the revised manuscript)

10. Line 203-207 Those lines should go to method section.

Line 203-207: This study used EC measurements at 42 sites to calibrate the parameter values and 43 sites to validate the model accuracy of the revised EC-LUE model. The parameters (ϵ_{msu} , ϵ_{msh} ,

ϕ , and VPD_0) of each vegetation type are shown in Table 3. We evaluated the model performance by using the tower-derived meteorology data and global reanalysis meteorology, respectively. In general, the revised EC-LUE model could effectively reproduce the spatial, seasonal, and annual variations in the tower-estimated GPP at most of the calibration and validation sites (Figs. 1–4).

Response: Yes, we agree that the contents about “calibration and validation” and “parameters” in these lines should be moved to method section. According to the suggestion of the second reviewer, we have used cross-validation method to estimate model parameters, and we rewrite this part and put them into method section “section 2.4 Model calibration and validation”:

“Cross-validation method was used to calibrate and validate the revised EC-LUE model. Fifty percent of the sites were randomly selected to calibrate model parameters for each vegetation type, and the remaining 50% of the sites were used to validate the model. This parameterization process was repeated until all possible combinations of 50% sites were achieved for each vegetation type. The nonlinear regression procedure (Proc NLIN) in the Statistical Analysis System (SAS, SAS Institute Inc., Cary, NC, USA) was applied to optimize the model parameters (ϵ_{msu} , ϵ_{msh} , ϕ , and VPD_0) using 8-day estimated GPP based on EC measurements. The mean GPP simulations of 8-day from all validation runs only were used to model validation. Mean calibrated parameter values from all model runs were used to simulate GPP over the global scale (Table 3).” (Line 189-195 in the revised manuscript)

After consideration, we keep the result contents in these lines “In general, the revised EC-LUE model could effectively reproduce the spatial, seasonal, and annual variations in the tower-estimated GPP at most of the calibration and validation sites (Figs. 1–3).” in “section 3.1 Model performance”.

11. Figure 4 (Major concern) Fig 4 could be expanded to better compare the performance of the revised EC-LUE model with other models in capturing the inter-annual and intraannual GPP variations, to show the improvement of the revised EC-LUE model. This is important because there are a number of the existing models (process-based and the empirical LUE models as well the machine learning method). While the results about spatial and temporal variations of the GPP (from the new model and other models) should be compressed or even dropped.

Response: Thank you. The main objective of our manuscript is focused on the improvement of the LUE models and produced a long-term GPP dataset. So, we compare the interannual variations of the revised EC-LUE model with other LUE models (CASA, CFix, CFlux, MODIS, VPM, VPRM, and the original EC-LUE model) as shown in Fig. 4. It is a good idea to compare with other kind models (process-based models and machine learning methods). However, we really appreciate the understanding that this comparison is quite beyond the field of this study. Moreover, due to large data gaps of measurements derived from eddy covariance towers, we need run process-based models at eddy covariance towers and obtain the corresponding simulations with observations of GPP in order to evaluate the model performance. This work needs contributions of model PIs, and which probably need take long time and great efforts. In addition, previous studies have provided the insights on this issue. Keenan et al. (2012) compared the performance of 16 process-based biophysical models and 3 satellite-based models (including the MODIS product) in reproducing the interannual variations in GPP. The result indicated the MODIS model performance was comparable to the process-based biophysical models. In our manuscript, the revised EC-LUE model (averaged $R^2 = 0.44$) was significantly better than the MODIS model (averaged $R^2 = 0.17$) at interannual scale. Therefore, we can conclude the similar result that our model was better than the process-based biophysical models compared in Keenan et al. (2012).

We rearranged the figures, Fig. 3 in the revised manuscript is the original Fig. 4.

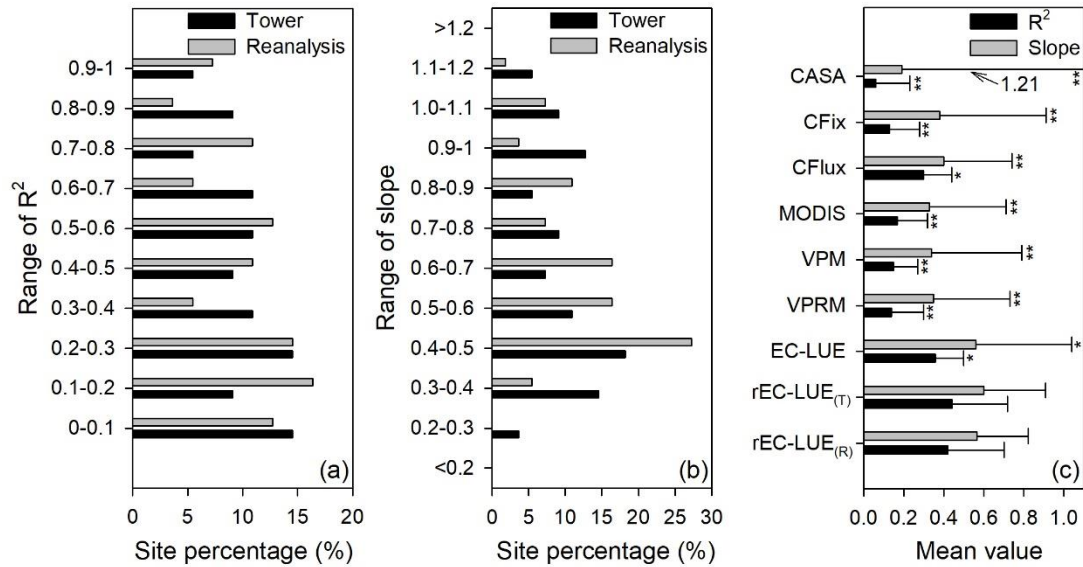


Figure 3: Site percentage of (a) correlation coefficients (R^2), and (b) regression slopes between the model simulated and tower-based interannual variabilities in GPP. (c) Averaged values (error bars represent the standard deviations) of R^2 and slope for various LUE models. rEC-LUE_(T) and rEC-LUE_(R) indicate the revised EC-LUE models derived from tower-derived meteorology data and meteorological reanalysis dataset. The R^2 and slopes of the other seven LUE models (i.e., EC-LUE, VPRM, VPM, MODIS, CFlux, CFix, and CASA) in the figure were obtained from the study by Yuan et al. (2014). **** and * indicate a significant difference in statistic variables (R^2 and slope) between the rEC-LUE_(T) and other LUE models (i.e., rEC-LUE_(T) and other seven LUE models) at p-value < 0.01 and p-value < 0.05, respectively.**

References

1. Cai, W., Yuan, W., Liang, S., Liu, S., Dong, W., Chen, Y., Liu, D., Zhang, H.: Large Differences in Terrestrial Vegetation Production Derived from Satellite-Based Light Use Efficiency Models, *Remote Sens.*, 6, 8945-8965, doi:10.3390/rs6098945, 2014.
2. Collatz, G.J., Ball, J.T., Grivet, C., Berry, J.A.: Physiological and environmental regulation of stomatal conductance, photosynthesis and transpiration: a model that includes a laminar boundary layer, *Agric. For. Meteorol.*, 54, 107-136, 1991.
3. Farquhar, G.D., von Caemmerer, S., Berry, J.A.: A biochemical model of photosynthetic CO₂ assimilation in leaves of C₃ species, *Planta*, 149, 78-90, doi:10.1007/bf00386231, 1980.
4. Keenan, T.F., Baker, I., Barr, A., Ciais, P., Davis, K., Dietze, M., Dragon, D., Gough, C.M., Grant, R., Hollinger, D., Hufkens, K., Poulter, B., McCaughey, H., Raczka, B., Ryu, Y., Schaefer, K., Tian, H.Q., Verbeeck, H., Zhao, M.S., Richardson, A.D.: Terrestrial biosphere model performance for inter-annual variability of land-atmosphere CO₂ exchange, *Global Change Biol.*, 18, 1971-1987, doi:10.1111/j.1365-2486.2012.02678.x, 2012.
5. Keenan, T.F., Prentice, I.C., Canadell, J.G., Williams, C.A., Wang, H., Raupach, M., Collatz, G.J.: Recent pause in the growth rate of atmospheric CO₂ due to enhanced terrestrial carbon uptake, *Nat. Commun.*, 710.1038/ncomms13428, 2016.
6. Korson, L., Drost-Hansen, W., Millero, F.J.: Viscosity of water at various temperatures, *J. Phys. Chem.*, 73, 34-39, doi:10.1021/j100721a006, 1969.

7. Prentice, I.C., Dong, N., Gleason, S.M., Maire, V., Wright, I.J.: Balancing the costs of carbon gain and water transport: testing a new theoretical framework for plant functional ecology, *Ecol. Lett.*, 17, 82-91, doi:10.1111/ele.12211, 2014.
8. Reichstein, M., Falge, E., Baldocchi, D., Papale, D., Aubinet, M., Berbigier, P., Bernhofer, C., Buchmann, N., Gilmanov, T., Granier, A., Grunwald, T., Havrankova, K., Ilvesniemi, H., Janous, D., Knohl, A., Laurila, T., Lohila, A., Loustau, D., Matteucci, G., Meyers, T., Miglietta, F., Ourcival, J.-M., Pumpanen, J., Rambal, S., Rotenberg, E., Sanz, M., Tenhunen, J., Seufert, G., Vaccari, F., Vesala, T., Yakir, D., Valentini, R.: On the separation of net ecosystem exchange into assimilation and ecosystem respiration: review and improved algorithm, *Global Change Biol.*, 11, 1424-1439, doi:10.1111/j.1365-2486.2005.001002.x, 2005.
9. Vuichard, N., Papale, D.: Filling the gaps in meteorological continuous data measured at FLUXNET sites with ERA-Interim reanalysis, *Earth Syst. Sci. Data*, 7, 157-171, doi:10.5194/essd-7-157-2015, 2015.
10. Yuan, W., Cai, W., Xia, J., Chen, J., Liu, S., Dong, W., Merbold, L., Law, B., Arain, A., Beringer, J., Bernhofer, C., Black, A., Blanken, P.D., Cescatti, A., Chen, Y., Francois, L., Gianelle, D., Janssens, I.A., Jung, M., Kato, T., Kiely, G., Liu, D., Marcolla, B., Montagnani, L., Raschi, A., Rouspard, O., Varlagin, A., Wohlfahrt, G.: Global comparison of light use efficiency models for simulating terrestrial vegetation gross primary production based on the La Thuile database, *Agric. For. Meteorol.*, 192, 108-120, doi:10.1016/j.agrformet.2014.03.007, 2014.
11. Zheng, Y., Shen, R.; Wang, Y., Li, X., Liu, S., Liang, S., Chen, Jing M., Ju, W., Zhang, L., Yuan, W.: Improved estimate of global gross primary production for reproducing its long-term variation, 1982-2017. figshare. Dataset. doi:10.6084/m9.figshare.8942336, 2019.

Response to Reviewer #2:

1. This paper reported some improvements of global gross primary production using the revised EC-LUE model. Overall, it lacks in detailed explanation and thorough validation to show the novelty of the proposed model if any. English must be significantly improved. Thus, I recommend rejecting the paper. Please see several major comments below.

Response: Thanks for your deep thoughts and comments. The poor model performance in reproducing the interannual variability of GPP has been one of the most important uncertainties of satellite-based models, which will restrict our ability for quantifying the long-term trend of GPP over regional and global scales. This study aims to improve the model performance of a LUE model in reproducing interannual variability and produce a new long-term global GPP dataset. Meanwhile, we revised the manuscript according to your comments, and added detailed information on model parameterization and validation (please refer the following responses).

2. Details are missing in many parts. Justification should follow when a decision or selection is done. For example, what is the rationale of dividing data into calibration and validation, and how was it done? How was the parameter optimization conducted? How was the collocation of different input data done? These are just a few of them. Readers don't know what and how the authors exactly did, which limit the understanding of the proposed model and its evaluation.

Response: Sorry for confusion. We checked carefully the manuscript and made sure to represent the method, data and result clear. Here, the reviewer mentioned the model parameterization method, and we responded details in the next comment.

3. Calibration vs. validation. As empirical models are dependent on data, a more robust approach should be adopted. Calibration sites were randomly selected? What if different calibration sites are used? A bootstrapping method might be adopted to see if consistent results can be achieved using different calibration data. Or n-fold cross validation would work. If consistent results were not obtained, the proposed model would be inherently unstable.

Response: Thanks for your constructive comments. In the revised manuscript, we used cross validation method to calibrate model parameters. Cross validation method need more sites for each vegetation types, so we added the study sites from 84 to 95. We updated all the related method and result sections thoroughly (including all the tables and figures, and the related methods and results). And we produced and analyzed the global GPP datasets using the new parameters. Here we show the cross-validation method and the optimized parameter table. Other related modifications are too long to show here, please see them in the revised manuscript.

The detailed description on the cross-validation method is:

“Cross-validation method was used to calibrate and validate the revised EC-LUE model. Fifty percent of the sites were randomly selected to calibrate model parameters for each vegetation type, and the remaining 50% of the sites were used to validate the model. This parameterization process was repeated until all possible combinations of 50% sites were achieved for each vegetation type. The nonlinear regression procedure (Proc NLIN) in the Statistical Analysis System (SAS, SAS Institute Inc., Cary, NC, USA) was applied to optimize the model parameters (ϵ_{msu} , ϵ_{msh} , ϕ , and VPD_0) using 8-day estimated GPP based on EC measurements. The mean GPP simulations of 8-day from all validation runs only were used to model validation. Mean calibrated parameter values from all model runs were used to

simulate GPP over the global scale (Table 3).” (Line 189-195 in the revised manuscript)

The table of the optimized parameters are shown in Table 3:

Table 3: Optimized parameters (ϵ_{msu} , ϵ_{msh} , ϕ , and VPD_0) of the revised EC-LUE model for different vegetation types.

Vegetation Types	DBF	ENF	EBF	MF	GRA	CRO-C3	CRO-C4	SAV	SHR	WET
ϵ_{msu} (g C MJ ⁻¹)	1.28 ± 0.36	1.72 ± 0.42	1.67 ± 0.85	1.38 ± 0.21	1.16 ± 0.15	1.25 ± 0.42	2.46 ± 0.78	2.24 ± 0.68	1.21 ± 0.25	1.34 ± 0.26
ϵ_{msh} (g C MJ ⁻¹)	3.59 ± 0.66	3.87 ± 0.58	4.35 ± 0.72	3.29 ± 0.63	1.91 ± 0.46	2.46 ± 0.52	5.64 ± 1.02	4.26 ± 0.95	2.71 ± 0.52	2.62 ± 0.49
ϕ (ppm)	32 ± 8.25	25 ± 7.59	20 ± 6.36	49 ± 11.25	57 ± 11.85	43 ± 9.56	54 ± 15.36	54 ± 12.23	34 ± 7.59	36 ± 10.32
VPD_0 (kPa)	1.15 ± 0.25	1.34 ± 0.26	0.57 ± 0.15	0.62 ± 0.14	1.69 ± 0.35	1.02 ± 0.19	1.53 ± 0.31	1.65 ± 0.26	1.34 ± 0.21	0.62 ± 0.12

Additionally, we examined the variability of model performance by using different combinations of calibration and validation sites (Fig. R1). We calculated the mean R^2 and RMSE across all validation sites for each combination, and used the coefficient of variation (CV) of R^2 and RMSE of all combinations to indicate the impacts of combinations on model performance. The averaged R^2 over all combinations ranged from 0.62 (EBF) to 0.88 (DBF) among various vegetation types, and the CV values of R^2 were mostly less than 0.11 (except EBF, CV = 0.32) (Fig. R1a-b). The averaged RMSE ranged from 1.33 g C m⁻² d⁻¹ (CRO-C3) to 5.84 g C m⁻² d⁻¹ (SRH) with CV varying from 0.06 to 0.30 (Fig. R1c-d). From statistics (mean, SD, and CV) of R^2 and RMSE, we can conclude our proposed model is robust with high accuracy.

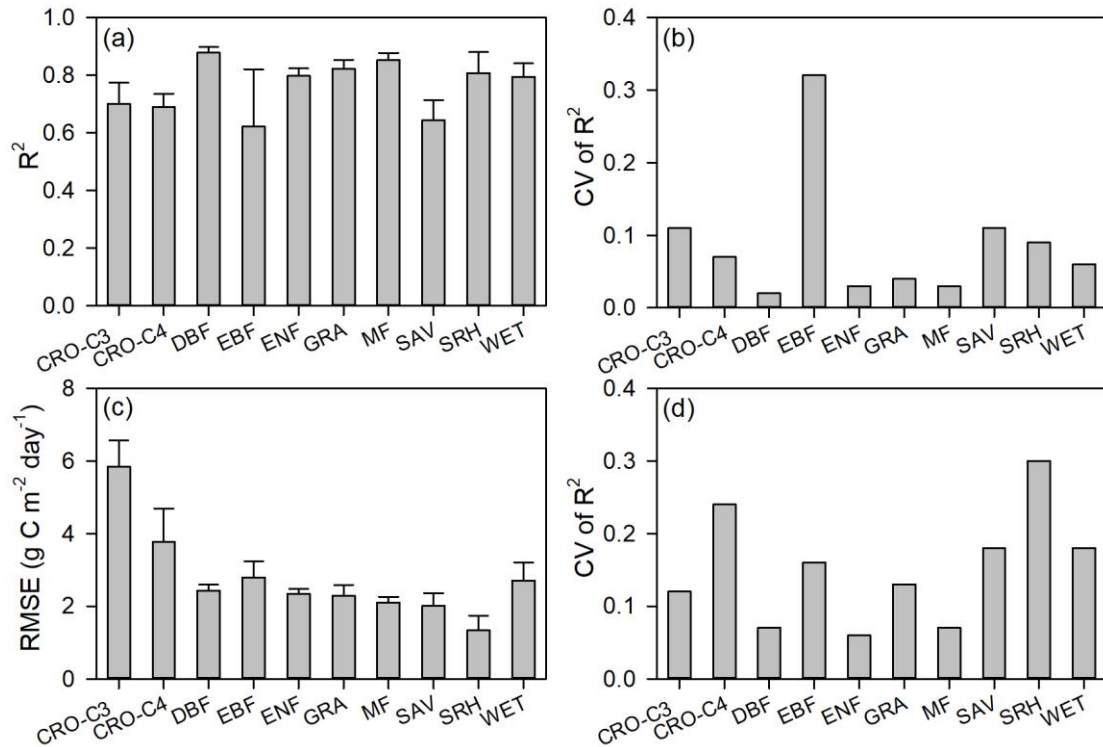


Figure R1: Model performance for all the combinations of calibration and validation sites in cross-validation. (a) Averaged values of R^2 (error bars represent the standard deviation, namely SD), (b) coefficient of variation (CV) of R^2 ($CV = SD/\text{mean}$); (c) Averaged values of RMSE (error bars represent the SD), (b) CV of RMSE.

4. Seasonal analysis using time-series data should be conducted. Figs 2 and 3 are not sufficient to say that the proposed model showed a good performance in reproducing the seasonal variations in GPP as they don't contain any seasonal information. You may conduct statistical analysis by season, not simply based on stations.

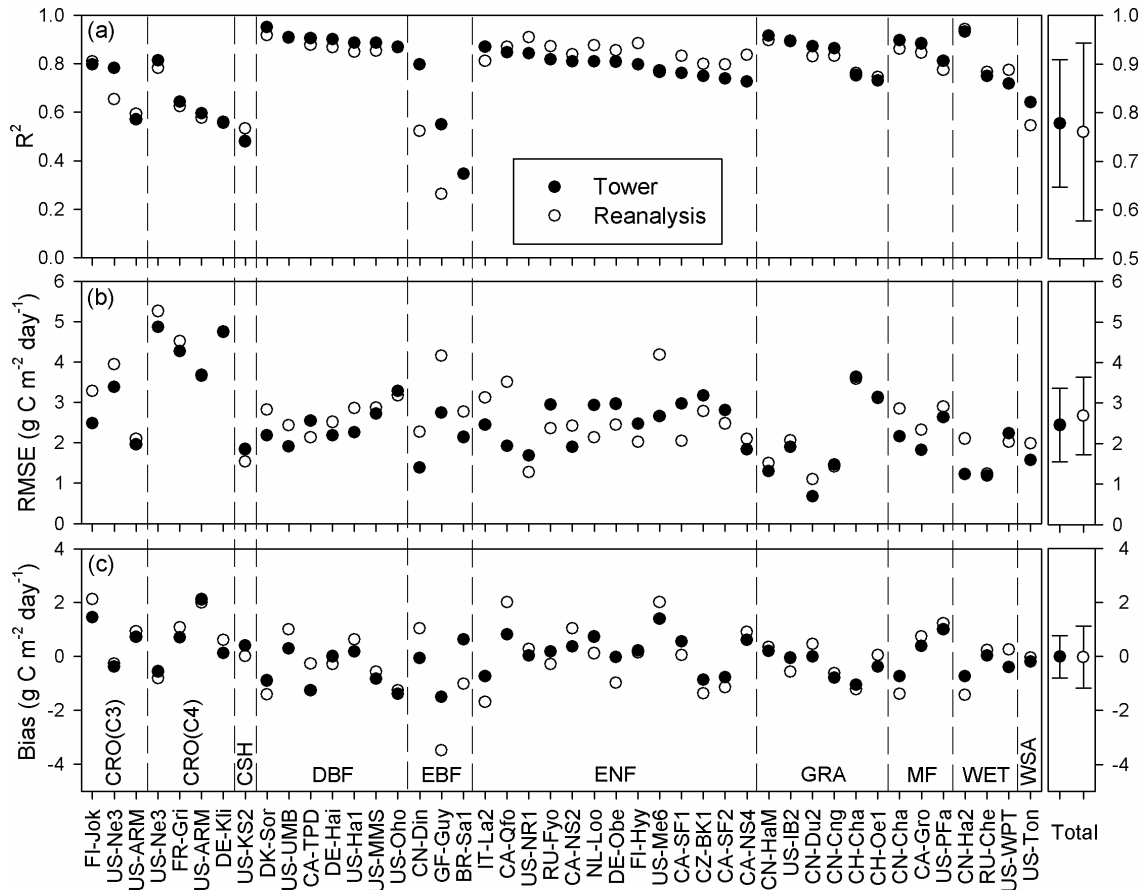


Figure 2: Comparisons of 8-day mean GPP between the observations at 42 calibration sites and the model simulations. Solid and open dots indicate the GPP simulations derived from tower-derived meteorology data and meteorological reanalysis dataset, respectively.

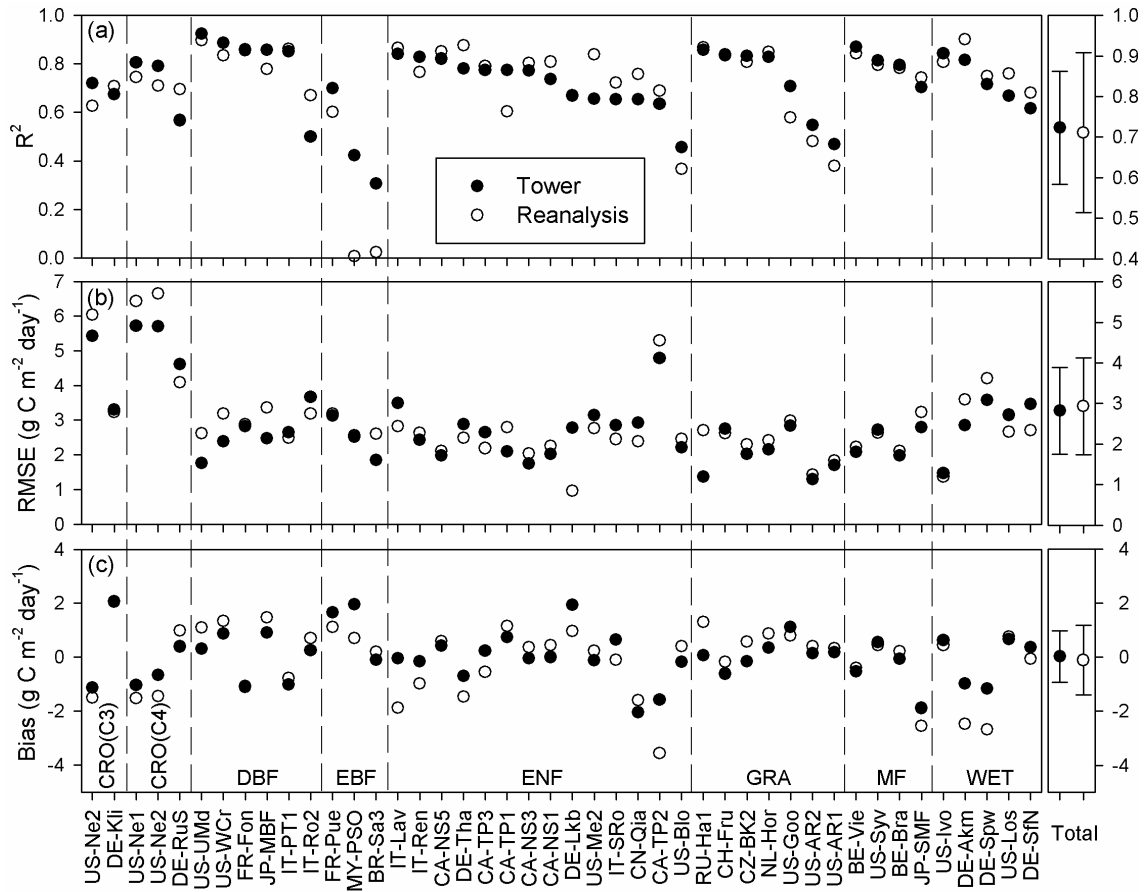


Figure 3: Comparisons of 8-day mean GPP between the observations at 43 validation sites and the model simulations. Solid and open dots indicate the GPP simulations derived from tower-derived meteorology data and meteorological reanalysis dataset, respectively.

Response: In the revised manuscript we used cross-validation method, so we combined Figs. 2-3 to Fig. 2. In Figs. 2-3 (in the original manuscript), we calculated the correlation (R^2) between simulated and observed GPP at 8-day step for each site, and the correlation (R^2) indicates the consistence of temporal changes between GPP simulations and observations. We added these explanations as following:

“In Fig. 2, we compared the modelled GPP and tower GPP at 8-day step for each site to examine the capacity of our model in reproducing the seasonal variations.” (Line 237-238 in the revised manuscript)

In addition, in the revised manuscript, we also added another index (Kendall’s coefficient of rank correlation τ) to further quantify the agreement between the simulated and tower estimated GPP at seasonal patterns (Fig. 2d). We updated the Methods (Section 2.4 Model calibration and validation), Results (Section 3.1 Model performance), and Fig. 2d in the revise manuscript as following.

Methods (Section 2.4 Model calibration and validation):

“Additionally, Kendall’s coefficient of rank correlation τ (Kanji, 1999) was used to quantify the agreement of seasonal changes between the simulated and tower estimated GPP. The Kendall coefficient measured the tendency coherence between predicted and observed GPP by comparing the ranks assigned to successive pairs. If $GPP_{sim,j} - GPP_{sim,i}$ and $GPP_{obs,j} - GPP_{obs,i}$ have the same sign (positive or negative), the pair would be concordant, or discordant. A time-series data with n observations, the Kendall’s coefficient of rank correlation τ can be expressed:

$$\tau = \frac{C-D}{n(n-1)/2} \quad (20)$$

where $n(n-1)/2$ is the total combination of pairs, C is the number of concordant pairs, and D is the number of discordant pairs. The Kendall's coefficient ranged from -1 ($C = 0$) to 1 ($D = 0$). The Kendall's coefficient is much closer to 1, which means a stronger positive relationship between the seasonal patterns of the simulated and tower estimated GPP." (Line 197-206 in the revised manuscript)

Results (Section 3.1 Model performance):

"The averaged Kendall's correlation coefficient (τ) was 0.63, indicating that the model simulated GPP had a strong seasonal coherence with tower estimated GPP. Similar to R^2 , the lower Kendall's correlation coefficient (τ) value sites were also located in the tropical forest areas." (Line 244-246 in the revised manuscript)

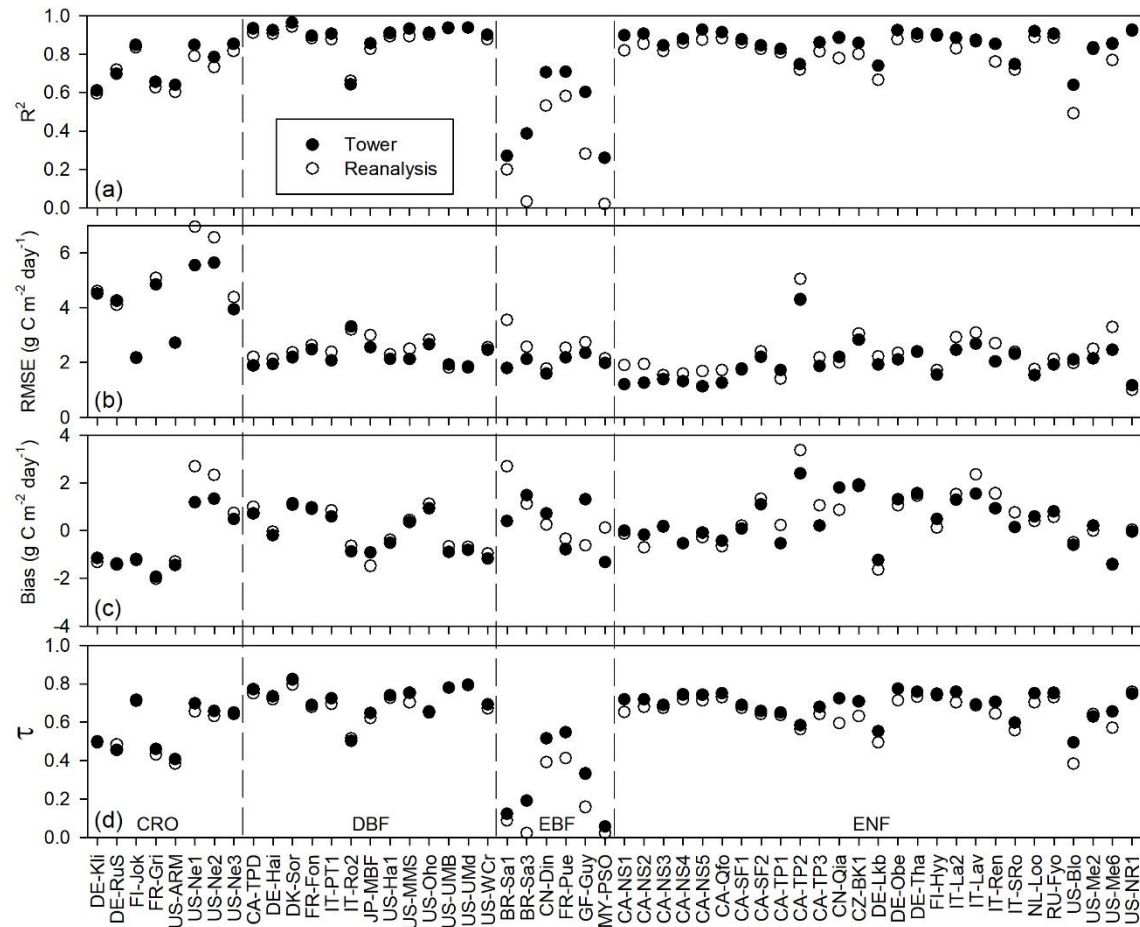
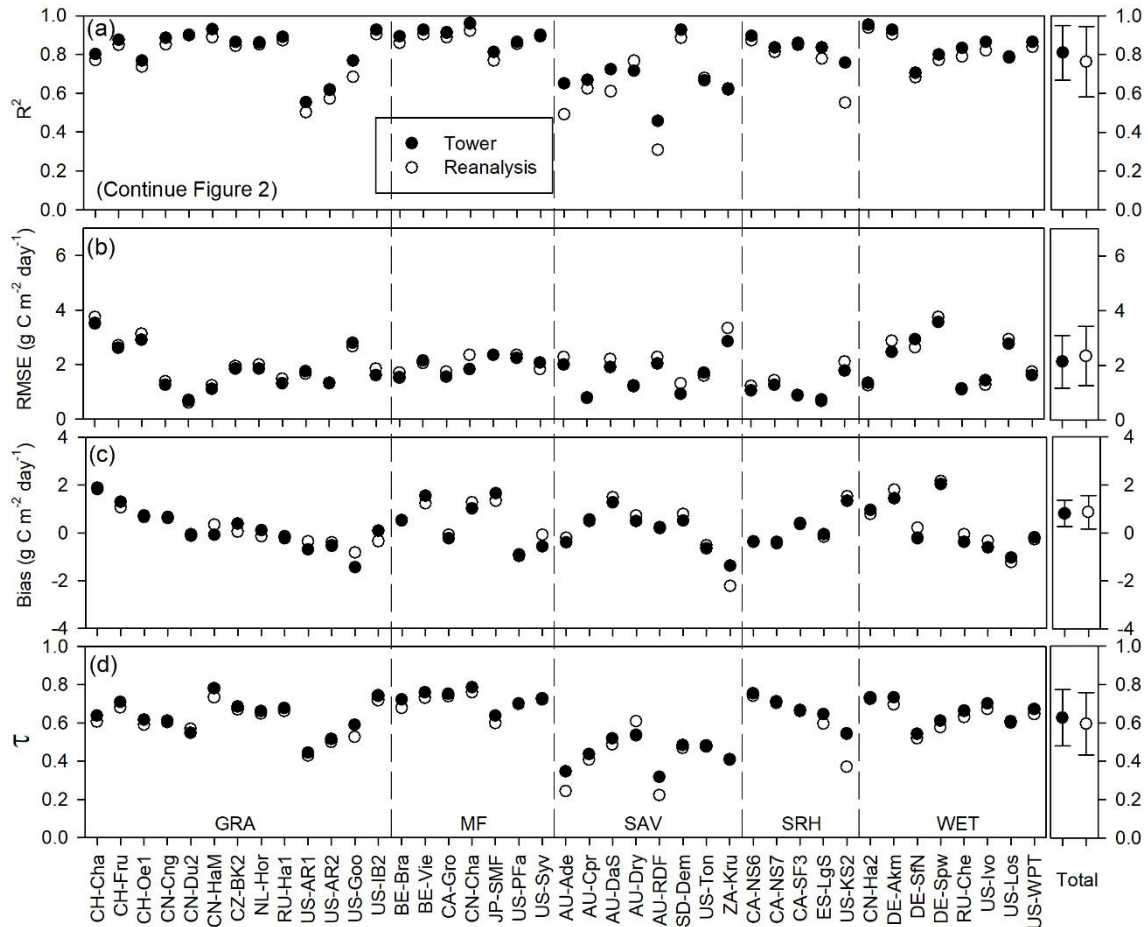


Figure 2: Comparisons of 8-day mean GPP between the model simulated GPP and tower estimated GPP. Solid and open dots indicate the GPP simulations derived from tower-derived meteorology data and meteorological reanalysis dataset, respectively.

Figure 2 (continue)



5. More supporting references should follow in lines 250-251 if you want to say the decreased GPP was due to excessive precipitation and hot temp. In other words, both precipitation and temperature in Amazon significantly increased from 1982 to 2017? Seasonal factors might affect? Line 250-251: The decreased GPP areas were mainly distributed in the tropic regions with abundant precipitation and high temperature, particularly in the Amazon forest.

Response: Sorry for confusion. It is not our purpose to say the abundant precipitation and high temperature is the cause of decreased GPP in tropic regions. We revised the sentence to:

“[The decreased GPP was found in the tropic regions, especially in the Amazon forest.](#)” (Line 274 in the revised manuscript).

The decreased GPP in the tropic regions were mainly due to the suppression of the increased atmospheric water demand indicated by atmosphere vapor pressure deficit (VPD). We have reported the detailed cause of GPP decreases responded to the increased VPD in our recent paper (Yuan et al., 2019), therefore, we appreciate your understanding that we did not discuss the details. In addition, the main objective of this manuscript is to introduce the revised EC-LUE model and long-term global GPP dataset produced by EC-LUE model.

6. Scale issues should be carefully examined. Input data have different scales and the ground GPP measurements don't have the same scale with input data. What kinds of approaches were conducted when matching input data on the same spatial domain? How did the authors mitigate or consider the different scale issues between site GPP data and input variables?

Response: At global scale, the spatial resolution of satellite-based GLASS LAI dataset is 0.05 °latitude by 0.05 °longitude. We downscaled the meteorological reanalysis data (temperature, direct PAR, diffuse PAR, and VPD) to 0.05 °latitude by 0.05 °longitude using the bilinear interpolation method to match the spatial resolution of LAI. We have reported the detailed method in the manuscript:

“We aggregated the daily variables (air temperature, VPD, direct PAR, and diffuse PAR) to 8-day interval temporal resolution. And these variables were resampled to the spatial resolution of 0.05 ° latitude by 0.05 ° longitude using the bilinear interpolation method.” (Line 136-138 in the revised manuscript)

At site level, we calibrated and validated the model using the tower observed meteorology data and global reanalysis meteorology data, respectively. The tower observed meteorology data were directly obtained from the measurement of FLUXNET and the global reanalysis meteorology data were extracted from the processed global 0.05 °×0.05 ° reanalysis data. The model performance slightly decreases when using the meteorological reanalysis compared to that driven by tower-derived meteorology data (please refer to the section 3.1 in the revised manuscript). To further mitigate the uncertainty, we used the parameters optimized by global reanalysis meteorology data to simulate the GPP at global scale.

And we discussed the uncertainty introduced by the mismatches between eddy covariance flux footprint and image pixels of the input dataset in section 4.3 Model uncertainty:

“Additionally, the uncertainty of the revised EC-LUE model may arise by scale mismatches between eddy covariance flux footprint and input dataset. The eddy covariance flux footprint is generally less than 3 km² and varies depending on the wind speed, wind direction and the atmospheric stability (Tan et al., 2006). In our studies, the revised EC-LUE model was run at 0.05 degree (~5 km²) spatial resolution. The uncertainty of simulated GPP introduced by the scale effect is inevitable but smaller than that introduced by the model structures, parameters or input datasets (Sjostrom et al., 2013; Zheng et al., 2018).” (Line 392-396 in the revised manuscript)

7. Lines 282-285. Needs more uncertainty analysis by factor (e.g., radiation) to support this.

Line 282-285: In contrast, 74% of the sites showed higher R² values (>0.5) for the revised EC-LUE model. The improvements of the revised EC-LUE model in reproducing interannual variations are owing to the integration of several important environmental drivers for vegetation production (i.e., atmospheric CO₂ concentration, radiation components, and VPD), which exhibited large variations and contributed significantly to vegetation production at interannual scale.

Response: This statement is based on the results presented by Fig. 3 in the revised manuscript (namely Fig. 4 in the original manuscript). The comparison showed the revised EC-LUE model has the better performance for reproducing the interannual variability in GPP compared to the original EC-LUE and other LUE models. It is a very good idea to identify the contributions of various factors to improve the model ability. However, to our knowledge, there is no recognized methods to conduct the uncertainty analysis by factors, and it will be very interesting to develop this method. However, we appreciate your understanding that it will be beyond the scope of this study, and this manuscript is data description paper and the main purpose is to introduce the model methods and describe the global dataset of GPP with long-term series.

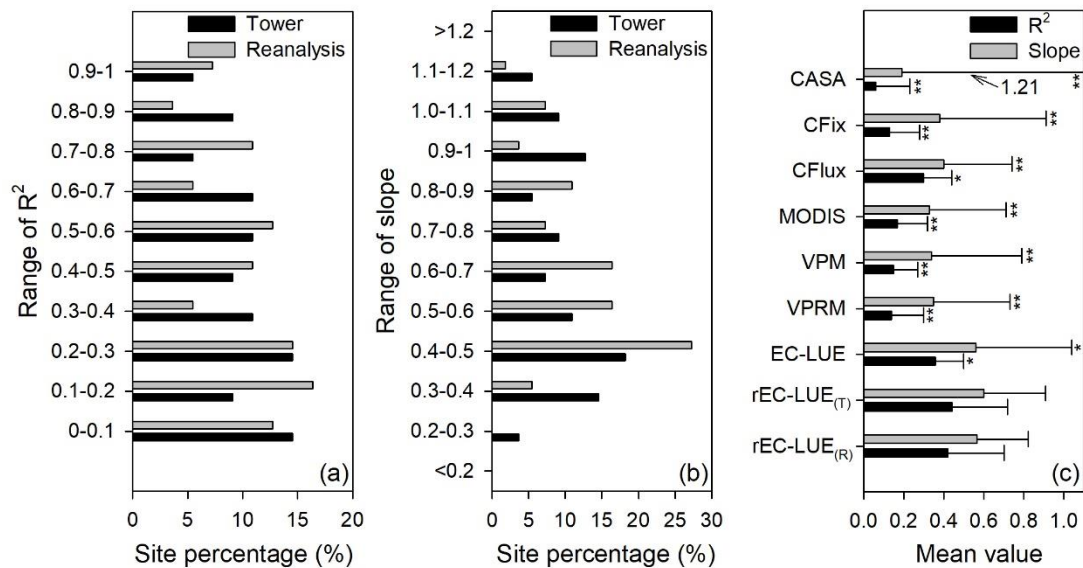


Figure 3: Site percentage of (a) correlation coefficients (R^2), and (b) regression slopes between the model simulated and tower-based interannual variabilities in GPP. (c) Averaged values (error bars represent the standard deviations) of R^2 and slope for various LUE models. rEC-LUE_(T) and rEC-LUE_(R) indicate the revised EC-LUE models derived from tower-derived meteorology data and meteorological reanalysis dataset. The R^2 and slopes of the other seven LUE models (i.e., EC-LUE, VPRM, VPM, MODIS, CFlux, CFix, and CASA) in the figure were obtained from the study by Yuan et al. (2014). **** and * indicate a significant difference in statistic variables (R^2 and slope) between the rEC-LUE_(T) and other LUE models (i.e., rEC-LUE_(T) and other seven LUE models) at p-value < 0.01 and p-value < 0.05, respectively.**

8. Line 325. throughout the seasons? or different results by season? Again, seasonal analysis should be conducted.

Line 325: The revised EC-LUE model showed the lowest accuracy for the evergreen broadleaf forests in the tropic areas (Figs. 2–3).

Response: “throughout the seasons”. As the response of comment #4, we test the seasonal performance of the revised EC-LUE model for each site. We also added another index (Kendall’s coefficient of rank correlation τ) to further quantify the agreement between the simulated and tower estimated GPP at seasonal patterns in the revised manuscript (Fig. 2d in the revised manuscript).

9. Figure 8. Comparison by region (or continent) would make the paper robust. Are there any merits of using the proposed model in terms of the spatial domain?

Response: As your suggestion, we added the comparison between our model and other models across bioclimatic zones in the Köppen-Geiger climate classification map (Beck et al., 2018) before the Fig. 8 (in the original manuscript). Because we have rearranged the figures in our manuscript, the comparison across bioclimatic zones is Fig. 7 in the revised manuscript. We added the following comparison:

“At regional scale, we compared the annual mean GPP between the revised EC-LUE model and other models across the bioclimatic zones in the Köppen-Geiger climate classification map (Beck et al., 2018) (Fig. 7). The GPP of the revised EC-LUE model was comparable to the mean value of other models for each bioclimatic zone (Fig. 7a). The GPP of different models exhibited large discrepancies in tropical regions (Af/Am/Aw) (Fig. 7a). The correlations (R^2) of GPP across all the bioclimatic zones between the revised EC-LUE model and other models ranged from 0.73 (LPX-Bern) to 0.95 (FLUXCOM

MARS, FLUXCOM RF) (Fig. 7b).'' (Line 325-331 in the revised manuscript)

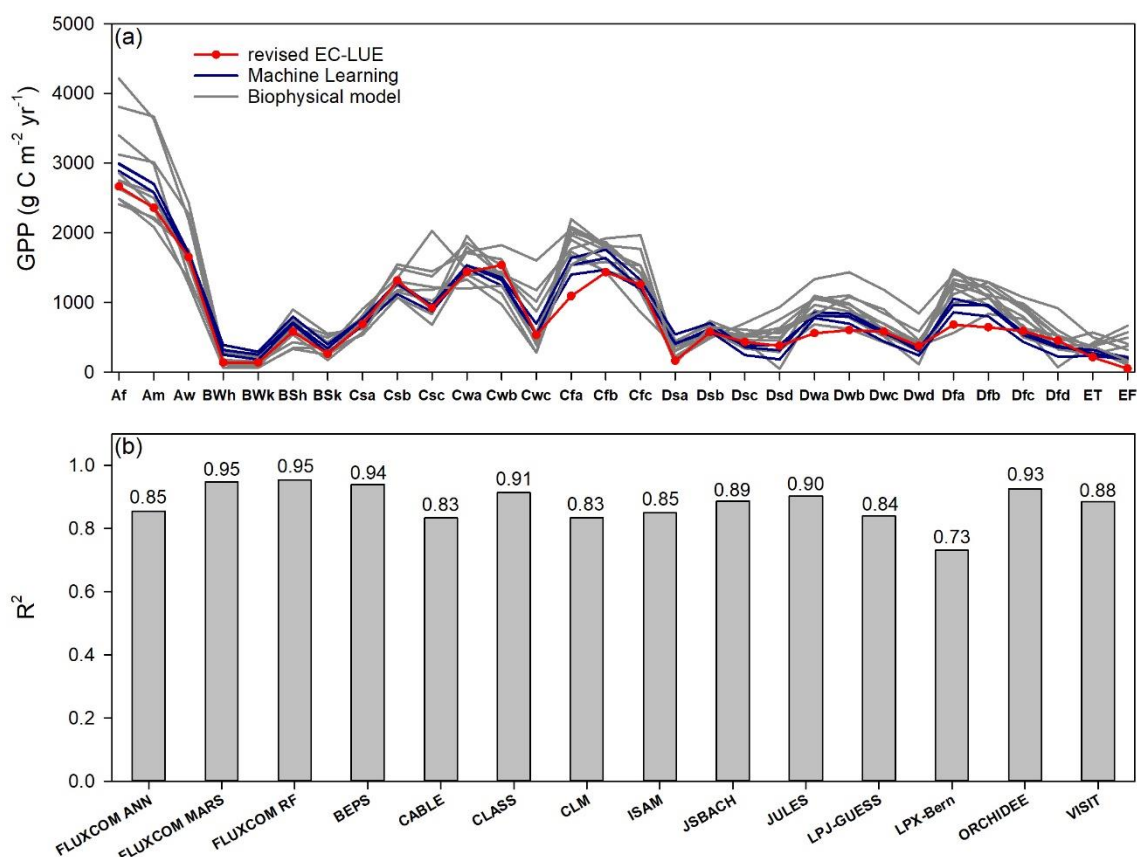


Figure 7: Comparisons of long-term (1982 to 2010s) averaged GPP between the revised EC-LUE model and other models across bioclimatic zones in the Köppen-Geiger climate classification map (Beck et al., 2018). (a) the regional averaged value (b) correlation coefficients (R^2) of GPP at all the bioclimatic zones between the revised EC-LUE model and other models. These models including machine learning models (FLUXCOM ANN, FLUXCOM MARS, FLUXCOM RF; Jung et al., 2017), biophysical models BEPS (Ju et al., 2006; Liu et al., 2018), and ten biophysical models in TRENDY (CABLE, CLASS, CLM, ISAM, JSBACH, JULES, LPJ-GUESS, LPX-Bern, ORCHIDEE, and VISIT). The abbreviations for the bioclimatic zones are as follows: Af, tropical, rainforest; Am, tropical, monsoon; Aw, tropical, savannah; BWh, arid, desert, hot; BWk, arid, desert, cold; BSh, arid, steppe, hot; BSk, arid, steppe, cold; Csa, temperate, dry summer, hot summer; Csb, temperate, dry summer, warm summer; Csc, temperate, dry summer, cold summer; Cwa, temperate, dry winter, hot summer; Cwb, temperate, dry winter, warm summer; Cwc, temperate, dry winter, cold summer; Cfa, temperate, no dry season, hot summer; Cfb, temperate, no dry season, warm summer; Cfc, temperate, no dry season, cold summer; Dsa, cold, dry summer, hot summer; Dsb, cold, dry summer, warm summer; Dsc, cold, dry summer, cold summer; Dsd, cold, dry summer, very cold winter; Dwa, cold, dry winter, hot summer; Dwb, cold, dry winter, warm summer; Dwc, cold, dry winter, cold summer; Dwd, cold, dry winter, very cold winter; Dfa, cold, no dry season, hot summer; Dfb, cold, no dry season, warm summer; Dfc, cold, no dry season, cold summer; Dfd, cold, no dry season, very cold winter; ET, polar, tundra; EF, polar, frost.

10. Lines 371-372. Don't see any conclusive results to say that the model has a unique superiority in reproducing the inter annual variations in GPP at both site level and global scales. Superiority to what? Any comparison with other models (e.g., machine learning or physical models) to show

the inter annual variations?

Line 371-372: The revised EC-LUE performed well in simulating the spatial, seasonal, and interannual variations in global GPP. Particularly, it has a unique superiority in reproducing the interannual variations in GPP at both site level and global scales.

Response: In our manuscript, we compared the model performance at interannual variations of the revised EC-LUE model with other LUE models, such as the original EC-LUE model, CASA, CFix, CFlux, MODIS, VPM, and VPRM. The result showed the revised EC-LUE indeed has a unique superiority in reproducing interannual variations than other LUE models. Over the sites with longer 5-year observations, the averaged R^2 between annual mean tower-estimated and model simulated GPP are 0.44 for the revised EC-LUE model, which is significantly higher than those of original EC-LUE model ($R^2 = 0.36$) and other LUE models (R^2 ranged from 0.06 to 0.30 with an average value of 0.16), and these results have been represented at Fig. 3 (in the revised manuscript).

We appreciate your understanding that we don't compare it with other kind models because the main objective of our manuscript is focused on the improvement of the LUE models and produced a long-term GPP dataset. Moreover, due to large data gaps of measurements derived from eddy covariance towers, we need run process-based models at eddy covariance towers and obtain the corresponding simulations with observations of GPP in order to evaluate the model performance. This work needs contributions of model PIs, and which probably need take long time and great efforts. In addition, previous studies have provided the insights on this issue. Keenan et al. (2012) compared the performance of 16 process-based biophysical models and 3 satellite-based models (including the MODIS product) in reproducing the interannual variations in GPP. The result indicated the MODIS model performance was comparable to the process-based biophysical models. In our manuscript, the revised EC-LUE model (averaged $R^2 = 0.44$) was significantly better than the MODIS model (averaged $R^2 = 0.17$) at interannual scale. Therefore, we can conclude the similar result that our model was better than the process-based biophysical models compared in Keenan et al. (2012).

In order to emphasize that we conducted the comparison with other LUE models, we revised these sentences you mentioned (Line 371-372 in the original manuscript) as following:

“The revised EC-LUE performed well in simulating the spatial, seasonal, and interannual variations in GPP across the globe. Particularly, it has a unique superiority in reproducing the interannual variations in GPP ($R^2 = 0.44$) compared with the original EC-LUE model ($R^2 = 0.36$) and other LUE models (R^2 ranged from 0.06 to 0.30 with an average value of 0.16).” (Line 405-407 in the revised manuscript)

The comparisons with other LUE models are shown in the abstract, result, and discussion section.

In the abstract section:

“Particularly, the revised EC-LUE model improved the model performance in reproducing the interannual variations in GPP, and the averaged R^2 between annual mean tower estimated and model simulated GPP is 0.44 over all 55 sites with observations longer than 5-years, which is significantly higher than those of original EC-LUE model ($R^2 = 0.36$) and other LUE models (R^2 ranged from 0.06 to 0.30 with an average value of 0.16).” (Line 29-33 in the revised manuscript)

In the result section:

“The result showed that the revised EC-LUE model could effectively determine the interannual variations in GPP (Fig. 3). Approximately 42% and 40% of the sites showed higher R^2 values (>0.5) by using the tower-derived meteorology data and the meteorological reanalysis dataset (Fig. 3a).

The averaged R^2 for the revised EC-LUE model was 0.44 by using the tower-derived meteorology data, which was significantly higher than the original EC-LUE model ($R^2 = 0.36$) and other LUE models (R^2 ranged from 0.06 to 0.30 with an average value of 0.16) (Fig. 3c). The averaged R^2 for the revised EC-LUE model was 0.42 by using the meteorological reanalysis dataset. The averaged slopes of the revised EC-LUE model were 0.60 and 0.57 by using the tower-derived meteorology data and the meteorological reanalysis dataset (Fig. 3c)” (Line 252-259 in the revised manuscript)

In the discussion section:

“Numerous studies have shown that most GPP models can reproduce the spatial changes in GPP but failed to reproduce the temporal variations (Keenan et al., 2012; Yuan et al., 2014). Therefore, the capacity to reproduce realistic interannual variations for a GPP model is significantly important. In our study, the revised EC-LUE model performed a higher accuracy in reproducing the interannual variations in GPP than did the original EC-LUE model and other LUE models. Yuan et al. (2014) reported that the averaged slope of the regression relation between the mean annual GPP simulated by seven LUE models and the mean annual GPP estimated from EC tower ranged from 0.19 to 0.56 (Fig. 3c). While the revised EC-LUE model showed a higher slope of regression relation (0.60), which is much closer to 1 than that obtained from other LUE models (Fig. 3c). The VPM GPP showed less interannual variations across most biomes ($R^2 < 0.5$), probably because of the insensitivity of the environmental stress factors at the interannual scale (Zhang et al., 2017). In contrast, 42% of the sites showed higher R^2 values (> 0.5) for the revised EC-LUE model.” (Line 296-305 in the revised manuscript)

11. English needs to be carefully revised.

Response: We thoroughly checked and improved English usages of the revised manuscript. And we also polished the English in a professional agency.

References

1. Beck, H.E., Zimmermann, N.E., McVicar, T.R., Vergopolan, N., Berg, A., Wood, E.F.: Present and future Köppen-Geiger climate classification maps at 1-km resolution, *Scientific Data*, doi:10.1038/sdata.2018.214, 2018.
2. Kanji, G.K., 1999. 100 Statistical Tests. SAGE Publications, London.
3. Keenan, T.F., Baker, I., Barr, A., Ciais, P., Davis, K., Dietze, M., Dragon, D., Gough, C.M., Grant, R., Hollinger, D., Hufkens, K., Poulter, B., McCaughey, H., Raczka, B., Ryu, Y., Schaefer, K., Tian, H.Q., Verbeeck, H., Zhao, M.S., Richardson, A.D.: Terrestrial biosphere model performance for inter-annual variability of land-atmosphere CO₂ exchange, *Global Change Biol.*, 18, 1971-1987, doi:10.1111/j.1365-2486.2012.02678.x, 2012.
4. Sjoström, M., Zhao, M., Archibald, S., Arneth, A., Cappelaere, B., Falk, U., de Grandcourt, A., Hanan, N., Kergoat, L., Kutsch, W., Merbold, L., Mougou, E., Nickless, A., Nouvellon, Y., Scholes, R.J., Veenendaal, E.M., Ardo, J.: Evaluation of MODIS gross primary productivity for Africa using eddy covariance data, *Remote Sens. Environ.*, 131, 275-286, doi:10.1016/j.rse.2012.12.023, 2013.
5. Tan, B., Woodcock, C.E., Hu, J., Zhang, P., Ozdogan, M., Huang, D., Yang, W., Knyazikhin, Y., Myneni, R.B.: The impact of gridding artifacts on the local spatial properties of MODIS data: Implications for validation, compositing, and band-to-band registration across resolutions, *Remote Sens. Environ.*, 105, 98-114, doi:10.1016/j.rse.2006.06.008, 2006.
6. Yuan, W., Cai, W., Xia, J., Chen, J., Liu, S., Dong, W., Merbold, L., Law, B., Arain, A., Beringer, J., Bernhofer, C., Black, A., Blanken, P.D., Cescatti, A., Chen, Y., Francois, L., Gianelle, D.,

- Janssens, I.A., Jung, M., Kato, T., Kiely, G., Liu, D., Marcolla, B., Montagnani, L., Raschi, A., Rouspard, O., Varlagin, A., Wohlfahrt, G.: Global comparison of light use efficiency models for simulating terrestrial vegetation gross primary production based on the La Thuile database, *Agric. For. Meteorol.*, 192, 108-120, doi:10.1016/j.agrformet.2014.03.007, 2014.
7. Yuan, W., Zheng, Y., Piao, S., Ciais, P., Lombardozzi, D., Wang, Y., Ryu, Y., Chen, G., Dong, W., Hu, Z., Jain, A.K., Jiang, C., Kato, E., Li, S., Lienert, S., Liu, S., Nabel, J.E.M.S., Qin, Z., Quine, T., Sitch, S., Smith, W.K., Wang, F., Wu, C., Xiao, Z., Yang, S.: Increased atmospheric vapor pressure deficit reduces global vegetation growth, *Science Advances*, 510.1126/sciadv.aax1396, 2019.
 8. Zhang, Y., Xiao, X., Wu, X., Zhou, S., Zhang, G., Qin, Y., Dong, J.: Data Descriptor: A global moderate resolution dataset of gross primary production of vegetation for 2000-2016, *Scientific Data*, 410.1038/sdata.2017.165, 2017.
 9. Zheng, Y., Zhang, L., Xiao, J., Yuan, W., Yan, M., Li, T., Zhang, Z.: Sources of uncertainty in gross primary productivity simulated by light use efficiency models: Model structure, parameters, input data, and spatial resolution, *Agric. For. Meteorol.*, 263, 242-257, doi:10.1016/j.agrformet.2018.08.003, 2018.

Improved estimate of global gross primary production for reproducing its long-term variation, 1982-2017

Yi Zheng¹, Ruoque Shen¹, Yawen Wang^{1,2}, Xiangqian Li¹, Shuguang Liu³, Shunlin Liang^{4,5}, Jing M. Chen^{6,7}, Weimin Ju^{7,8}, Li Zhang⁹, Wenping Yuan^{1,2*}

- 5 ¹School of Atmospheric Sciences, Sun Yat-sen University, ~~Guangzhou 510245~~[Zhuhai 519082](#), Guangdong, China;
²Southern Laboratory of Ocean Science and Engineering (Guangdong, Zhuhai), Zhuhai 519000, Guangdong, China
³College of Life Science and Technology, Central South University of Forestry and Technology (CSUFT), Changsha, Hunan 410004, China
⁴Department of Geographical Sciences, University of Maryland, College Park, MD 20742 USA
10 ⁵School of Remote Sensing Information Engineering, Wuhan University, Wuhan 430072, Hubei, China
⁶Department of Geography, University of Toronto, Canada, M5G 3G3
⁷International Institute for Earth System Sciences, Nanjing University, Nanjing, China.
⁸Jiangsu Center for Collaborative Innovation in Geographical Information Resource Development and Application, Nanjing, China.
15 ⁹Key Laboratory of Digital Earth Science, Institute of Remote Sensing and Digital Earth, Chinese Academy of Sciences, Beijing 100094, China

Correspondence to: yuanwpcn@126.com (W. Yuan).

Abstract. Satellite-based models have been widely used to simulate vegetation gross primary production (GPP) at [the](#) site, regional, or global scales in recent years. However, accurately reproducing the interannual variations in GPP remains a major challenge, and the long-term changes in GPP remain highly uncertain. In this study, we generated a long-term global GPP dataset at 0.05 °latitude by 0.05 °longitude ~~at~~[and](#) 8-day interval by revising a light use efficiency model (i.e. EC-LUE [model](#)). In the revised EC-LUE model, we integrated the regulations of several major environmental variables: atmospheric CO₂ concentration, radiation components, and atmospheric vapor pressure deficit (VPD). These environmental variables showed substantial long-term changes, which could greatly impact the global vegetation productivity. Eddy covariance (EC) measurements at [8495](#) towers from the FLUXNET2015 dataset, covering nine major ecosystem types ~~of~~[around](#) the globe, were used to calibrate and validate the model. [In general, the revised EC-LUE model could effectively reproduce the spatial, seasonal, and annual variations in the tower estimated GPP at most sites.](#) The revised EC-LUE model could explain ~~83% and 68%~~[71% of the spatial variations in annual GPP over 95 sites. At more than 95% of the ~~spatial variations in the annual GPP at 42 calibration sites, the correlation coefficients \(R²\) of seasonal changes between tower estimated and 43 validation sites, respectively. In particular, the revised EC-LUE model could very well reproduce \(-74% sites R² > model simulated GPP are larger than 0.5; averaged R² = 0.65\).~~ Particularly, the revised EC-LUE model improved the model performance in reproducing the interannual variations in GPP ~~at 51,~~ and the averaged R² between annual mean tower estimated and model simulated GPP is 0.44 over all 55 sites with observations ~~greater~~\[longer\]\(#\) than 5-years. ~~At,~~ which is significantly higher than those of original EC-LUE model \(R² = 0.36\) and other LUE models \(R² ranged from 0.06 to 0.30 with an average value of 0.16\). At the global scale, ~~sensitivity~~\[GPP derived from light use efficiency models, machine learning models, and process-based biophysical\]\(#\)](#)

models exist substantial differences in magnitude and interannual variations. The revised EC-LUE model quantified the mean global GPP from 1982 to 2017 as $106.2 \pm 2.9 \text{ Pg C yr}^{-1}$ with the trend $0.15 \text{ Pg C yr}^{-1}$. Sensitivity analysis indicated that the GPP simulated by the revised EC-LUE model was sensitive to atmospheric CO_2 concentration, VPD, and radiation. Over the period of 1982–2017, the CO_2 fertilization effect on the global GPP ($0.22 \pm 0.07 \text{ Pg C yr}^{-1}$) could be partly offset by increased VPD ($-0.17 \pm 0.06 \text{ Pg C yr}^{-1}$). The long-term changes of environmental variables could be well reflected in the global GPP dataset. The CO_2 fertilization effect on the global GPP ($0.14 \pm 0.001 \text{ Pg C yr}^{-1}$) could be offset by the increased VPD ($-0.16 \pm 0.02 \text{ Pg C yr}^{-1}$). The global GPP derived from different datasets exist substantial uncertainty in magnitude and interannual variations. The magnitude of global summed GPP simulated by the revised EC-LUE model was comparable to other global models. While the revised EC-LUE model has a unique superiority in simulating the interannual variations in GPP at both site level and global scales. The revised EC-LUE model provides. Overall, the revised EC-LUE model is able to provide a reliable long-term estimate of global GPP because of integrating the important environmental variables. The GPP dataset is available at <https://doi.org/10.6084/m9.figshare.8942336> (Zheng et al., 2019).

1 Introduction

Vegetation gross primary production (GPP) is the largest carbon flux component within terrestrial ecosystems and plays an essential role in regulating the global carbon cycle (Canadell et al., 2007; Zhao et al., 2010). As a primary variable of the terrestrial ecosystem cycle, GPP estimates will substantially determine other variables of the carbon cycle (Yuan et al., 2011). Satellite-based GPP models have been developed based on the light use efficiency (LUE) principle (Monteith, 1972; Potter et al., 1993; Running et al., 2004; Xiao et al., 2005; Yuan et al., 2007). Thus far, LUE models have been a major tool for investigating the spatio-temporal changes in GPP and the environmental dominates, either independently or by combining with other ecosystem models (Keenan et al., 2016; Smith et al., 2016).

However, current LUE models exhibit a poor performance in reproducing the interannual variations in GPP. A previous study indicated that seven LUE models only could only explain 6–36% of the interannual variations in GPP at 51 eddy covariance (EC) towers (Yuan et al., 2014). Similarly, a model comparison showed that none of the examined 16 process-based biophysical models nor the 3 satellite-based models remote sensing products (BESS, MODIS C5, and MODIS C5.1) could consistently reproduce the observed interannual variations in carbon exchange GPP at 11 forest sites in North America (Keenan et al., 2012). Seven LUE models simulated the long-term trends of global GPP varied from -0.15 to $1.09 \text{ Pg C yr}^{-1}$ over the period 2000–2010 (Cai et al., 2014). An important reason for the poor performance in modeling the interannual variability is that the effect of environmental regulations on vegetation production is not completely integrated into the LUE models (Stocker et al., 2019). In particular, the long-term changes in several environmental variables are very important for accurately simulating the GPP series at the decadal scale.

Several environmental variables should be included in GPP models. Firstly, as we all know the rising atmospheric CO_2 concentration in the past few decades substantially stimulated global vegetation growth (Zhu et al., 2016; Liu et al., 2017).

Field experiments using greenhouses or open-top chambers showed that an increase of ~~approximate~~approximately 300 ppm in CO₂ concentration can increase ~~C3 plant~~the photosynthesis of C3 plants on the order of 60% (Norby et al., 1999). Free-air CO₂ enrichment (FACE) experiments generally confirmed the enhancement in net primary production (NPP) with the rising CO₂ concentration (Ainsworth and Long, 2005). For example, four FACE experiments indicated that the forest NPP consistently increased at the median of 23 ± 2% when the ambient CO₂ concentration was elevated to approximately 550 ppm (Norby et al., 2005). According to observations, the atmospheric CO₂ concentration has risen by approximately 20% from 340 ppm (1982) to 410 ppm (2018) (<https://www.esrl.noaa.gov/>). However, the effects of CO₂ fertilization on GPP have not been integrated in most current satellite-based LUE models.

Secondly, solar radiation, or more specifically the photosynthetic active radiation (PAR) substantially influences the vegetation production of the terrestrial ecosystem (Alton et al., 2007; Kanniah et al., 2012; Krupkova et al., 2017). Study indicated that the solar radiation incident at the earth surface underwent significant decadal variations (Wild et al., 2005). A comprehensive analysis based on the datasets of worldwide distributed sites indicated significant decreases in solar radiation (2% per decade) from the late 1950s to 1990 in the regions of Asia, Europe, North America, and Africa (Gilgen et al., 1998). A later assessment by Wild et al. (2005) showed that the radiation increased at widespread locations since the mid-1980s.

However, ~~it is~~ not only the total amount of solar radiation or PAR incident at the earth surface; but ~~also~~, more importantly, their partitioning into direct and diffuse radiations, ~~that~~ impact the vegetation productivity (Urban et al., 2007; Kanniah et al., 2012). Increased proportion of diffuse radiation enhances vegetation photosynthesis, because a higher blue/red light ratio within the diffuse radiation may lead to higher light use efficiency (Gu et al., 2002; Alton et al., 2007). For example, the sharply increased diffuse radiation induced by the 1991 Mount Pinatubo eruption enhanced the noontime vegetation productivity of a deciduous forest in the next 2 years (Gu et al. 2003). Besides volcanic aerosols, clouds could also reduce the total and direct radiation, while increase the proportion of diffuse radiation. Yuan et al. (2010) found that the higher LUE at European forests than North America was because of the higher ratio of cloudy days in Europe. Yuan et al. (2014) further proved that the significantly underestimated GPP during cloudy days by six LUE models was because the effects of diffuse radiation on LUE were neglected in these models.

Thirdly, atmospheric vapor pressure deficit (VPD) is another factor that should be included in GPP models. As an important driver of atmospheric water demand for plants, VPD influences terrestrial ecosystem function and photosynthesis (Rawson et al., 1977); Yuan, et al., 2019. Rising air temperature increases the saturated vapor pressure at a rate of ~7%/K according to the Classius–Clapeyron relationship, and therefore, VPD will increase if the atmospheric water vapor content does not increase by exactly the same amount ~~of~~as the saturated vapor pressure. Numerous studies indicated significant changes in the relative humidity (ratio of actual water vapor pressure to saturated water vapor pressure) in both humid areas and continental areas located far from oceanic humidity (Van Wijngaarden and Vincent, 2004; Pierce et al., 2013). In particular, the global averaged land surface relative humidity decreased sharply after the late 1990s (Simmons et al. 2010; Willett et al. 2014). The leaf and canopy photosynthetic rate ~~decline~~declines when the atmospheric VPD increases due to stomatal closure (Fletcher et al., 2007). A recent study highlighted that increases in VPD rather than changes in precipitation ~~will~~would be a dominant influence on

vegetation productivity (Konings et al., 2017). However, currently the influence of long-term VPD variations is not well expressed in many LUE models ~~currently~~.

We have developed a LUE model, namely the EC-LUE model, by integrating remote sensing data and eddy covariance data to simulate daily GPP (Yuan et al., 2007; 2010). The model has been evaluated using the observations at EC towers located in Europe, North America, China, and East Asia, covering various ecosystem types (Yuan et al., 2007; 2010; Li et al., 2013). In this study, we revised the EC-LUE model by integrating the impacts of several environmental variables (i.e., atmospheric CO₂ concentration, radiation components, and atmospheric VPD) across a long-term temporal scale. Firstly, we evaluated the effectiveness of the revised EC-LUE model in determining the spatial, seasonal, and interannual variations in GPP from multiple eddy covariance sites. ~~Then~~ Secondly, a global GPP dataset at 0.05 ° spatial resolution was generated based on the optimized model. Finally, we analyzed the contributions of the aforementioned environmental variables to the global GPP and discussed the spatial and interannual variations in GPP from different ~~global GPP~~ datasets.

2 Data and Methods

2.1 Description of the revised EC LUE model

~~The terrestrial vegetation GPP can be expressed as follows in the revised EC LUE model:~~

$$GPP = (\epsilon_{msu} \times APAR_{su} + \epsilon_{msh} \times APAR_{sh}) \times C_s \times \min(T_s, W_s) \quad (1)$$

~~where ϵ_{msu} is the maximum LUE of sunlit leaves; $APAR_{su}$ is the PAR absorbed by sunlit leaves; ϵ_{msh} is the maximum LUE of shaded leaves; $APAR_{sh}$ is the PAR absorbed by shaded leaves; C_s , T_s , and W_s represent the downward regulation scalars of atmospheric CO₂ concentration ($[CO_2]$), air temperature, and VPD on LUE ranging from 0 to 1; min represents the minimum value.~~

~~The effect of atmospheric CO₂ concentration on GPP is determined by the following equations (Farquhar et al., 1980; Collatz et al., 1991):~~

$$C_s = \frac{C_i - \phi}{C_i + 2\phi} \quad (2)$$

$$C_i = C_a \times \chi \quad (3)$$

~~where ϕ is the CO₂ compensation point in the absence of dark respiration (ppm); C_i is the leaf internal CO₂ concentration; C_a is the atmospheric CO₂ concentration; χ is the ratio of leaf internal to atmospheric CO₂ which can be estimated as follows (Prentice et al., 2014; Keenan et al., 2016):~~

$$\chi = \frac{\epsilon}{\epsilon + \sqrt{VPD}} \quad (4)$$

$$\epsilon = \sqrt{\frac{356.51K}{1.6\eta^*}} \quad (5)$$

$$K = K_c \left(1 + \frac{P_0}{K_0}\right) \quad (6)$$

$$K_c = 39.97 \times e^{\frac{79.43 \times (T - 298.15)}{298.15RT}} \quad (7)$$

$$K_o = 27480 \times e^{\frac{36.38 \times (T - 298.15)}{298.15RT}} \quad (8)$$

where K_c and K_o are the Michaelis-Menten constants for CO_2 and O_2 ; P_o is the partial pressure of O_2 ; T_a is air temperature (K); η^* is the viscosity of water relative to its value at 25 °C depending on the air temperature (Korson et al., 1969); R is the molar gas constant (8.314 J mol⁻¹ K⁻¹).

~~T_s and W_s can be expressed as follows:~~

$$T_s = \frac{(T - T_{\min}) \times (T - T_{\max})}{(T - T_{\min}) \times (T - T_{\max}) - (T - T_{\text{opt}}) \times (T - T_{\text{opt}})} \quad (9)$$

$$W_s = \frac{\text{VPD}_0}{\text{VPD}_0 + \text{VPD}} \quad (10)$$

where T_{\min} , T_{opt} , and T_{\max} are the minimum, optimum, and maximum temperatures (K) for vegetation photosynthesis, respectively (Yuan et al., 2007); VPD_0 is the half saturation coefficient of the VPD constraint equation (kPa).

~~APAR_{su} and APAR_{sh} can be expressed as follows (Chen et al., 1999):~~

$$\text{APAR}_{\text{su}} = (\text{PAR}_{\text{dir}} \times \frac{\cos(\beta)}{\cos(\theta)} + \frac{\text{PAR}_{\text{dif}} - \text{PAR}_{\text{dif,u}}}{\text{LAI}} + C) \times \text{LAI}_{\text{su}} \quad (11)$$

$$\text{APAR}_{\text{sh}} = \left(\frac{\text{PAR}_{\text{dif}} - \text{PAR}_{\text{dif,u}}}{\text{LAI}} + C \right) \times \text{LAI}_{\text{sh}} \quad (12)$$

$$\text{PAR}_{\text{dif,u}} = \text{PAR}_{\text{dif}} \times \exp\left(\frac{-0.5 \times \Omega \times \text{LAI}}{\cos(\theta)}\right) \quad (13)$$

where PAR_{dir} is the direct PAR; PAR_{dif} is the diffuse PAR; $\text{PAR}_{\text{dif,u}}$ is the diffuse PAR under the canopy; C represents the multiple scattering effects of direct radiation; Ω is the clumping index, which is set according to vegetation types (Tang et al., 2007); θ is the solar zenith angle; β is the mean leaf sun angle, which is set to 60°; $\bar{\theta}$ is the representative zenith angle for diffuse radiation transmission and can be expressed by LAI (Chen et al., 1999):

$$\cos(\bar{\theta}) = 0.537 + 0.025 \times \text{LAI} \quad (14)$$

The LAIs of shaded leaves (LAI_{sh}) and sunlit leaves (LAI_{su}) in Eqs. (11) and (12) are computed following Chen et al (1999):

$$\text{LAI}_{\text{su}} = 2 \times \cos(\theta) \times \left(1 - e^{-0.5 \times \Omega \times \frac{\text{LAI}}{\cos(\theta)}} \right) \quad (15)$$

$$\text{LAI}_{\text{sh}} = \text{LAI} - \text{LAI}_{\text{su}} \quad (16)$$

The parameters ϵ_{msu} , ϵ_{msh} , ϕ , and VPD_0 were calibrated using the estimated GPP from EC towers. The initial ranges of ϵ_{msu} and ϵ_{msh} were set to 0–12 g C MJ⁻¹, ϕ was set to 0–100 ppm, VPD_0 was set to 0–4 kPa. The optimized values of these parameters were adopted until the root mean square error (RMSE) of the model simulated and the EC-estimated daily GPP approached to the minimum value.

2.2 Data from the eddy covariance towers

The FLUXNET2015 dataset (<http://www.fluxdata.org>) includes over 200 variables of carbon fluxes, energy fluxes, and meteorological data variables collected and processed at sites by the FLUXNET community. In our study,

160 ~~eighty-four~~ninety-five EC sites in FLUXNET2015 dataset were utilized to optimize the parameters and evaluate the performance of the revised EC-LUE model, including nine major terrestrial ecosystem vegetation types (Table 1): evergreen broadleaf forests (EBF), evergreen needleleaf forests (ENF), deciduous broadleaf forests (DBF), mixed forests (MF), grasslands (GRA), savannas (SAV), shrubland (SHR), wetlands (WET), and croplands (CRO). More information about the characteristics of these sites can be referred to the FLUXNET website. For each site, the ~~aggregated~~ daily GPP, PAR, air temperature (Ta), and VPD were used in our study. The GPP variable (GPP_NT_VUT_REF) used in this study was estimated from night-time partitioning method. The corresponding net ecosystem exchange (NEE) was generated using variable friction velocity (USTAR) threshold for each year (VUT), in which 40 versions of NEE were created by using different percentiles of USTAR thresholds. The model efficiency between each version and the others 39 versions were calculated to test their similarities and the reference (REF) NEE was selected as the one with higher model efficiency sum (the most similar to the others 39). The daily meteorological variables were gap-filled ~~and/or~~ downscaled from the ERA-interim reanalysis dataset in both space and time (Vuichard and Papale, 2015). ~~The carbon flux measurements (i.e., net ecosystem exchange (NEE)) were gap-filled and partitioned into GPP and ecosystem respiration (Re) using a nighttime based approach (Reichstein et al. 2005).~~ The gap-filled technique of the carbon flux measurements and meteorological variables is the marginal distribution sampling (MDS) method described in Reichstein et al. (2005). For each variable, we aggregated the daily values to 8-day time step. Only the 8-day measurements with more than 5-day valid values were used.

<<Table 1>>

2.32 Data at the global scale

~~The input data of the revised EC-LUE model~~The global scale datasets used in this study are shown in ~~Table2~~Table 2. The ~~global scale~~ meteorological reanalysis dataset was derived from the second Modern-Era Retrospective analysis for Research and Applications (MERRA-2) dataset. It was produced by NASA's Global Modeling and Assimilation Office that ~~uses~~used an upgraded version of the GEOS-5 (Rienecker et al., 2011). It has been validated carefully using surface meteorological datasets and enhanced assimilation system to reduce the uncertainty in various meteorological variables globally. In our study, we obtained the daily mean air temperature (Ta, °C), mean dew point temperature (Td, °C), total direct PAR_r (PAR_{dr}, MJ m⁻² d⁻¹), and total diffuse PAR (PAR_{df}, MJ m⁻² d⁻¹) at 0.625 °in longitude by 0.5 °in latitude from 1982 to 2017. VPD was calculated from air temperature and dew point temperature:

$$SVP = 6.112 \times e^{\frac{17.67T_a}{T_a+243.5}} \quad (471)$$

$$RH = e^{\frac{17.625T_d}{T_d+243.04} - \frac{17.625T_a}{T_a+243.04}} \quad (482)$$

$$VPD = SVP \times (1 - RH) \quad (493)$$

where SVP is the saturated vapor pressure (k Pa), and RH is the relative humidity. We aggregated the daily variables (air temperature, VPD, direct PAR, and diffuse PAR) to 8-day interval temporal resolution. And these variables were resampled to the spatial resolution of 0.05 °latitude by 0.05 °longitude using the bilinear interpolation method.

The 8-day Global Land Surface Satellite-leaf area index (GLASS LAI) dataset at 0.05 °latitude by 0.05 °longitude was adopted to indicate vegetation growth from 1982 to 2017. It was produced using the general regression neural networks (GRNNs) trained with the fused MOD15 LAI and CYCLOPES LAI and the preprocessed MODIS/AVHRR reflectance data over the BELMANIP sites (Xiao et al., 2016). Products validation and comparison showed that the GLASS LAI product was spatially complete and temporally continuous with lower uncertainty (Xu et al., 2018).

Additionally, the MCD12Q1 product with IGBP classification scheme was used as land cover map ~~and the~~ [The ISLSCP II C4 Vegetation Percentage map was used to separate the C3 and C4 crops](#). The NOAA’s Earth System Research Laboratory (ESRL) CO₂ concentration dataset was used to express the CO₂ fertilization effect.

200 <<Table 2>>

2.3 The revised EC-LUE model

The terrestrial vegetation GPP can be expressed as follows in the revised EC-LUE model:

$$GPP = (\varepsilon_{msu} \times APAR_{su} + \varepsilon_{msh} \times APAR_{sh}) \times C_s \times \min(T_s, W_s) \quad (4)$$

205 where ε_{msu} is the maximum LUE of sunlit leaves; $APAR_{su}$ is the PAR absorbed by sunlit leaves; ε_{msh} is the maximum LUE of shaded leaves; $APAR_{sh}$ is the PAR absorbed by shaded leaves; C_s , T_s , and W_s represent the downward regulation scalars of atmospheric CO₂ concentration ([CO₂]), air temperature, and VPD on LUE ranging from 0 to 1; min represents the minimum value.

The effect of atmospheric CO₂ concentration on GPP is determined by the following equations (Farquhar et al., 1980; Collatz et al., 1991):

$$210 C_s = \frac{C_i - \varphi}{C_i + 2\varphi} \quad (5)$$

$$C_i = C_a \times \chi \quad (6)$$

where φ is the CO₂ compensation point in the absence of dark respiration (ppm); C_i is the leaf internal CO₂ concentration; C_a is the atmospheric CO₂ concentration; χ is the ratio of leaf internal to atmospheric CO₂ concentration which can be estimated as follows (Prentice et al., 2014; Keenan et al., 2016):

$$215 \chi = \frac{\varepsilon}{\varepsilon + \sqrt{VPD}} \quad (7)$$

$$\varepsilon = \sqrt{\frac{356.51K}{1.6\eta^*}} \quad (8)$$

where ε is a parameter related to the ‘carbon cost of water’, which means the sensitivity of VPD to χ ; K is the Michaelis–Menten coefficient of Rubisco; η^* is the viscosity of water relative to its value at 25 °C (Korson et al., 1969).

$$K = K_c \left(1 + \frac{P_o}{K_o}\right) \quad (9)$$

220 where P_o is the partial pressure of O₂; K_c and K_o are the Michaelis–Menten constants for CO₂ and O₂ (Keenan et al., 2016):

$$K_c = 39.97 \times e^{\frac{79.43 \times (T_a - 298.15)}{298.15 \times R \times T_a}} \quad (10)$$

$$K_o = 27480 \times e^{\frac{36.38 \times (T_a - 298.15)}{298.15 \times R \times T_a}} \quad (11)$$

where T_a is air temperature (unit: K); R is the molar gas constant ($8.314 \text{ J mol}^{-1} \text{ K}^{-1}$).

T_s and W_s can be expressed as follows:

$$225 \quad T_s = \frac{(T_a - T_{\min}) \times (T_a - T_{\max})}{(T_a - T_{\min}) \times (T_a - T_{\max}) - (T_a - T_{\text{opt}}) \times (T_a - T_{\text{opt}})} \quad (12)$$

$$W_s = \frac{VPD_0}{VPD_0 + VPD} \quad (13)$$

where T_{\min} , T_{opt} , and T_{\max} are the minimum, optimum, and maximum temperatures for vegetation photosynthesis, respectively (Yuan et al., 2007); VPD_0 is the half-saturation coefficient of the VPD constraint equation (k Pa).

$APAR_{su}$ and $APAR_{sh}$ can be expressed as follows (Chen et al., 1999):

$$230 \quad APAR_{su} = (PAR_{\text{dir}} \times \frac{\cos(\beta)}{\cos(\theta)} + \frac{PAR_{\text{dif}} - PAR_{\text{dif,u}}}{LAI} + C) \times LAI_{su} \quad (14)$$

$$APAR_{sh} = (\frac{PAR_{\text{dif}} - PAR_{\text{dif,u}}}{LAI} + C) \times LAI_{sh} \quad (15)$$

$$PAR_{\text{dif,u}} = PAR_{\text{dif}} \times \exp(\frac{-0.5 \times \Omega \times LAI}{\cos(\bar{\theta})}) \quad (16)$$

where PAR_{dir} is the direct PAR; PAR_{dif} is the diffuse PAR; $PAR_{\text{dif,u}}$ is the diffuse PAR under the canopy; C represents the multiple scattering effects of direct radiation; Ω is the clumping index, which is set according to vegetation types (Tang et al., 2007); θ is the solar zenith angle; β is the mean leaf-sun angle, which is set to 60° ; $\bar{\theta}$ is the representative zenith angle for diffuse radiation transmission and can be expressed by LAI (Chen et al., 1999):

$$235 \quad \cos(\bar{\theta}) = 0.537 + 0.025 \times LAI \quad (17)$$

The LAIs of shaded leaves (LAI_{sh}) and sunlit leaves (LAI_{su}) in Eqs. (14) and (15) are computed following Chen et al (1999):

$$LAI_{su} = 2 \times \cos(\theta) \times \left(1 - e^{-0.5 \times \Omega \times \frac{LAI}{\cos(\bar{\theta})}}\right) \quad (18)$$

$$240 \quad LAI_{sh} = LAI - LAI_{su} \quad (19)$$

2.4 Model calibration and validation

Cross-validation method was used to calibrate and validate the revised EC-LUE model. Fifty percent of the sites were randomly selected to calibrate model parameters for each vegetation type, and the remaining 50% of the sites were used to validate the model. This parameterization process was repeated until all possible combinations of 50% sites were achieved for each vegetation type. The nonlinear regression procedure (Proc NLIN) in the Statistical Analysis System (SAS, SAS Institute Inc., Cary, NC, USA) was applied to optimize the model parameters (ϵ_{msu} , ϵ_{msh} , ϕ , and VPD_0) using 8-day estimated GPP based on EC measurements. The mean GPP simulations of 8-day from all validation runs only were used to model validation. Mean calibrated parameter values from all model runs were used to simulate GPP over the global scale (Table 3).

245 Three metrics, the coefficient of determination (R^2), RMSE, and bias (the difference between observations and simulations) were adopted to evaluate the performance of the revised EC-LUE model. Additionally, Kendall's coefficient of rank correlation

250

τ (Kanji, 1999) was used to quantify the agreement of seasonal changes between the simulated and tower estimated GPP. The Kendall coefficient measured the tendency coherence between predicted and observed GPP by comparing the ranks assigned to successive pairs. If $GPP_{sim,j} - GPP_{sim,i}$ and $GPP_{obs,j} - GPP_{obs,i}$ have the same sign (positive or negative), the pair would be concordant, or discordant. A time-series data with n observations, the Kendall's coefficient of rank correlation τ can be expressed:

$$\tau = \frac{C-D}{n(n-1)/2} \quad (20)$$

where $n(n-1)/2$ is the total combination of pairs, C is the number of concordant pairs, and D is the number of discordant pairs. The Kendall's coefficient ranged from -1 ($C = 0$) to 1 ($D = 0$). The Kendall's coefficient is much closer to 1, which means a stronger positive relationship between the seasonal patterns of the simulated and tower estimated GPP.

Using the averaged value of the optimized parameters (Table 3), a global GPP dataset at $0.05^\circ \times 0.05^\circ$ spatial resolution and 8-day temporal resolution over 1982-2017 was produced.

<<Table 3>>

2.5 Environmental contributions to long-term changes in GPP

To evaluate the contribution of the major environmental variables to GPP, including the atmospheric CO_2 concentration ($[CO_2]$), climate, and satellite-based LAI, two types of experimental simulations ~~where~~ were performed. The first simulation experiment (S_{ALL}) was a normal model run, with all the environmental drivers changing over time. In the second type of simulation experiments (S_{CLI0} , S_{LAI0} , and S_{CO20}), two driving factors could be varied with time while maintaining the third constant at an initial baseline level. For example, the S_{CLI0} simulation experiment allowed the LAI and atmospheric $[CO_2]$ to vary with time while the climate variables were kept constant at 1982 values. The S_{LAI0} ~~and~~ (S_{CO20}) simulation experiments kept LAI ~~and~~ (atmospheric $[CO_2]$) constant at 1982 values and varied the other two variables.

Considering the differences between the simulation results of the first type (S_{ALL}) and the second type (S_{CO20} and S_{LAI0}) of experiments, the GPP sensitivities to atmospheric $[CO_2]$ (β_{CO2}) and LAI (β_{LAI}) were estimated as follows:

$$\Delta GPP_{(S_{ALL}-S_{CO20})i} = \beta_{CO2} \times \Delta CO2_{(S_{ALL}-S_{CO20})i} + \varepsilon \quad (2021)$$

$$\Delta GPP_{(S_{ALL}-S_{LAI0})i} = \beta_{LAI} \times \Delta LAI_{(S_{ALL}-S_{LAI0})i} + \varepsilon \quad (2122)$$

where ΔGPP_i , $\Delta CO2_i$, and ΔLAI_i denote the differences in the GPP simulations, atmospheric $[CO_2]$, and LAI between the two model experiments from 1982 to 2017, and ε is the stochastic error term.

The GPP sensitivities to the three climate variables: air temperature (β_{Ta}), VPD (β_{VPD}), and PAR (β_{PAR}) were calculated using a multiple regression approach:

$$\Delta GPP_{(S_{ALL}-S_{CLI0})i} = \beta_{Ta} \times \Delta Ta_{(S_{ALL}-S_{CLI0})i} + \beta_{VPD} \times \Delta VPD_{(S_{ALL}-S_{CLI0})i} + \beta_{PAR} \times \Delta PAR_{(S_{ALL}-S_{CLI0})i} + \varepsilon \quad (2223)$$

where ΔTa_i , ΔVPD_i , and ΔPAR_i denote the differences in Ta , VPD, and PAR time series between the two model experiments (S_{ALL} and S_{CLI0}), respectively. The regression coefficient β was estimated using the maximum likelihood analysis.

2.5 Statistical analysis

Coefficient of determination (R^2), RMSE, and bias (the difference between observations and simulations) were adopted to evaluate the performance of the revised EC-LUE model.

285 3 Results

3.1 Parameter optimization and model validation

290 ~~This study used EC measurements at 42 sites to calibrate the parameter values and 43 sites to validate the model accuracy of the revised EC-LUE model. The parameters (ϵ_{ms05} , ϵ_{ms15} , ϕ , and VPD_0) of each vegetation type are shown in Table 3. We evaluated the model performance by using the tower-derived meteorology data and global reanalysis meteorology, respectively.~~

In general, the revised EC-LUE model could effectively ~~reproducing~~ reproduce the spatial, seasonal, and annual variations in the tower-estimated GPP at most ~~of the calibration and validation~~ sites (Figs. 1–4).

<<Table 3>>

295 ~~By using the tower-derived meteorology data, the~~ The revised EC-LUE model explained ~~76~~71% and 64% of the spatial variations in GPP across all the ~~calibration and validation sites with no obvious systematic errors (Fig. 1(a)). Furthermore, the model respectively explained 83% and 67% of the spatial variations in GPP at the calibration and validation sites. In contrast, the model performance decreased when using~~ EC sites by using the tower-derived meteorology data and the meteorological reanalysis dataset, ~~explaining only 52% of the spatial variations in the GPP and slightly overestimating the GPP at the sites with low/moderate GPP values (Fig. 1(b)).~~ respectively (Fig. 1).

300 <<Figure 1>>

Similarly, the revised EC-LUE model also shows a good performance in reproducing the seasonal variations in the GPP at most EC sites (~~Figs~~Fig. 2–3). ~~By~~ In Fig. 2, we compared the modeled GPP and tower GPP at 8-day step for each site to examine the capacity of our model in reproducing the seasonal variations. The averaged R^2 were 0.81 and 0.76 by using the tower-derived meteorology data, ~~the averaged R^2 over the calibration and validation sites was 0.78 and 0.72 and the meteorological reanalysis dataset, respectively. Over 92~~Using the tower-derived meteorology data, over 95% of the ~~calibration and validation~~ sites showed high R^2 (>0.5). The ~~two~~low R^2 (<0.4) sites (i.e., MY-PSO, BR-Sa1 and BR-Sa3) were tropical forests without pronounced seasonal ~~pattern~~patterns of GPP (Fig. 2(a); Fig. 3(a)-2a). The RMSE and the absolute value of bias varied from 0.6869 (CN-Du2) to 5.7263 (US-Ne1Ne2) $\text{g C m}^{-2} \text{d}^{-1}$ and from 0.002004 (CA-NS1) to 2.12 (US-ARM40 (CA-TP2)) $\text{g C m}^{-2} \text{d}^{-1}$, respectively. The averaged RMSE and the absolute value of bias over all the sites were 2.6413 and 310 0.6781 $\text{g C m}^{-2} \text{d}^{-1}$, respectively (Fig. 2(b)–(2b-c); Fig. 3(b)–(c)). The averaged Kendall's correlation coefficient (τ) was 0.63, indicating that the model simulated GPP had a strong seasonal coherence with tower estimated GPP. Similar to R^2 , the lower Kendall's correlation coefficient (τ) value sites were also located in the tropical forest areas. Additionally, there ~~is~~was

no obvious difference between the seasonal GPP performance ~~when~~by using the tower-derived meteorology data and ~~the~~ meteorological reanalysis dataset (~~Figs~~Fig. 2–3).

315 <<Figure 2/~~Figure 3~~>>

The ability of the LUE models to reproduce the interannual variations in GPP was investigated at ~~54~~55 EC towers with observations greater than 5-years (Table 1; Fig. 4~~3~~). We examined the relations between the mean annual GPP simulations and observations at each site and used the coefficient correlation (R^2) and slope of the regression relationship to investigate the model capability in simulating the interannual variations in GPP. The result showed that the revised EC-LUE model could effectively determine the interannual variations in GPP (Fig. 4~~3~~). Approximately ~~74~~42% and 40% of the sites showed higher R^2 values (>0.5) ~~for both~~by using the tower-derived meteorology data and ~~the meteorological reanalysis meteorology derived models~~dataset (Fig. 4(a)~~)).~~3a). ~~The mean values of averaged R^2 between~~for the revised EC-LUE model ~~simulated GPP and was~~ 0.44 by using the tower-~~estimated GPP were 0.65 and 0.61 for the models derived from tower-derived meteorology and reanalysis meteorology, and both the R^2 values are~~data, which was significantly higher than the original EC-LUE model ($R^2 = 0.36$) and other LUE models (~~((<~~ R^2 ranged from 0.06 to 0.30 with an average value of 0.16) (Fig. 4(e)~~)).~~3c). ~~The averaged R^2 for the revised EC-LUE model was 0.42 by using the meteorological reanalysis dataset.~~ The averaged slopes of the revised EC-LUE model were 0.71~~60~~ and 0.64~~for~~57 by using the tower-derived meteorology data and ~~the meteorological reanalysis meteorology derived models, while the slope of the original EC LUE model was 0.56~~dataset (Fig. 4(e)~~)).~~3c).

325 <<Figure 3>>

330 <<Figure 4>>

3.2 Spatio-temporal patterns of global GPP

A global GPP dataset at 0.05 °latitude by 0.05 °longitude ~~and 8-day interval~~ was generated ranging from 1982 to 2017 based on the revised EC-LUE model. The long-term averaged value of the global summed GPP was ~~125.3 ± 3.13~~106.2 ± 2.9 Pg C yr⁻¹ across the vegetated area. Fig. 5~~4~~ shows the global ~~distributed patterns~~distribution pattern of the annual averaged GPP for each pixel. The GPP was high over the tropical forest areas, such as Amazon and Southeast Asia, where the moisture and temperature conditions are sufficient for photosynthesis (Fig. 5(a)~~)).~~4a). The GPP decreased with the decreasing gradients of temperature and precipitation (Fig. 5(b)~~)).~~4b). The ~~moderate GPP was located in~~ temperate and subhumid regions ~~have moderate GPP~~; and the lowest GPP ~~is~~was located in arid or cold regions, where either precipitation or temperature is limited (Fig. 5(b)~~)).~~4b).

335 <<Figure 4>>

340 <<Figure 5>>

GPP trends over the period of 1982–2017 were determined for each pixel using a linear regression analysis (Fig. 6~~5~~). In general, the revised EC-LUE model predicted an increased trend in the annual mean GPP from 1982 to 2017. Approximately 69.5% of the vegetated areas, mainly located in temperate and humid regions, showed increased trends. The spatial ~~distributed patterns~~pattern of ~~the~~ GPP trend along with the temperature and precipitation gradients was more heterogeneous than that of

345

the mean annual GPP (Fig. 5(b);4b; Fig. 6(b));5b). The decreased GPP ~~areas were mainly distributed~~was found in the tropic regions ~~with abundant precipitation and high temperature, particularly, especially~~ in the Amazon forest. The extremely cold or arid areas exhibited less variations in GPP (Fig. 6(b));5b).

<<Figure 5>>

350 <<Figure 6>>

3.3 Contributions of environmental variables to GPP

To quantify the contributions of the environmental variables to the long-term changes in GPP, we explored the sensitivity of global summed GPP to climate variables (i.e., VPD, Ta, and PAR), LAI, and atmospheric CO₂ (Fig. 7(6)). The global summed GPP generated from different experimental simulations (section 2.45) exhibited differently in terms of the annual mean value, trend, and standard deviation (Fig. 7(a));6a). The normal simulated GPP (S_{ALL} GPP, all the environmental drivers changing over time) significantly increased at the rate of 0.4715 Pg C yr⁻¹, while the increasing rate of S_{CLI0} GPP (climate variables were kept constant at 1982 values) was even greater (0.3641 Pg C yr⁻¹). On the contrary, the S_{LAI0} GPP (LAI was kept constant at 1982 values) ~~showed a significantly decreasing trend (-0.06 Pg C yr⁻¹)~~, and the S_{CO20} GPP (atmospheric [CO₂] was kept constant at 1982 values) showed ~~an~~insignificantly ~~increasing~~decreasing trend at the rate of -0.04 Pg C yr⁻¹ and -0.07 Pg C
360 yr⁻¹ (Fig. 7(a));6a). The GPP sensitivity analysis showed that the global GPP decreased by approximately -6.67 ± 5.04 Pg C with a 0.1 kPa increase in VPD. ~~This is, which was~~ comparable to the increase in GPP with ~~a 100 ppm rise in atmospheric [CO₂] (i.e., β_{CO2} = 7.62 ± 0.04 Pg C 100 ppm⁻¹) or 0.1 unit greening of LAI (i.e., β_{LAI} = 5.984.78 ± 0.0972 Pg C 0.1 unit⁻¹) or 100 MJ increase in PAR (i.e., β_{PAR} = 5.76 ± 0.2373 ± 3.22 Pg C 100 MJ⁻¹)~~ (Fig. 7(b));6b). The global GPP increased by 12.31 ± 0.61 Pg C with a 100 ppm⁻¹ rise of atmospheric [CO₂] (i.e., β_{CO2} = 12.31 ± 0.61 Pg C 100 ppm⁻¹). Over the period of 1982–
365 2017, the increased VPD resulted in the global GPP decreases of -0.1617 ± 0.0206 Pg C yr⁻¹, which ~~offset~~could partly counteract the fertilization effect of CO₂ (0.1422 ± 0.00107 Pg C yr⁻¹). The global GPP showed a decreased trend after 2001 due to the joint effect of increased VPD and decreased PAR (Fig. 7(e));6c). While the increased trend of GPP before 2000 was ~~mainly~~affected by the increased PAR and rising atmospheric [CO₂], greening of LAI, and increased PAR (Fig. 7(e));6c).

<<Figure 6>>

370 <<Figure 7>>

4 Discussion

4.1 Model accuracy analysis

Numerous studies have shown that most GPP models can reproduce the spatial changes in GPP but failed to reproduce the temporal variations (Keenan et al., 2012; Yuan et al., 2014). Therefore, the capacity to reproduce realistic interannual variations
375 for a GPP model is significantly important. In our study, the revised EC-LUE model performed a higher accuracy in reproducing the interannual variations in GPP than did the original EC-LUE model and other LUE models. Yuan et al. (2014)

reported that the averaged slope of the regression relation between the mean annual GPP simulated by seven LUE models and the mean annual GPP estimated from EC tower ~~data~~ ranged from 0.19 to 0.56 (Fig. ~~4(e)~~; ~~3c~~). While the revised EC-LUE model showed a higher slope of regression relation (0.~~71~~60), which is much closer to 1 than that obtained from other LUE models (Fig. ~~4(e)~~; ~~3c~~). The VPM GPP showed less interannual ~~variation~~variations across most biomes ($R^2 < 0.5$), probably because of the insensitivity of the environmental stress factors at the interannual scale (Zhang et al., 2017). In contrast, ~~74~~42% of the sites showed higher R^2 values (> 0.5) for the revised EC-LUE model. The improvements of the revised EC-LUE model in reproducing interannual variations are owing to the integration of several important environmental drivers for vegetation production (i.e., atmospheric CO_2 concentration, radiation components, and VPD), which exhibited large variations and contributed significantly to vegetation production at interannual scale.

By integrating the atmospheric CO_2 concentration, the revised EC-LUE model suggested a CO_2 sensitivity (β_{CO_2}) of ~~7.62~~12.31 $\pm 0.0461 Pg C per 100 ppm (Fig. ~~7(b)~~; ~~6b~~), which indicates an increase of 11.6~~4~~% in GPP with a rise of 100 ppm in atmospheric $[\text{CO}_2]$. Our estimate is comparable to the observed response of NPP to the increased CO_2 in the FACE experiments (13% per 100 ppm) and estimates of other ecosystem models (5–20% per 100 ppm) (Piao et al., 2013). The elevated atmospheric CO_2 concentration substantially contributes to ~~the~~ vegetation productivity.$

The evaporation fraction (EF), namely the ratio of evapotranspiration (ET) to net radiation (R_n), was used to indicate the water stress on vegetation growth in the original EC-LUE model (Yuan et al., 2007; 2010). While the atmospheric VPD was used to indicate water stress to avoid the aggregated errors from ET simulations in the revised EC-LUE model. Physiologically, vegetation production is sensitive to both atmospheric VPD and soil moisture availability to roots. Recent studies highlighted that the increase in VPD had a larger limitation to the surface conductance and evapotranspiration than soil moisture over short time scales in many biomes (Novick et al., 2016; Sulman et al., 2016). Other studies have also suggested substantial impacts of VPD on vegetation growth (de Cárcer et al., 2018; Ding et al., 2018), forest mortality (Williams et al., 2013), and crop yields (Lobell et al., 2014). It is increasingly important to integrate the atmospheric water constraint to the carbon and water flux ~~modelling~~modeling.

4.2 Comparison of global GPP ~~product~~products

Global and regional GPP estimates remain highly uncertain despite the substantial advances in remote sensing technology, ground observations, and theory of carbon flux modeling (Zheng et al., 2018; Ryu et al., 2019). At regional scale, we compared the annual mean GPP between the revised EC-LUE model and other models across the bioclimatic zones in the Köppen-Geiger climate classification map (Beck et al., 2018) (Fig. 7). The GPP of the revised EC-LUE model was comparable to the mean value of other models for each bioclimatic zone (Fig. 7a). The GPP of different models exhibited large discrepancies in tropical regions (Af/Am/Aw) (Fig. 7a). The correlations (R^2) of GPP across all the bioclimatic zones between the revised EC-LUE model and other models ranged from 0.73 (LPX-Bern) to 0.95 (FLUXCOM MARS, FLUXCOM RF) (Fig. 7b).

<<Figure 7>>

410 ~~2019). Our~~ At global scale, our study showed large differences in the magnitude of global GPP estimated by various models varying from 92.7 to 168.7 Pg C yr⁻¹ (Figs. 8–9). The LUE models simulated the global GPP ranging from 92.7 to 133.7 Pg C yr⁻¹ (Fig. ~~9(a1))~~9a1). Several machine learning approaches estimated the global GPP ranging from ~~108.9~~111.0 to 144.2 Pg C yr⁻¹ (Fig. ~~9(a2))~~9a2). A comparison of ten global terrestrial ecosystem models of TRENDY showed that the global GPP ranged from ~~118.6~~107.8 to ~~168.7~~154.9 Pg C yr⁻¹ (Fig. ~~9(a3))~~9a3). The revised EC-LUE model quantified the mean global GPP from 1982 to 2017 as ~~125.3 ± 3.1~~106.2 ± 2.9 Pg C yr⁻¹. Other studies also support ~~our~~the conclusion that there are large uncertainties in the GPP estimates. By comparing diverse GPP models and products, Anav et al. (2015) reported that the global GPP ranged from 112 to 169 Pg C yr⁻¹. Seven satellite-based LUE models estimated the global GPP ranged from 95.1 to 139.7 Pg C yr⁻¹ over the period of 2000–2010 (Cai et al., 2014).

<<Figure 8>>

420 The interannual variability and trend in GPP also vary substantially with different models. This study showed that the interannual variability (standard deviation) ranged from 0.~~3332~~ to ~~6.795.89~~ Pg C yr⁻¹, with the trends varying from ~~-0.0705~~ to 0.84 Pg C yr⁻² (Fig. 9). The biophysical models showed large interannual variability, with the standard deviation ranging from 1.38 to ~~6.795.89~~ Pg C yr⁻¹. The LUE models estimated the interannual variability ~~varying~~varied from 1.30 to 3.13 Pg C yr⁻¹. In contrast, the machine learning models exhibited less interannual variability with standard deviation under 1.0 Pg C yr⁻¹. The interannual variability of the revised EC-LUE model was ~~3.1~~2.9 Pg C yr⁻¹ (Figs. ~~9(b1)–(9b1–b3))~~). In general, the GPP interannual variability before the year 2000 year was greater than that after the year 2001 for most of the biophysical models and LUE models (Figs. ~~9(b1)–(9b1–b3))~~). Most GPP models showed an increased trend or insignificant trend during all valid years and before 2000. Similar to the standard deviation, the trends of machine learning models were less than other models. Compared with the other models, CLASS and the revised EC-LUE model showed a significant decreasing trend after 2001 (Figs. ~~9(e1)–(9c1–c3))~~), probably because of the joint effect of increased VPD and decreased PAR (Fig. ~~7(e))~~6c).

430 <<Figure 9>>

4.3 Model uncertainty

435 The revised EC-LUE model showed the lowest accuracy for the evergreen broadleaf forests in the tropic areas (~~Figs~~Fig. 2–3). Similarly, other satellite-based models exhibited a large uncertainty in the GPP simulations over tropical forest areas (Ryu et al., 2011; Yuan et al., 2014). MODIS GPP product (MOD17) underestimated the GPP at high productivity sites over the tropical evergreen forests (de Almeida et al., 2018). Regarding the quality of satellite data, a high cloud cover exists over tropical regions, introducing large uncertainties to FAPAR/LAI and other vegetation indices (e.g., NDVI and EVI). For example, less reliable MOD15 FAPAR data duringfrom January to April because of the cloudiness contamination, which could substantially affect the seasonality of GPP estimates (de Almeida et al., 2018). ~~In addition~~Furthermore, the quality of satellite data even affects the evaluation of the interannual variations. Saleska et al. (2007) reported that a large scale green-up in the Amazon evergreen forests during the drought in 2005 using MODIS EVI data. However, an opposite conclusion was arrived when cloud-contaminated data were excluded from the analysis, showing no obvious green-up in the Amazon evergreen forests

during the drought in 2005 (Samanta et al., 2010). Additionally, several subsequent studies found increased LAI and EVI during the dry season in the Amazon evergreen forests; however, a recent study highlighted that the apparent seasonal changes in EVI result from the variations in the sun-sensor geometry rather than vegetation greenness (Morton et al., 2014).

445 The latest study highlighted that the aggregate canopy phenology rather than the climate changes is the main ~~causes~~cause of the seasonal changes in photosynthesis in evergreen broadleaf forests (Wu et al., 2016). In ~~particularly~~particular, the new leaf growing synchronously with dry season litterfall may shift the old canopy to be younger, which can explain the significant seasonal increase (~27%) in the ecosystem photosynthesis. Therefore, the vertical changes in leaf age and photosynthesis ability with canopy depth are important to simulate the seasonal variations in carbon flux in tropical forests (Wu et al., 2017).

450 These leaf trait related parameters can be simulated from the narrow-band spectra of leaves (Serbin et al., 2012; Dechant et al., 2017). Nevertheless, because of the limitation in obtaining the large scale hyperspectral remote sensing data, regional or global estimation of these parameters are currently unavailable.

The revised EC-LUE model does not integrate the regulation of soil nitrogen content on vegetation production. Atmospheric nitrogen deposition has exhibited a large increasing trend in the past few decades because of the excessive fossil fuel
455 combustion in the industrial and transportation sectors and the abuse of nitrogenous fertilizer in the agricultural practice (Galloway et al., 2004). And the global land atmospheric nitrogen deposition is expected to further increase dramatically from 25–40 Tg N yr⁻¹ in the 2000s to 60–100 Tg N yr⁻¹ in 2100 (Lamarque et al., 2005). A meta-analysis of worldwide nitrogen addition experiments found that nitrogen addition could have a significantly positive effect on vegetation productivity (Liu and Greaver, 2009). As most terrestrial ecosystems are nitrogen limited, quantifying the spatio-temporal distributions of
460 vegetation nitrogen content at large scales is essential to improve the accuracy of carbon flux estimation. Several studies quantified the leaf nitrogen content by detecting the nitrogen absorption spectra from the narrow-band of hyperspectral data (Cho, 2007). However, leaf water, starch, lignin, and cellulose overlap with the absorption characters of nitrogen in the shortwave infrared bands, making it difficult to retrieve the nitrogen content (Kokaly and Clark, 1999). ~~Additionally~~What's
more, canopy structures, background, and ~~the~~ illumination/viewing geometry, can further decrease the capacity to detect leaf
465 nitrogen (Yoder and Pettigrew-Crosby, 1995; Knyazikhin et al., 2013). Advances in inversion and statistical models of leaf or canopy nitrogen have emerged (Asner et al., 2011; Dechant et al., 2017; Wang et al., 2018), but these methods require further evaluation over large regions and the global map of leaf or canopy nitrogen is not available yet.

Additionally, the uncertainty of the revised EC-LUE model may arise by scale mismatches between eddy covariance flux footprint and input dataset. The eddy covariance flux footprint is generally less than 3 km² and varies depending on the wind speed, wind direction and atmospheric stability (Tan et al., 2006). In our studies, the revised EC-LUE model was run at 0.05 degree (~5 km²) spatial resolution. The uncertainty of simulated GPP introduced by the scale effect is inevitable but smaller than that introduced by the model structures, parameters or input datasets (Sjostrom et al., 2013; Zheng et al., 2018).

470

5 Data availability

475 The 0.05 ° × 0.05 ° global GPP dataset for 1982-2017 is available at <https://doi.org/10.6084/m9.figshare.8942336> (Zheng et al., 2019). The dataset is provided in hdf format at 8-day interval. The valid value is ranged from 0 to 3000, and the background ~~filled~~ value is 65535. The scale factor of the data is 0.01. Each hdf file represents an 8-day GPP at daily value (unit: g C m² day⁻¹). To obtain the summation of each 8-day (or 5-day or 6-day) period, please multiply the GPP value by corresponding days (8 for the first 45 values, and 5 or 6 for the last value in a year).

6 Conclusion

480 In this study, we produced a long-term global GPP dataset by integrating several major long-term environmental variables ~~into a light use efficiency model, including~~ atmospheric CO₂ concentration, radiation components, and atmospheric water vapor pressure. These environmental variables showed substantial long-term changes and contributed significantly to vegetation production at interannual scale. The revised EC-LUE performed well in simulating the spatial, seasonal, and interannual variations in ~~global-GPP: across the globe.~~ Particularly, it has a unique superiority in reproducing the interannual variations in GPP ~~at both site level~~ ($R^2 = 0.44$) compared with the original EC-LUE model ($R^2 = 0.36$) and ~~global scales.~~ ~~Therefore, the~~ other LUE models (R^2 ranged from 0.06 to 0.30 with an average value of 0.16). ~~The GPP dataset~~ derived from the revised EC-LUE model provides an alternative and reliable estimates of global GPP at the long-term scale by integrating the important environmental variables.

490 **Author contributions.** W. Yuan and Y. Zheng designed the research, performed the analysis, and wrote the paper; R. Shen, Y. Wang, and X. Li performed the analysis; S. Liu, S. Liang, J. Chen, W. Ju, and L. Zhang edited and revised the manuscript.

Competing interests. The authors declare that they have no conflict of interest.

Acknowledgements

This study was supported by National Key Basic Research Program of China (2016YFA0602701), Changjiang Young Scholars Programme of China (Q2016161), Training Project of Sun Yat-sen University (16lgjc53), Fok Ying Tung Education Foundation (151015), and Beijing Normal University Project (2015KJJCA14). ~~The covariance data used in the study was acquired and shared by the FLUXNET community.~~ The covariance data used in the study was acquired and shared by the FLUXNET community, including these networks: AmeriFlux, AfriFlux, AsiaFlux, CarboAfrica, CarboEuropeIP, CarboItaly, CarboMont, ChinaFlux, Fluxnet-Canada, GreenGrass, ICOS, KoFlux, LBA, NECC, OzFlux-TERN, TCOS-Siberia, and USCCC. The ERA-Interim reanalysis data are provided by ECMWF and processed by LSCE. The FLUXNET eddy covariance data processing and harmonization was carried out by the European Fluxes Database Cluster, AmeriFlux Management Project,

500

[and Fluxdata project of FLUXNET, with the support of CDIAC and ICOS Ecosystem Thematic Center, and the OzFlux, ChinaFlux and AsiaFlux offices.](#)

References

- 505 Ainsworth, E.A., Long, S.P.: What have we learned from 15 years of free-air CO₂ enrichment (FACE)? A meta-analytic review of the responses of photosynthesis, canopy, *New Phytol.*, 165, 351-371, doi:10.1111/j.1469-8137.2004.01224.x, 2005.
- Alton, P.B., North, P.R., Los, S.O.: The impact of diffuse sunlight on canopy light-use efficiency, gross photosynthetic product and net ecosystem exchange in three forest biomes, *Global Change Biol.*, 13, 776-787, doi:10.1111/j.1365-2486.2007.01316.x, 2007.
- Anav, A., Friedlingstein, P., Beer, C., Ciais, P., Harper, A., Jones, C., Murray-Tortarolo, G., Papale, D., Parazoo, N.C., Peylin, 510 P., Piao, S., Sitch, S., Viovy, N., Wiltshire, A., Zhao, M.: Spatiotemporal patterns of terrestrial gross primary production: A review, *Rev. Geophys.*, 53, 785-818, doi:10.1002/2015rg000483, 2015.
- Asner, G.P., Martin, R.E., Knapp, D.E., Tupayachi, R., Anderson, C., Carranza, L., Martinez, P., Houcheime, M., Sinca, F., Weiss, P.: Spectroscopy of canopy chemicals in humid tropical forests, *Remote Sens. Environ.*, 115, 3587-3598, doi:10.1016/j.rse.2011.08.020, 2011.
- 515 [Beck, H.E., Zimmermann, N.E., McVicar, T.R., Vergopolan, N., Berg, A., Wood, E.F.: Present and future Koppen-Geiger climate classification maps at 1-km resolution, *Scientific Data*, doi:10.1038/sdata.2018.214, 2018.](#)
- Cai, W., Yuan, W., Liang, S., Zhang, X., Dong, W., Xia, J., Fu, Y., Chen, Y., Liu, D., Zhang, Q.: Improved estimations of gross primary production using satellite-derived photosynthetically active radiation, *J. Geophys. Res. G: Biogeosci.*, 119, 110-123, doi:10.1002/2013jg002456, 2014.
- 520 Cai, W., Yuan, W., Liang, S., Liu, S., Dong, W., Chen, Y., Liu, D., Zhang, H.: Large Differences in Terrestrial Vegetation Production Derived from Satellite-Based Light Use Efficiency Models, *Remote Sens.*, 6, 8945-8965, doi:10.3390/rs6098945, 2014.
- Canadell, J.G., Le Quere, C., Raupach, M.R., Field, C.B., Buitenhuis, E.T., Ciais, P., Conway, T.J., Gillett, N.P., Houghton, R.A., Marland, G.: Contributions to accelerating atmospheric CO₂ growth from economic activity, carbon intensity, and 525 efficiency of natural sinks, *Proc. Natl. Acad. Sci. U.S.A.*, 104, 18866-18870, doi:10.1073/pnas.0702737104, 2007.
- Chen, J.M., Liu, J., Cihlar, J., Goulden, M.L.: Daily canopy photosynthesis model through temporal and spatial scaling for remote sensing applications, *Ecol. Modell.*, 124, 99-119, doi:10.1016/s0304-3800(99)00156-8, 1999.
- Cho, M.A., Skidmore, A., Corsi, F., van Wieren, S.E., Sobhan, I.: Estimation of green grass/herb biomass from airborne hyperspectral imagery using spectral indices and partial least squares regression, *International Journal of Applied Earth 530 Observation and Geoinformation*, 9, 414-424, doi:10.1016/j.jag.2007.02.001, 2007.
- Collatz, G.J., Ball, J.T., Grivet, C., Berry, J.A.: Physiological and environmental regulation of stomatal conductance, photosynthesis and transpiration: a model that includes a laminar boundary layer, *Agric. For. Meteorol.*, 54, 107-136, 1991.

- de Almeida, C.T., Delgado, R.C., Galvao, L.S., de Oliveira Cruz e Aragao, L.E., Concepcion Ramos, M.: Improvements of the MODIS Gross Primary Productivity model based on a comprehensive uncertainty assessment over the Brazilian Amazonia, ISPRS J. Photogramm. Remote Sens., 145, 268-283, doi:10.1016/j.isprsjprs.2018.07.016, 2018.
- de Cácer, P.S., Vitasse, Y., Peñuelas, J., Jasse, V.E.J., Buttler, A., Signarbieux, C.: Vapor-pressure deficit and extreme climatic variables limit tree growth, Global Change Biol., 24, 1108-1122, doi:10.1111/gcb.13973, 2018.
- Dechant, B., Cuntz, M., Vohland, M., Schulz, E., Doktor, D.: Estimation of photosynthesis traits from leaf reflectance spectra: Correlation to nitrogen content as the dominant mechanism, Remote Sens. Environ., 196, 279-292, doi:10.1016/j.rse.2017.05.019, 2017.
- Ding, J., Yang, T., Zhao, Y., Liu, D., Wang, X., Yao, Y., Peng, S., Wang, T., Piao, S.: Increasingly Important Role of Atmospheric Aridity on Tibetan Alpine Grasslands, Geophys. Res. Lett., 45, 2852-2859, doi:10.1002/2017gl076803, 2018.
- Farquhar, G.D., von Caemmerer, S., Berry, J.A.: A biochemical model of photosynthetic CO₂ assimilation in leaves of C₃ species, Planta, 149, 78-90, doi:10.1007/bf00386231, 1980.
- Fletcher, A.L., Sinclair, T.R., Allen, L.H.: Transpiration responses to vapor pressure deficit in well watered 'slow-wilting' and commercial soybean, Environ. Exp. Bot., 61, 145-151, doi:10.1016/j.envexpbot.2007.05.004, 2007.
- Galloway, J.N., Dentener, F.J., Capone, D.G., Boyer, E.W., Howarth, R.W., Seitzinger, S.P., Asner, G.P., Cleveland, C.C., Green, P.A., Holland, E.A., Karl, D.M., Michaels, A.F., Porter, J.H., Townsend, A.R., Vorosmarty, C.J.: Nitrogen cycles: past, present, and future, Biogeochemistry, 70, 153-226, doi:10.1007/s10533-004-0370-0, 2004.
- Gilgen, H., Wild, M., Ohmura, A.: Means and trends of shortwave irradiance at the surface estimated from Global Energy Balance Archive data, J. Clim., 11, 2042-2061, doi:10.1175/1520-0442-11.8.2042, 1998.
- Gu, L.H., Baldocchi, D., Verma, S.B., Black, T.A., Vesala, T., Falge, E.M., Dowty, P.R.: Advantages of diffuse radiation for terrestrial ecosystem productivity, J. Geophys. Res. D: Atmos., 10710.1029/2001jd001242, 2002.
- Kanniah, K.D., Beringer, J., North, P., Hutley, L.: Control of atmospheric particles on diffuse radiation and terrestrial plant productivity: A review, Progress in Physical Geography-Earth and Environment, 36, 209-237, doi:10.1177/0309133311434244, 2012.
- Ju, W., Chen, J.M., Black, T.A., Barr, A.G., Liu, J., Chen, B.: Modelling multi-year coupled carbon and water fluxes in a boreal aspen forest, Agric. For. Meteorol., 140, 136-151, doi:10.1016/j.agrformet.2006.08.008, 2006.
- [Jung, M., Reichstein, M., Schwalm, C.R., Huntingford, C., Sitch, S., Ahlstrom, A., Arneeth, A., Camps-Valls, G., Ciais, P., Friedlingstein, P., Gans, F., Ichii, K., Ain, A.K.J., Kato, E., Papale, D., Poulter, B., Raduly, B., Rodenbeck, C., Tramontana, G., Viovy, N., Wang, Y.-P., Weber, U., Zaehle, S., Zeng, N.: Compensatory water effects link yearly global land CO₂ sink changes to temperature, Nature, 541, 516-520, doi:10.1038/nature20780, 2017.](#)
- [Kanji, G.K., 1999. 100 Statistical Tests. SAGE Publications, London.](#)
- Keenan, T.F., Baker, I., Barr, A., Ciais, P., Davis, K., Dietze, M., Dragon, D., Gough, C.M., Grant, R., Hollinger, D., Hufkens, K., Poulter, B., McCaughey, H., Raczka, B., Ryu, Y., Schaefer, K., Tian, H., Verbeeck, H., Zhao, M., Richardson, A.D.:

- Terrestrial biosphere model performance for inter-annual variability of land-atmosphere CO₂ exchange, *Global Change Biol.*, 18, 1971-1987, doi:10.1111/j.1365-2486.2012.02678.x, 2012.
- Keenan, T.F., Prentice, I.C., Canadell, J.G., Williams, C.A., Wang, H., Raupach, M., Collatz, G.J.: Recent pause in the growth rate of atmospheric CO₂ due to enhanced terrestrial carbon uptake, *Nat. Commun.*, 7, 1038/ncomms13428, 2016.
- 570 Knyazikhin, Y., Schull, M.A., Stenberg, P., Mottus, M., Rautiainen, M., Yang, Y., Marshak, A., Latorre Carmona, P., Kaufmann, R.K., Lewis, P., Disney, M.I., Vanderbilt, V., Davis, A.B., Baret, F., Jacquemoud, S., Lyapustin, A., Myneni, R.B.: Hyperspectral remote sensing of foliar nitrogen content, *Proc. Natl. Acad. Sci. U.S.A.*, 110, E185-E192, doi:10.1073/pnas.1210196109, 2013.
- Kokaly, R.F., Clark, R.N.: Spectroscopic determination of leaf biochemistry using band-depth analysis of absorption features and stepwise multiple linear regression, *Remote Sens. Environ.*, 67, 267-287, doi:10.1016/s0034-4257(98)00084-4, 1999.
- 575 Konings, A.G., Williams, A.P., Gentine, P.: Sensitivity of grassland productivity to aridity controlled by stomatal and xylem regulation, *Nat. Geosci.*, 10, 284-+, doi:10.1038/ngeo2903, 2017.
- Korson, L., Drost-Hansen, W., Millero, F.J.: Viscosity of water at various temperatures, *J. Phys. Chem.*, 73, 34-39, doi:10.1021/j100721a006, 1969.
- 580 Krupkova, L., Markova, I., Havrankova, K., Pokorny, R., Urban, O., Sigut, L., Pavelka, M., Cienciala, E., Marek, M.V.: Comparison of different approaches of radiation use efficiency of biomass formation estimation in Mountain Norway spruce, *Trees-Structure and Function*, 31, 325-337, doi:10.1007/s00468-016-1486-2, 2017.
- Lamarque, J.F., Kiehl, J.T., Brasseur, G.P., Butler, T., Cameron-Smith, P., Collins, W.D., Collins, W.J., Granier, C., Hauglustaine, D., Hess, P.G., Holland, E.A., Horowitz, L., Lawrence, M.G., McKenna, D., Merilees, P., Prather, M.J., Rasch, P.J., Rotman, D., Shindell, D., Thornton, P.: Assessing future nitrogen deposition and carbon cycle feedback using a multimodel approach: Analysis of nitrogen deposition, *J. Geophys. Res. D: Atmos.*, 110, 10.1029/2005jd005825, 2005.
- 585 Li, X.L., Liang, S.L., Yu, G.R., Yuan, W.P., Cheng, X., Xia, J.Z., Zhao, T.B., Feng, J.M., Ma, Z.G., Ma, M.G., Liu, S.M., Chen, J.Q., Shao, C.L., Li, S.G., Zhang, X.D., Zhang, Z.Q., Chen, S.P., Ohta, T., Varlagin, A., Miyata, A., Takagi, K., Saiqusa, N., Kato, T.: Estimation of gross primary production over the terrestrial ecosystems in China, *Ecol. Modell.*, 261, 80-92, doi:10.1016/j.ecolmodel.2013.03.024, 2013.
- 590 Liu, L., Greaver, T.L.: A review of nitrogen enrichment effects on three biogenic GHGs: the CO₂ sink may be largely offset by stimulated N₂O and CH₄ emission, *Ecol. Lett.*, 12, 1103-1117, doi:10.1111/j.1461-0248.2009.01351.x, 2009.
- Liu, S., Bond-Lamberty, B., Boyesen, L.R., Ford, J.D., Fox, A., Gallo, K., Hatfield, J., Henebry, G.M., Huntington, T.G., Liu, Z., Loveland, T.R., Norby, R.J., Sohl, T., Steiner, A.L., Yuan, W., Zhang, Z., Zhao, S.: Grand Challenges in Understanding the Interplay of Climate and Land Changes, *Earth Interactions*, 21, 1-43, doi:10.1175/ei-d-16-0012.1, 2017.
- Liu, Y., Xiao, J., Ju, W., Zhu, G., Wu, X., Fan, W., Li, D., Zhou, Y.: Satellite-derived LAI products exhibit large discrepancies and can lead to substantial uncertainty in simulated carbon and water fluxes, *Remote Sens. Environ.*, 206, 174-188, doi:10.1016/j.rse.2017.12.024, 2018.

- Lobell, D.B., Roberts, M.J., Schlenker, W., Braun, N., Little, B.B., Rejesus, R.M., Hammer, G.L.: Greater Sensitivity to Drought Accompanies Maize Yield Increase in the US Midwest, *Science*, 344, 516-519, doi:10.1126/science.1251423, 2014.
- 600 Monteith, J.: Solar radiation and productivity in tropical ecosystems, *J. Appl. Ecol.*, 9, 747-766, 1972.
- Morton, D.C., Nagol, J., Carabajal, C.C., Rosette, J., Palace, M., Cook, B.D., Vermote, E.F., Harding, D.J., North, P.R.J.: Amazon forests maintain consistent canopy structure and greenness during the dry season, *Nature*, 506, 221-+, doi:10.1038/nature13006, 2014.
- 605 Norby, R.J., DeLucia, E.H., Gielen, B., Calfapietra, C., Giardina, C.P., King, J.S., Ledford, J., McCarthy, H.R., Moore, D.J.P., Ceulemans, R., De Angelis, P., Finzi, A.C., Karnosky, D.F., Kubiske, M.E., Lukac, M., Pregitzer, K.S., Scarascia-Mugnozza, G.E., Schlesinger, W.H., Oren, R.: Forest response to elevated CO₂ is conserved across a broad range of productivity, *Proc. Natl. Acad. Sci. U.S.A.*, 102, 18052-18056, doi:10.1073/pnas.0509478102, 2005.
- Norby, R.J., Wullschleger, S.D., Gunderson, C.A., Johnson, D.W., Ceulemans, R.: Tree responses to rising CO₂ in field experiments: implications for the future forest, *Plant Cell Environ.*, 22, 683-714, doi:10.1046/j.1365-3040.1999.00391.x, 1999.
- 610 [Novick, K.A., Ficklin, D.L., Stoy, P.C., Williams, C.A., Bohrer, G., Oishi, A.C., Papuga, S.A., Blanken, P.D., Noormets, A., Sulman, B.N., Scott, R.L., Wang, L., Phillips, R.P.: The increasing importance of atmospheric demand for ecosystem water and carbon fluxes, *Nat. Clim. Change*, 6, 1023-1027, doi:10.1038/nclimate3114, 2016.](#)
- Piao, S., Sitch, S., Ciais, P., Friedlingstein, P., Peylin, P., Wang, X., Ahlstrom, A., Anav, A., Canadell, J.G., Cong, N., Huntingford, C., Jung, M., Levis, S., Levy, P.E., Li, J., Lin, X., Lomas, M.R., Lu, M., Luo, Y., Ma, Y., Myneni, R.B., Poulter, B., Sun, Z., Wang, T., Viovy, N., Zaehle, S., Zeng, N.: Evaluation of terrestrial carbon cycle models for their response to climate variability and to CO₂ trends, *Global Change Biol.*, 19, 2117-2132, doi:10.1111/gcb.12187, 2013.
- 615 Pierce, D.W., Westerling, A.L., Oyler, J.: Future humidity trends over the western United States in the CMIP5 global climate models and variable infiltration capacity hydrological modeling system, *Hydrol. Earth Syst. Sci.*, 17, 1833-1850, doi:10.5194/hess-17-1833-2013, 2013.
- 620 Potter, C.S., Randerson, J.T., Field, C.B., Matson, P.A., Vitousek, P.M., Mooney, H.A., Klooster, S.A.: Terrestrial ecosystem production: A process model-based on global satellite and surface data, *Global Biogeochem. Cycles*, 7, 811-841, doi:10.1029/93gb02725, 1993.
- Prentice, I.C., Dong, N., Gleason, S.M., Maire, V., Wright, I.J.: Balancing the costs of carbon gain and water transport: testing a new theoretical framework for plant functional ecology, *Ecol. Lett.*, 17, 82-91, doi:10.1111/ele.12211, 2014.
- 625 Rawson, H.M., Begg, J.E., Woodward, R.G.: The effect of atmospheric humidity on photosynthesis, transpiration and water use efficiency of leaves of several plant species, *Planta*, 134, 5-10, doi:10.1007/bf00390086, 1977.
- Reichstein, M., Falge, E., Baldocchi, D., Papale, D., Aubinet, M., Berbigier, P., Bernhofer, C., Buchmann, N., Gilmanov, T., Granier, A., Grunwald, T., Havrankova, K., Ilvesniemi, H., Janous, D., Knohl, A., Laurila, T., Lohila, A., Loustau, D., 630 Matteucci, G., Meyers, T., Miglietta, F., Ourcival, J.-M., Pumpanen, J., Rambal, S., Rotenberg, E., Sanz, M., Tenhunen, J., Seufert, G., Vaccari, F., Vesala, T., Yakir, D., Valentini, R.: On the separation of net ecosystem exchange into assimilation

- and ecosystem respiration: review and improved algorithm, *Global Change Biol.*, 11, 1424-1439, doi:10.1111/j.1365-2486.2005.001002.x, 2005.
- Rienecker, M.M., Suarez, M.J., Gelaro, R., Todling, R., Bacmeister, J., Liu, E., Bosilovich, M.G., Schubert, S.D., Takacs, L.,
635 Kim, G.-K., Bloom, S., Chen, J., Collins, D., Conaty, A., Da Silva, A., Gu, W., Joiner, J., Koster, R.D., Lucchesi, R., Molod, A., Owens, T., Pawson, S., Pegion, P., Redder, C.R., Reichle, R., Robertson, F.R., Ruddick, A.G., Sienkiewicz, M., Woollen, J.: MERRA: NASA's modern-era retrospective analysis for research and applications, *J. Clim.*, 24, 3624-3648, doi:10.1175/jcli-d-11-00015.1, 2011.
- Running, S.W., Nemani, R.R., Heinsch, F.A., Zhao, M.S., Reeves, M., Hashimoto, H.: A continuous satellite-derived measure
640 of global terrestrial primary production, *Bioscience*, 54, 547-560, doi:10.1641/0006-3568(2004)054[0547:acsmog]2.0.co;2, 2004.
- Ryu, Y., Baldocchi, D.D., Kobayashi, H., van Ingen, C., Li, J., Black, T.A., Beringer, J., van Gorsel, E., Knohl, A., Law, B.E., Rouspard, O.: Integration of MODIS land and atmosphere products with a coupled-process model to estimate gross primary productivity and evapotranspiration from 1 km to global scales, *Global Biogeochem. Cycles*, 2510.1029/2011gb004053, 2011.
- 645 Ryu, Y., Berry, J.A., Baldocchi, D.D.: What is global photosynthesis? History, uncertainties and opportunities, *Remote Sens. Environ.*, 223, 95-114, doi:10.1016/j.rse.2019.01.016, 2019.
- Saleska, S.R., Didan, K., Huete, A.R., da Rocha, H.R.: Amazon forests green-up during 2005 drought, *Science*, 318, 612-612, doi:10.1126/science.1146663, 2007.
- Samanta, A., Ganguly, S., Hashimoto, H., Devadiga, S., Vermote, E., Knyazikhin, Y., Nemani, R.R., Myneni, R.B.: Amazon
650 forests did not green-up during the 2005 drought, *Geophys. Res. Lett.*, 3710.1029/2009gl042154, 2010.
- Serbin, S.P., Dillaway, D.N., Kruger, E.L., Townsend, P.A.: Leaf optical properties reflect variation in photosynthetic metabolism and its sensitivity to temperature, *J. Exp. Bot.*, 63, 489-502, doi:10.1093/jxb/err294, 2012.
- Simmons, A.J., Willett, K.M., Jones, P.D., Thorne, P.W., Dee, D.P.: Low-frequency variations in surface atmospheric humidity, temperature, and precipitation: Inferences from reanalyses and monthly gridded observational data sets, *J. Geophys. Res. D:*
655 *Atmos.*, 11510.1029/2009jd012442, 2010.
- [Sjostrom, M., Zhao, M., Archibald, S., Arneth, A., Cappelaere, B., Falk, U., de Grandcourt, A., Hanan, N., Kergoat, L., Kutsch, W., Merbold, L., Mougin, E., Nickless, A., Nouvellon, Y., Scholes, R.J., Veenendaal, E.M., Ardo, J.: Evaluation of MODIS gross primary productivity for Africa using eddy covariance data, *Remote Sens. Environ.*, 131, 275-286, doi:10.1016/j.rse.2012.12.023, 2013.](#)
- 660 Smith, W.K., Reed, S.C., Cleveland, C.C., Ballantyne, A.P., Anderegg, W.R.L., Wieder, W.R., Liu, Y.Y., Running, S.W.: Large divergence of satellite and Earth system model estimates of global terrestrial CO₂ fertilization, *Nat. Clim. Change*, 6, 306-310, doi:10.1038/nclimate2879, 2016.
- Stocker, B.D., Zscheischler, J., Keenan, T.F., Prentice, I.C., Seneviratne, S.I., Peñuelas, J.: Drought impacts on terrestrial primary production underestimated by satellite monitoring, *Nat. Geosci.*, 12, 264-270, doi:10.1038/s41561-019-0318-6, 2019.

- 665 Sulman, B.N., Roman, D.T., Yi, K., Wang, L., Phillips, R.P., Novick, K.A.: High atmospheric demand for water can limit forest carbon uptake and transpiration as severely as dry soil, *Geophys. Res. Lett.*, 43, 9686-9695, doi:10.1002/2016gl069416, 2016.
- [Tan, B., Woodcock, C.E., Hu, J., Zhang, P., Ozdogan, M., Huang, D., Yang, W., Knyazikhin, Y., Myneni, R.B.: The impact of gridding artifacts on the local spatial properties of MODIS data: Implications for validation, compositing, and band-to-band registration across resolutions, *Remote Sens. Environ.*, 105, 98-114, doi:10.1016/j.rse.2006.06.008, 2006.](#)
- 670 Tang, S., Chen, J.M., Zhu, Q., Li, X., Chen, M., Sun, R., Zhou, Y., Deng, F., Xie, D.: LAI inversion algorithm based on directional reflectance kernels, *J. Environ. Manage.*, 85, 638-648, doi:10.1016/j.jenvman.2006.08.018, 2007.
- Urban, O., Janous, D., Acosta, M., Czerny, R., Markova, I., Navratil, M., Pavelka, M., Pokorny, R., Sprtova, M., Zhang, R., Spunda, V., Grace, J., Marek, M.V.: Ecophysiological controls over the net ecosystem exchange of mountain spruce stand.
- 675 Comparison of the response in direct vs. diffuse solar radiation, *Global Change Biol.*, 13, 157-168, doi:10.1111/j.1365-2486.2006.01265.x, 2007.
- Van Wijngaarden, W.A., Vincent, L.A.: Trends in relative humidity in Canada from 1953–2003. In 15th Symp. on Global Change and Climate Variations, 2004.
- Vuichard, N., Papale, D.: Filling the gaps in meteorological continuous data measured at FLUXNET sites with ERA-Interim reanalysis, *Earth Syst. Sci. Data*, 7, 157-171, doi:10.5194/essd-7-157-2015, 2015.
- 680 Wang, Z., Skidmore, A.K., Darvishzadeh, R., Wang, T.: Mapping forest canopy nitrogen content by inversion of coupled leaf-canopy radiative transfer models from airborne hyperspectral imagery, *Agric. For. Meteorol.*, 253, 247-260, doi:10.1016/j.agrformet.2018.02.010, 2018.
- Wild, M., Gilgen, H., Roesch, A., Ohmura, A., Long, C.N., Dutton, E.G., Forgan, B., Kallis, A., Russak, V., Tsvetkov, A.: From dimming to brightening: Decadal changes in solar radiation at Earth's surface, *Science*, 308, 847-850, doi:10.1126/science.1103215, 2005.
- 685 Willett, K.M., Dunn, R.J.H., Thorne, P.W., Bell, S., de Podesta, M., Parker, D.E., Jones, P.D., Williams, C.N., Jr.: HadISDH land surface multi-variable humidity and temperature record for climate monitoring, *Climate of the Past*, 10, 1983-2006, doi:10.5194/cp-10-1983-2014, 2014.
- 690 Williams, A.P., Allen, C.D., Macalady, A.K., Griffin, D., Woodhouse, C.A., Meko, D.M., Swetnam, T.W., Rauscher, S.A., Seager, R., Grissino-Mayer, H.D., Dean, J.S., Cook, E.R., Gangodagamage, C., Cai, M., McDowell, N.G.: Temperature as a potent driver of regional forest drought stress and tree mortality, *Nat. Clim. Change*, 3, 292-297, doi:10.1038/nclimate1693, 2013.
- 695 Wu, J., Albert, L.P., Lopes, A.P., Restrepo-Coupe, N., Hayek, M., Wiedemann, K.T., Guan, K., Stark, S.C., Christoffersen, B., Prohaska, N., Tavares, J.V., Marostica, S., Kobayashi, H., Ferreira, M.L., Campos, K.S., da Silva, R., Brando, P.M., Dye, D.G., Huxman, T.E., Huete, A.R., Nelson, B.W., Saleska, S.R.: Leaf development and demography explain photosynthetic seasonality in Amazon evergreen forests, *Science*, 351, 972-976, doi:10.1126/science.aad5068, 2016.

- Wu, J., Guan, K., Hayek, M., Restrepo-Coupe, N., Wiedemann, K.T., Xu, X., Wehr, R., Christoffersen, B.O., Miao, G., da Silva, R., de Araujo, A.C., Oliviera, R.C., Camargo, P.B., Monson, R.K., Huete, A.R., Saleska, S.R.: Partitioning controls on Amazon forest photosynthesis between environmental and biotic factors at hourly to interannual timescales, *Global Change Biol.*, 23, 1240-1257, doi:10.1111/gcb.13509, 2017.
- Xiao, X.M., Zhang, Q.Y., Hollinger, D., Aber, J., Moore, B.: Modeling gross primary production of an evergreen needleleaf forest using [medis](#)[MODIS](#) and climate data, *Ecol. Appl.*, 15, 954-969, doi:10.1890/04-0470, 2005.
- Xiao, Z., Liang, S., Wang, J., Xiang, Y., Zhao, X., Song, J.: Long-Time-Series Global Land Surface Satellite Leaf Area Index Product Derived From MODIS and AVHRR Surface Reflectance, *IEEE Trans. Geosci. Remote Sens.*, 54, 5301-5318, doi:10.1109/tgrs.2016.2560522, 2016.
- Xu, B., Li, J., Park, T., Liu, Q., Zeng, Y., Yin, G., Zhao, J., Fan, W., Yang, L., Knyazikhin, Y., Myneni, R.B.: An integrated method for validating long-term leaf area index products using global networks of site-based measurements, *Remote Sens. Environ.*, 209, 134-151, doi:10.1016/j.rse.2018.02.049, 2018.
- Yoder, B.J., Pettigrew-Crosby, R.E.: Predicting nitrogen and chlorophyll content and concentrations from reflectance spectra (400-2500 nm) at leaf and canopy scales, *Remote Sens. Environ.*, 53, 199-211, doi:10.1016/0034-4257(95)00135-n, 1995.
- Yuan, W., Cai, W., Xia, J., Chen, J., Liu, S., Dong, W., Merbold, L., Law, B., Arain, A., Beringer, J., Bernhofer, C., Black, A., Blanken, P.D., Cescatti, A., Chen, Y., Francois, L., Gianelle, D., Janssens, I.A., Jung, M., Kato, T., Kiely, G., Liu, D., Marcolla, B., Montagnani, L., Raschi, A., Rouspard, O., Varlagin, A., Wohlfahrt, G.: Global comparison of light use efficiency models for simulating terrestrial vegetation gross primary production based on the La Thuile database, *Agric. For. Meteorol.*, 192, 108-120, doi:10.1016/j.agrformet.2014.03.007, 2014.
- Yuan, W., Liu, S., Zhou, G., Zhou, G., Tieszen, L.L., Baldocchi, D., Bernhofer, C., Gholz, H., Goldstein, A.H., Goulden, M.L., Hollinger, D.Y., Hu, Y., Law, B.E., Stoy, P.C., Vesala, T., Wofsy, S.C., AmeriFlux, C.: Deriving a light use efficiency model from eddy covariance flux data for predicting daily gross primary production across biomes, *Agric. For. Meteorol.*, 143, 189-207, doi:10.1016/j.agrformet.2006.12.001, 2007.
- Yuan, W., Luo, Y., Li, X., Liu, S., Yu, G., Zhou, T., Bahn, M., Black, A., Desai, A.R., Cescatti, A., Marcolla, B., Jacobs, C., Chen, J., Aurela, M., Bernhofer, C., Gielen, B., Bohrer, G., Cook, D.R., Dragoni, D., Dunn, A.L., Gianelle, D., Gruenwald, T., Ibrom, A., Leclerc, M.Y., Lindroth, A., Liu, H., Marchesini, L.B., Montagnani, L., Pita, G., Rodeghiero, M., Rodrigues, A., Starr, G., Stoy, P.C.: Redefinition and global estimation of basal ecosystem respiration rate, *Global Biogeochem. Cycles*, 2510.1029/2011gb004150, 2011.
- Yuan, W., Liu, S., Yu, G., Bonnefond, J.-M., Chen, J., Davis, K., Desai, A.R., Goldstein, A.H., Gianelle, D., Rossi, F., Suyker, A.E., Verma, S.B.: Global estimates of evapotranspiration and gross primary production based on MODIS and global meteorology data, *Remote Sens. Environ.*, 114, 1416-1431, doi:10.1016/j.rse.2010.01.022, 2010.
- [Yuan, W., Zheng, Y., Piao, S., Ciais, P., Lombardozi, D., Wang, Y., Ryu, Y., Chen, G., Dong, W., Hu, Z., Jain, A.K., Jiang, C., Kato, E., Li, S., Lienert, S., Liu, S., Nabel, J.E.M.S., Qin, Z., Quine, T., Sitch, S., Smith, W.K., Wang, F., Wu, C., Xiao,](#)

[Z., Yang, S.: Increased atmospheric vapor pressure deficit reduces global vegetation growth. Science Advances, 510.1126/sciadv.aax1396, 2019.](https://doi.org/10.1126/sciadv.aax1396)

Zhang, Y., Xiao, X., Wu, X., Zhou, S., Zhang, G., Qin, Y., Dong, J.: Data Descriptor: A global moderate resolution dataset of gross primary production of vegetation for 2000-2016, Scientific Data, 410.1038/sdata.2017.165, 2017.

735 Zhao, M., Running, S.W.: Drought-Induced Reduction in Global Terrestrial Net Primary Production from 2000 Through 2009, Science, 329, 940-943, doi:10.1126/science.1192666, 2010.

Zheng, Y., Shen, R.; Wang, Y., Li, X., Liu, S., Liang, S., Chen, Jing M., Ju, W., Zhang, L., Yuan, W.: Improved estimate of global gross primary production for reproducing its long-term variation, 1982-2017. figshare. Dataset. ~~doi~~doi:10.6084/m9.figshare.8942336, 2019.

740 Zheng, Y., Zhang, L., Xiao, J., Yuan, W., Yan, M., Li, T., Zhang, Z.: Sources of uncertainty in gross primary productivity simulated by light use efficiency models: Model structure, parameters, input data, and spatial resolution, Agric. For. Meteorol., 263, 242-257, doi:10.1016/j.agrformet.2018.08.003, 2018.

Zhu, Z., Piao, S., Myneni, R.B., Huang, M., Zeng, Z., Canadell, J.G., Ciais, P., Sitch, S., Friedlingstein, P., Arneeth, A., Cao, C., Cheng, L., Kato, E., Koven, C., Li, Y., Lian, X., Liu, Y., Liu, R., Mao, J., Pan, Y., Peng, S., Penuelas, J., Poulter, B., Pugh,

745 T.A.M., Stocker, B.D., Viovy, N., Wang, X., Wang, Y., Xiao, Z., Yang, H., Zaehle, S., Zeng, N.: Greening of the Earth and its drivers, Nat. Clim. Change, 6, 791-796, doi:10.1038/nclimate3004, 2016.

750 Table 1: Information on the eddy covariance (EC) sites used in this study ~~for model calibration and validation.~~

Site Name	Latitude	Longitude	Vegetation Type	Study Period
<i>Model calibration</i> *DE-Kli	<u>50.89°N</u>	<u>13.52°E</u>	<u>CRO</u>	<u>2004-2012</u>
DE-RuS	<u>50.87°N</u>	<u>6.45°E</u>	<u>CRO</u>	<u>2011-2012</u>
FI-Jok	60.90°N	23.51°E	CRO- C3	2000 2001-2003
<i>US-Ne3</i> *FR-Gri	48.84°N <u>41.17°N</u>	1.95°E <u>96.43°W</u>	CRO- C3 / C4	2001-2011 2005-2012
*US-ARM	36.61°N	97.49°W	CRO- C3 / C4	2003-2012
*FR-GriUS-Ne1	48.84°N <u>41.16°N</u>	1.95°E <u>96.47°W</u>	CRO- C4	2004-2011 2001-2012
DE-Kli *US-Ne2	41.16°N <u>50.89°N</u>	96.47°W <u>13.52°E</u>	CRO- C4	2004-2011 2001-2012
US-KS2	28.61°N	80.67°W	SHR	2003-2006
*DK-Sor	55.49°N	11.64°E	DBF	1996-2014
*US-UMBNe3	41.17°N <u>45.56°N</u>	96.43°W <u>84.71°W</u>	DBF CRO	2000-2011 2001-2012
CA-TPD	42.64°N	80.56°W	DBF	2012- 2014
*DE-Hai	51.08°N	10.45°E	DBF	2000- 2011 2012
*DK-Sor	<u>55.49°N</u>	<u>11.64°E</u>	DBF	<u>2001-2012</u>
*FR-Fon	<u>48.48°N</u>	<u>2.78°E</u>	DBF	<u>2005-2012</u>
IT-PT1	<u>45.20°N</u>	<u>9.06°E</u>	DBF	<u>2002-2004</u>
*IT-Ro2	<u>42.39°N</u>	<u>11.92°E</u>	DBF	<u>2002-2008; 2010-2012</u>
JP-MBF	<u>44.39°N</u>	<u>142.32°E</u>	DBF	<u>2004-2005</u>
*US-Ha1	42.54°N	72.17°W	DBF	1991-2011 1992-2012
*US-MMS	39.32°N	86.41°W	DBF	1999- 2011 2012
*US-Oho	41.55°N	83.84°W	DBF	2004- 2011 2012
*US-UMB	<u>45.56°N</u>	<u>84.71°W</u>	DBF	<u>2000-2012</u>
*US-UMd	<u>45.56°N</u>	<u>84.70°W</u>	DBF	<u>2008-2012</u>
*US-WCr	<u>45.81°N</u>	<u>90.08°W</u>	DBF	<u>1999-2006; 2011-2012</u>
*BR-Sa1	<u>2.86°S</u>	<u>54.96°W</u>	EBF	<u>2002-2005; 2008-2011</u>
BR-Sa3	<u>3.02°S</u>	<u>54.97°W</u>	EBF	<u>2001-2003</u>
CN-Din	23.17°N	112.54°E	EBF	2003-2005
*FR-Pue	<u>43.74°N</u>	<u>3.60°E</u>	EBF	<u>2000-2012</u>
*GF-Guy	5.28°N	52.92°W	EBF	2004- 2014 2012

*BR-Sa+MY- PSO	2.86°S97°N	54.96°W102.31°E	EBF	2008-2011	2003-2009
IT-La2	45.95°N	11.29°E	ENF		2001
*CA-QfoNS1	49.69°N55.88°N	74.34°W98.48°W	ENF	2003-2010	2002-2005
*US-NR1	40.03°N	105.55°W	ENF	1999-2011	
*RU-Fyo	56.46°N	32.92°E	ENF	1998-2011	
*CA-NS2	55.91°N	98.52°W	ENF	2001-2005	
*NL-Loo	52.17°N	5.74°E	ENF	1996-2011	
*DE-Obe	50.78°N	13.72°E	ENF	2008-2011	
*FI-Hyy	61.85°N	24.30°E	ENF	1996-2011	
US-Me6	44.32°N	121.61°W	ENF	2010-2011	
CA-SF1	54.49°N	105.82°W	ENF	2003-2006	
*CZ-BK1	49.50°N	18.54°E	ENF	2004-2011	
*CA-SF2NS3	54.25°N55.91°N	105.88°W98.38°W	ENF	2001	2002-2005
CA-NS4	55.91°N	98.38°W	ENF	2003-2005	
CN-HaM	37.37°N	101.18°E	GRA	2002-2004	
US-IB2	41.84°N	88.24°W	GRA	2004-2011	
CN-Du2	42.05°N	116.28°E	GRA	2007-2008	
CN-Cng	44.59°N	123.51°E	GRA	2007-2010	
*CH-Cha	47.21°N	8.41°E	GRA	2006-2008;	2010-2011
*CH-Oe1	47.29°N	7.73°E	GRA	2002-2008	
CN-Cha	42.40°N	128.10°E	MF	2003-2005	
*CA-Gro	48.22°N	82.16°W	MF	2003-2011	
*US-PFa	45.95°N	90.27°W	MF	1996-2011	
CN-Ha2	37.61°N	101.33°E	WET	2003-2005	
RU-Che	68.61°N	161.34°E	WET	2002-2005	
US-WPT	41.46°N	83.00°W	WET	2011-2013	
*US-Ton	38.43°N	120.97°W	SAV	2001-2011	
<i>Model validation</i>					
*US-Ne2	41.16°N	96.47°W	CRO-C3/C4	2001-2011	
*DE-Kli	50.89°N	13.52°E	CRO-C3	2004-2014	
*US-Ne1	41.16°N	96.47°W	CRO-C4	2001-2011	
DE-RuS	50.87°N	6.45°E	CRO-C4	2011-2014	
*US-UMd	45.56°N	84.70°W	DBF	2007-2014	

*US-WC†	45.81°N	90.08°W	DBF	1999-2006
*FR-Fon	48.48°N	2.78°E	DBF	2005-2011
JP-MBF	44.39°N	142.32°E	DBF	2004-2005
IT-PT1	45.20°N	9.06°E	DBF	2002-2004
*IT-Ro2	42.39°N	11.92°E	DBF	2002-2011
*FR-Pue	43.74°N	3.60°E	EBF	2000-2011
MY-PSO	2.97°N	102.31°E	EBF	2003-2009
BR-Sa3	3.02°S	54.97°W	EBF	2000-2003
*IT-Lav	45.96°N	11.28°E	ENF	2003-2011
*IT-Ren	46.59°N	11.43°E	ENF	1999-2004; 2009-2011
*CA-NS5	55.86°N	98.49°W	ENF	2001-2005
*DE-ThaCA-Qfo	<u>50.96°N</u> <u>49.69°N</u>	<u>13.57°E</u> <u>74.34°W</u>	ENF	<u>1997-2011</u> <u>2003-2010</u>
*CA-TP3SF1	<u>42.71°N</u> <u>54.49°N</u>	<u>80.35°W</u> <u>105.82°W</u>	ENF	2003- 2011 <u>2006</u>
*CA-SF2	<u>54.25°N</u>	<u>105.88°W</u>	<u>ENF</u>	<u>2001-2005</u>
*CA-TP1	42.66°N	80.56°W	ENF	2003- 2011 <u>2012</u>
*CA-NS3TP2	<u>55.91°N</u> <u>42.77°N</u>	<u>98.38°W</u> <u>80.46°W</u>	ENF	<u>2001-2005</u> <u>2003-2007</u>
CA-NS1	55.88°N	98.48°W	ENF	2002-2005
DE-Lkb	49.10°N	13.30°E	ENF	2009-2011
*US-Me2	44.45°N	121.56°W	ENF	2002-2011
*IT-SRoCA-TP3	<u>43.73°N</u> <u>42.71°N</u>	<u>10.28°E</u> <u>80.35°W</u>	ENF	1999 <u>2003-2012</u>
CN-Qia	26.74°N	115.06°E	ENF	2003-2005
*CZ-BK1	<u>49.50°N</u>	<u>18.54°E</u>	<u>ENF</u>	<u>2004-2012</u>
DE-Lkb	<u>49.10°N</u>	<u>13.30°E</u>	<u>ENF</u>	<u>2009-2012</u>
*DE-Obe	<u>50.78°N</u>	<u>13.72°E</u>	<u>ENF</u>	<u>2008-2012</u>
*DE-Tha	<u>50.96°N</u>	<u>13.57°E</u>	<u>ENF</u>	<u>1996-2012</u>
*FI-Hyy	<u>61.85°N</u>	<u>24.30°E</u>	<u>ENF</u>	<u>1996-2012</u>
IT-La2	<u>45.95°N</u>	<u>11.29°E</u>	<u>ENF</u>	<u>2001</u>
*CA-TP2IT-Lav	<u>42.77°N</u> <u>45.96°N</u>	<u>80.46°W</u> <u>11.28°E</u>	ENF	2003- 2007 <u>2012</u>
*IT-Ren	<u>46.59°N</u>	<u>11.43°E</u>	<u>ENF</u>	<u>1999-2012</u>
*IT-SRo	<u>43.73°N</u>	<u>10.28°E</u>	<u>ENF</u>	<u>2001-2012</u>
*NL-Loo	<u>52.17°N</u>	<u>5.74°E</u>	<u>ENF</u>	<u>1996-2012</u>
*RU-Fyo	<u>56.46°N</u>	<u>32.92°E</u>	<u>ENF</u>	<u>1998-2012</u>
*US-Blo	38.90°N	120.63°W	ENF	1997-2007
RU-Ha1*US-Me2	<u>54.73°N</u> <u>44.45°N</u>	<u>90.00°E</u> <u>121.56°W</u>	<u>GRA</u> <u>ENF</u>	2002- 2004 <u>2012</u>

<u>US-Me6</u>	<u>44.32°N</u>	<u>121.61°W</u>	<u>ENF</u>	<u>2011-2012</u>
<u>*US-NR1</u>	<u>40.03°N</u>	<u>105.55°W</u>	<u>ENF</u>	<u>1999-2012</u>
<u>*CH-Cha</u>	<u>47.21°N</u>	<u>8.41°E</u>	<u>GRA</u>	<u>2006-2008; 2010-2012</u>
<u>*CH-Fru</u>	<u>47.12°N</u>	<u>8.54°E</u>	<u>GRA</u>	<u>2006-2008; 2010- 20112012</u>
<u>*CH-Oe1</u>	<u>47.29°N</u>	<u>7.73°E</u>	<u>GRA</u>	<u>2002-2008</u>
<u>CN-Cng</u>	<u>44.59°N</u>	<u>123.51°E</u>	<u>GRA</u>	<u>2007-2010</u>
<u>CN-Du2</u>	<u>42.05°N</u>	<u>116.28°E</u>	<u>GRA</u>	<u>2007-2008</u>
<u>CN-HaM</u>	<u>37.37°N</u>	<u>101.18°E</u>	<u>GRA</u>	<u>2002-2003</u>
<u>*CZ-BK2</u>	<u>49.49°N</u>	<u>18.54°E</u>	<u>GRA</u>	<u>2006-2011</u>
<u>*NL-Hor</u>	<u>52.24°N</u>	<u>5.07°E</u>	<u>GRA</u>	<u>2004-2011</u>
<u>RU-Ha1</u>	<u>54.73°N</u>	<u>90.00°E</u>	<u>GRA</u>	<u>2002-2004</u>
<u>US-AR1</u>	<u>36.43°N</u>	<u>99.42°W</u>	<u>GRA</u>	<u>2009-2012</u>
<u>US-AR2</u>	<u>36.64°N</u>	<u>99.60°W</u>	<u>GRA</u>	<u>2009-2012</u>
<u>*US-Goo</u>	<u>34.25°N</u>	<u>89.87°W</u>	<u>GRA</u>	<u>2002-2006</u>
<u>*US-AR2IB2</u>	<u>36.64°N41.84°N</u>	<u>99.60°W88.24°W</u>	<u>GRA</u>	<u>20092005; 2007-2011</u>
<u>*BE-BraUS- AR1</u>	<u>51.31°N</u> <u>36.43°N</u>	<u>99.42°W</u> <u>4.52°E</u>	<u>GRAMF</u>	<u>2009-20111999-2002; 2004-2012</u>
<u>*BE-Vie</u>	<u>50.31°N</u>	<u>6.00°E</u>	<u>MF</u>	<u>1999-20111997-2012</u>
<u>*CA-Gro</u>	<u>48.22°N</u>	<u>82.16°W</u>	<u>MF</u>	<u>2004-2012</u>
<u>CN-Cha</u>	<u>42.40°N</u>	<u>128.10°E</u>	<u>MF</u>	<u>2003-2005</u>
<u>JP-SMF</u>	<u>35.26°N</u>	<u>137.08°E</u>	<u>MF</u>	<u>2003-2006</u>
<u>*US-PFa</u>	<u>45.95°N</u>	<u>90.27°W</u>	<u>MF</u>	<u>1996-2012</u>
<u>*US-Syv</u>	<u>46.24°N</u>	<u>89.35°W</u>	<u>MF</u>	<u>2001-2006; 2012</u>
<u>AU-Ade</u>	<u>13.08°S</u>	<u>131.12°E</u>	<u>SAV</u>	<u>2007-2009</u>
<u>AU-Cpr*BE- Bra</u>	<u>34.00°S</u> <u>51.31°N</u>	<u>4.52°E</u> <u>140.59°E</u>	<u>MFSAV</u>	<u>1999-2011-2012</u>
<u>*AU-DaS</u>	<u>14.16°S</u>	<u>131.39°E</u>	<u>SAV</u>	<u>2008-2012</u>
<u>AU-Dry</u>	<u>15.26°S</u>	<u>132.37°E</u>	<u>SAV</u>	<u>2009-2012</u>
<u>AU-RDF</u>	<u>14.56°S</u>	<u>132.48°E</u>	<u>SAV</u>	<u>2011-2012</u>
<u>SD-Dem</u>	<u>13.28°N</u>	<u>30.48°E</u>	<u>SAV</u>	<u>2007-2009</u>
<u>*US-Ton</u>	<u>38.43°N</u>	<u>120.97°W</u>	<u>SAV</u>	<u>2001-2012</u>
<u>ZA-Kru</u>	<u>25.02°S</u>	<u>31.50°E</u>	<u>SAV</u>	<u>2009-2012</u>
<u>CA-NS6</u>	<u>55.92°N</u>	<u>98.96°W</u>	<u>SRH</u>	<u>2002-2005</u>
<u>CA-NS7</u>	<u>56.64°N</u>	<u>99.95°W</u>	<u>SRH</u>	<u>2003-2005</u>
<u>JP-SMF*CA- SF3</u>	<u>35.26°N54.09°N</u>	<u>137.08°E106.01°W</u>	<u>MFSRH</u>	<u>2002-2006</u>
<u>ES-LgS</u>	<u>37.10°N</u>	<u>2.97°W</u>	<u>SRH</u>	<u>2007-2009</u>
<u>US-KS2</u>	<u>28.61°N</u>	<u>80.67°W</u>	<u>SRH</u>	<u>2003-2006</u>

<u>CN-Ha2</u>	<u>37.61°N</u>	<u>101.33°E</u>	<u>WET</u>	<u>2003-2005</u>
<u>DE-Akm</u>	<u>53.87°N</u>	<u>13.68°E</u>	<u>WET</u>	<u>2010-2012</u>
<u>DE-SfN</u>	<u>47.81°N</u>	<u>11.33°E</u>	<u>WET</u>	<u>2012</u>
<u>DE-Spw</u>	<u>51.89°N</u>	<u>14.03°E</u>	<u>WET</u>	<u>2010-2012</u>
<u>RU-Che</u>	<u>68.61°N</u>	<u>161.34°E</u>	<u>WET</u>	<u>2002-2004</u>
US-Ivo	68.49°N	155.75°W	WET	2004-2007
DE-Akm	53.87°N	13.68°E	WET	2009-2014
DE-Spw	51.89°N	14.03°E	WET	2010-2011
*US-Los	46.08°N	89.98°W	WET	2000-2001-2008 ; 2010
DE-SfN US- WPT	47.81°N <u>41.46°N</u>	11.33°E <u>83.00°W</u>	WET	<u>2011-2012-2014</u>

* indicates the site ~~was~~ used to investigate the interannual variations in GPP with observations greater than 5-years.

Table 2: Input ~~data~~ datasets used to drive the revised EC-LUE model.

Variable	Dataset/provider	Source
Air temperature	MERRA2	https://gmao.gsfc.nasa.gov/reanalysis/MERRA-2/
Dew point temperature	MERRA2	https://gmao.gsfc.nasa.gov/reanalysis/MERRA-2/
Direct PAR	MERRA2	https://gmao.gsfc.nasa.gov/reanalysis/MERRA-2/
Diffuse PAR	MERRA2	https://gmao.gsfc.nasa.gov/reanalysis/MERRA-2/
LAI	GLASS	http://www.glass.umd.edu/Download.html
Landcover map	MCD12Q1	https://lpdaac.usgs.gov/products/mcd12q1v006/
<u>C4 crop percentage</u>	<u>ISLSCP II C4 Vegetation Percentage</u>	<u>https://doi.org/10.3334/ORNLDAAAC/932</u>
CO ₂ concentration	NOAA's Earth System Research Laboratory	www.esrl.noaa.gov/gmd/ccgg/trends/

755

Table 3: Optimized parameters (ϵ_{msu} , ϵ_{msh} , ϕ , and VPD_0) of the revised EC-LUE model for different vegetation types.

Vegetation Types	DBF	ENF	EBF	MF	GRA	CRO-C3	CRO-C4	SAV	SHR	WET
ϵ_{msu} (g C MJ ⁻¹)	<u>1.4628</u> ± 0.36	<u>1.8072</u> ± 0.42	<u>1.7167</u> ± 0.85	<u>1.4638</u> ± 0.21	<u>1.16</u> ± 0.8315	<u>1.1725</u> ± 0.42	<u>2.3546</u> ± 0.78	<u>2.0524</u> ± 0.68	<u>1.21</u> ± 0.8625	<u>1.2334</u> ± 0.26
ϵ_{msh} (g C MJ ⁻¹)	<u>3.3359</u> ± 0.66	<u>3.9587</u> ± 0.58	<u>3.97435</u> ± 0.72	<u>3.4629</u> ± 0.63	<u>1.7591</u> ± 0.46	<u>2.3846</u> ± 0.52	<u>5.5464</u> ± 1.02	<u>34.26</u> ± 0.95	<u>2.4271</u> ± 0.52	<u>2.4562</u> ± 0.49
ϕ (ppm)	32 ± 8.25	25 ± 7.59	20 ± 6.36	49 ± 11.25	57 ± 11.85	43 ± 9.56	54 ± 15.36	54 ± 12.23	34 ± 7.59	36 ± 10.32
VPD_0 (kPa)	<u>1.15</u> ± 0.9325	<u>1.34</u> ± 0.7226	<u>0.4457</u> ± 0.15	<u>0.5862</u> ± 0.14	<u>1.3169</u> ± 0.35	<u>1.02</u> ± 0.8219	<u>1.53</u> ± 0.9431	<u>1.2465</u> ± 0.26	<u>1.2334</u> ± 0.21	<u>0.4262</u> ± 0.12

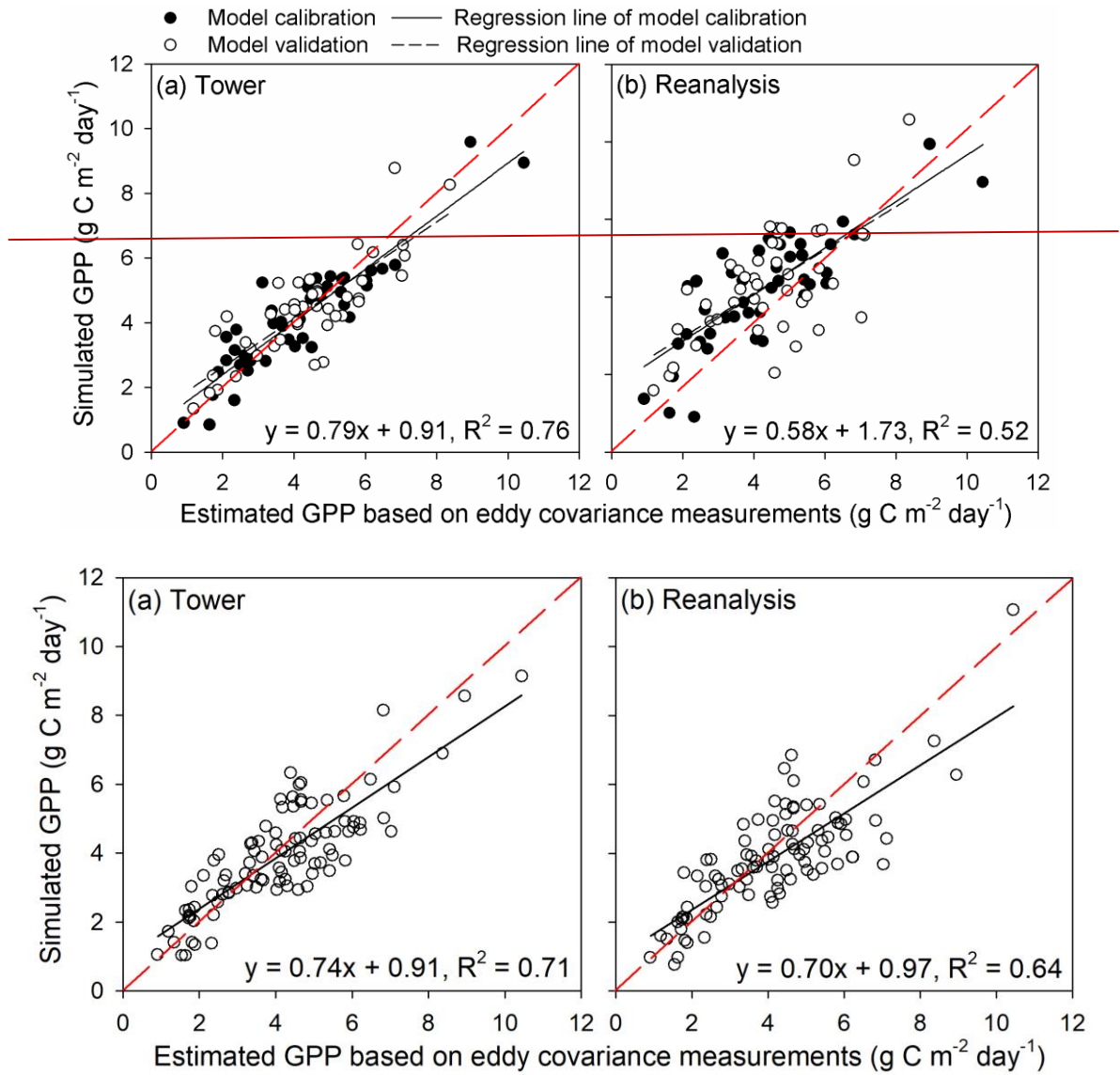


Figure 1: Comparisons between annual mean GPP estimated from EC towers and annual mean GPP simulated by the revised EC-LUE model. The modeled GPP were simulated using (a) tower-derived meteorology (calibration: $y = 0.82x + 0.75, R^2 = 0.83$; validation: $y = 0.75x + 1.13, R^2 = 0.68$) and (b) global reanalysis meteorology (calibration: $y = 0.60x + 1.66, R^2 = 0.62$; validation: $y = 0.56x + 1.84, R^2 = 0.40$). The black lines are the regression lines, and the red dash lines are the 1:1 lines. The insert equations are the regression equations derived from all the sites.

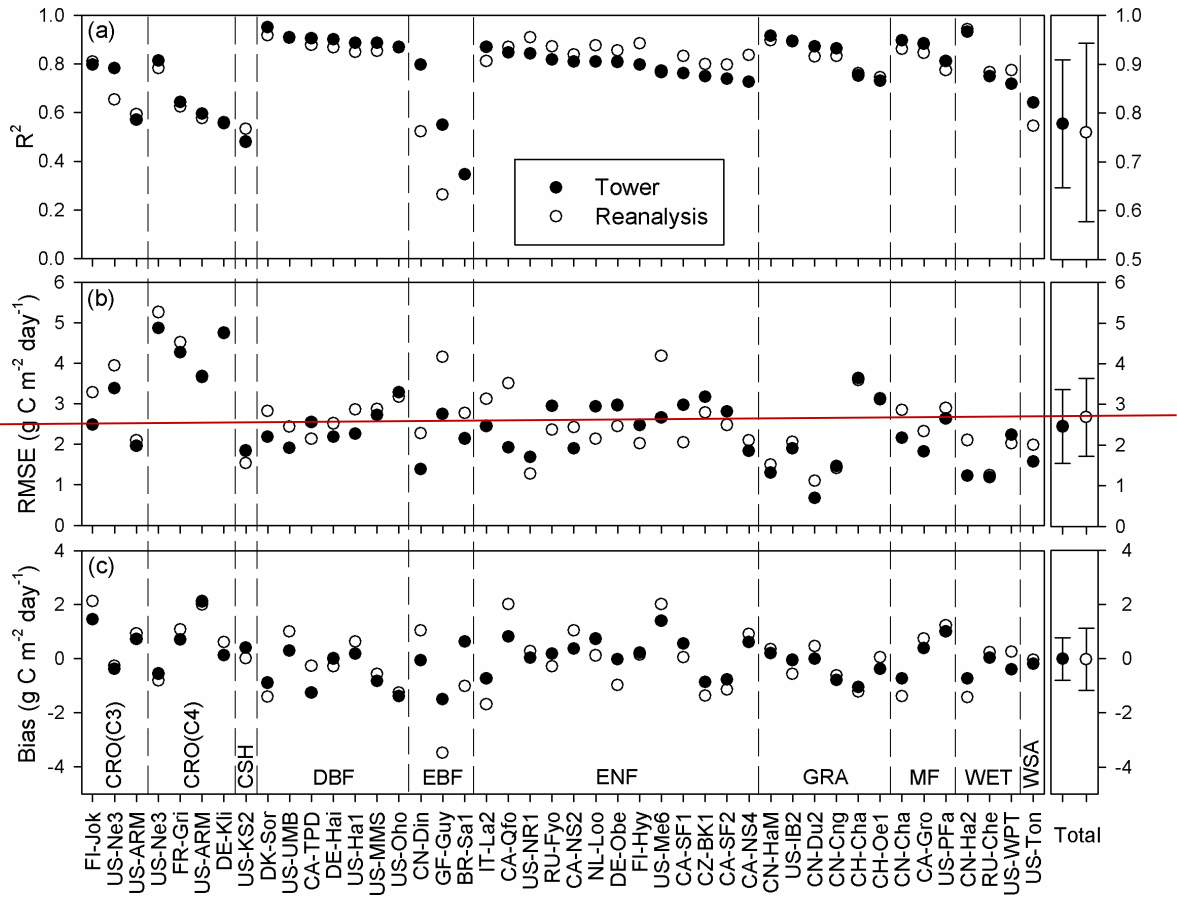


Figure 2: Comparisons of 8-day mean GPP between the observations at 42 calibration sites and the model simulations. Solid and open dots indicate the GPP simulations derived from tower-derived meteorology data and meteorological reanalysis dataset, respectively.

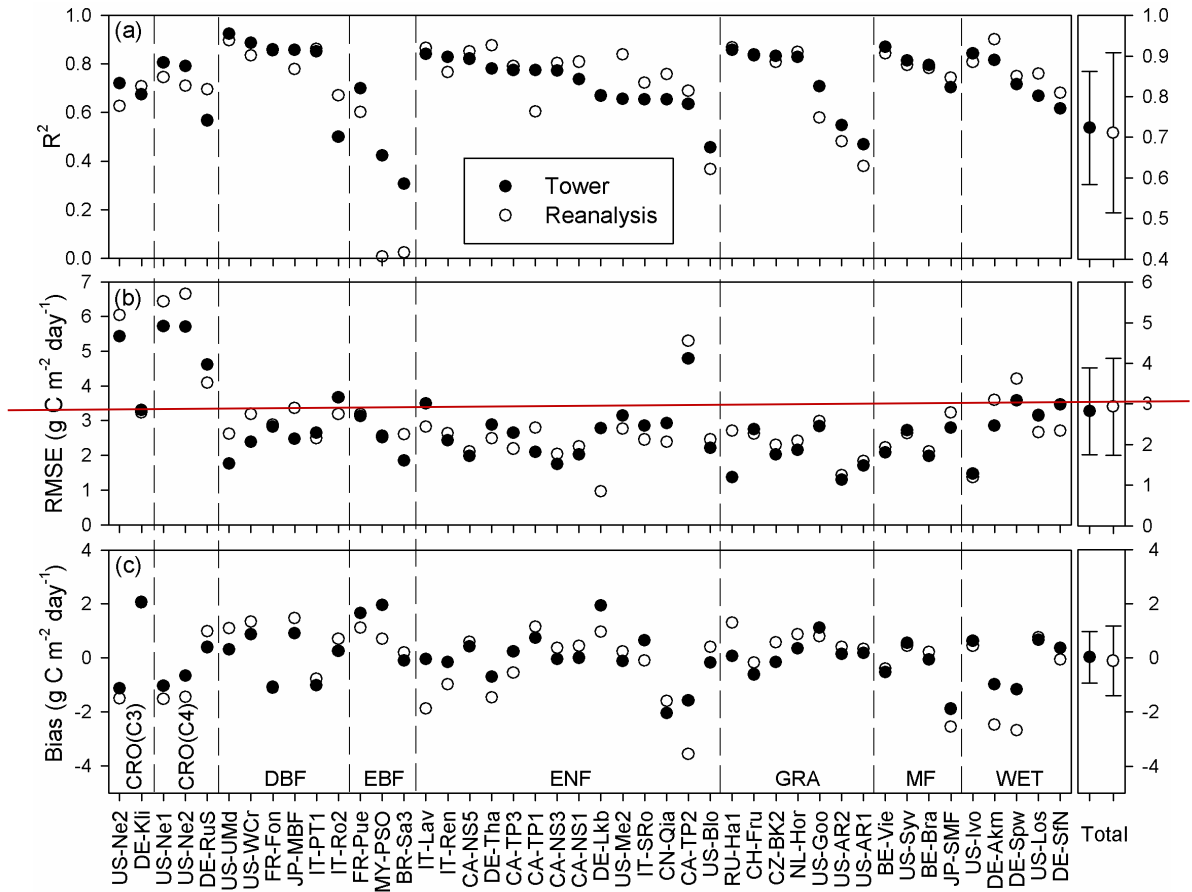


Figure 3: Comparisons of 8-day mean GPP between the observations at 43 validation sites and the model simulations. Solid and open dots indicate the GPP simulations derived from tower-derived meteorology data and meteorological reanalysis dataset, respectively.

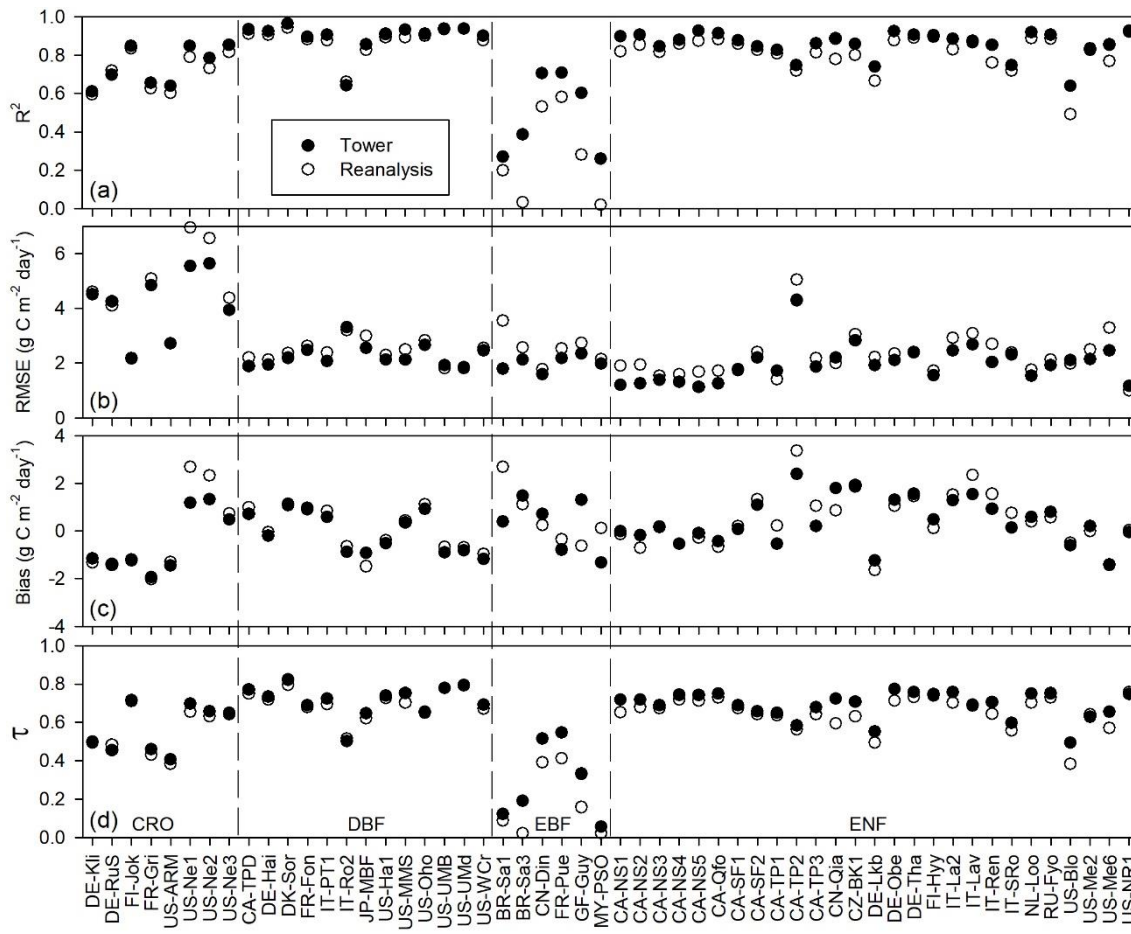
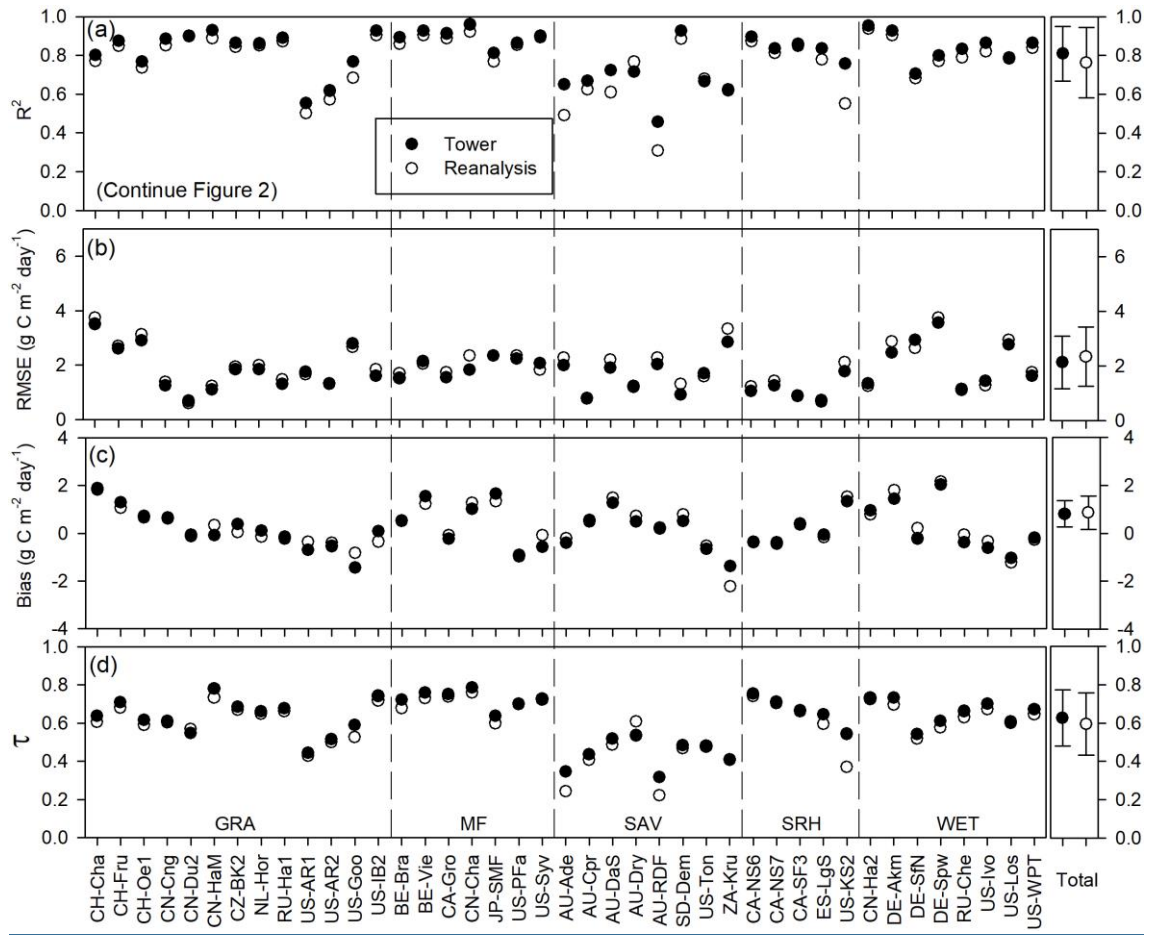


Figure 2: Comparisons of 8-day mean GPP between the model simulated GPP and tower estimated GPP. Solid and open dots indicate the GPP simulations derived from tower-derived meteorology data and meteorological reanalysis dataset, respectively.



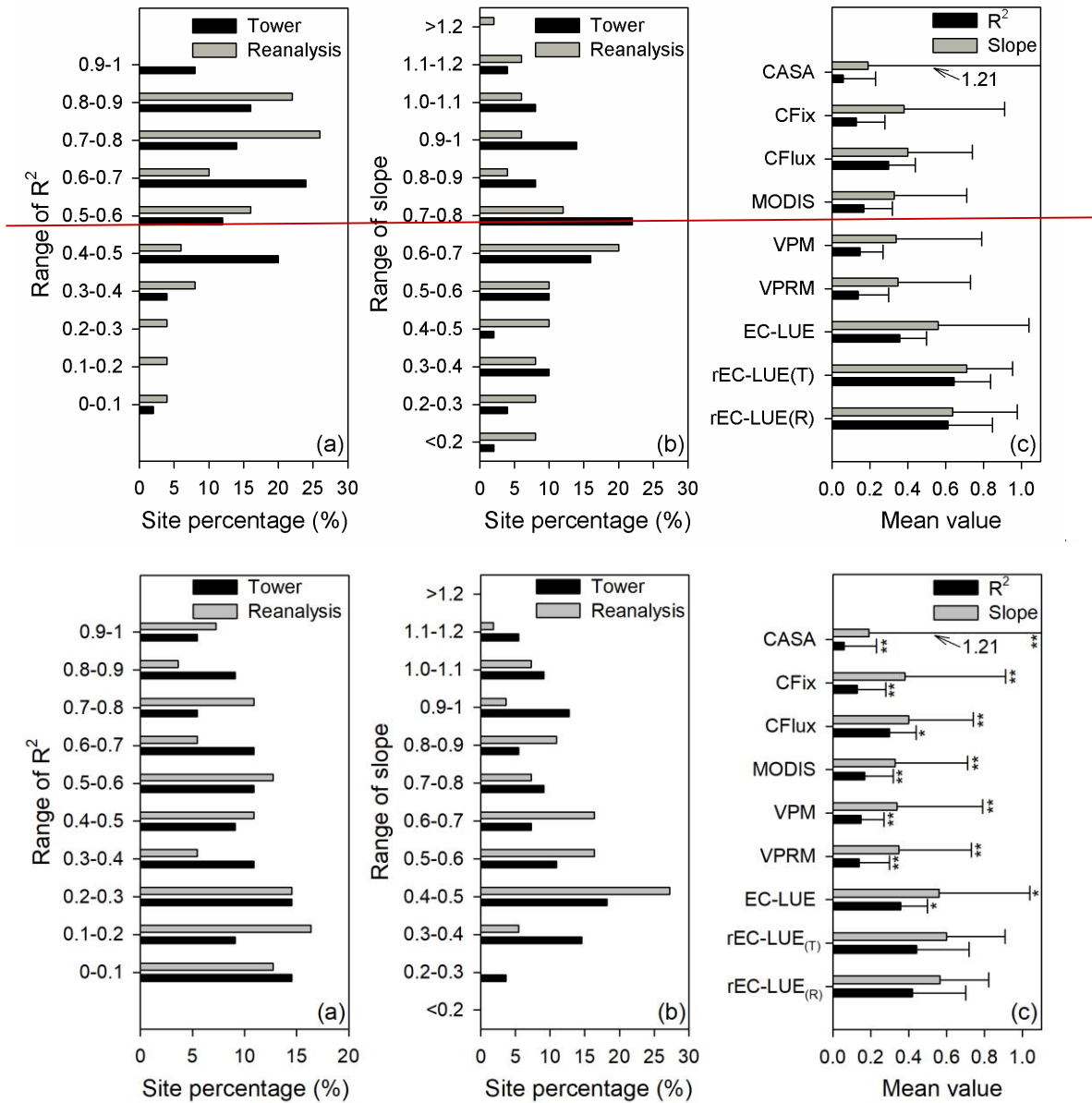


Figure 3: Site percentage of (a) correlation coefficients (R^2), and (b) regression slopes between the model simulated and tower-based interannual variabilities in GPP. (c) Averaged values (error bars represent the standard deviations) of R^2 and slope for various LUE models. rEC-LUE_(T) and rEC-LUE_(R) indicate the revised EC-LUE models derived from tower-derived meteorology data and meteorological reanalysis dataset. The mean-value-of R^2 and slopes of the other seven LUE models (i.e., EC-LUE, VPRM, VPM, MODIS, CFlux, CFix, and CASA) in the figure were obtained from the study by Yuan et al. (2014). **** and * indicate a significant difference in statistic variables (R^2 and slope) between the rEC-LUE_(T) and other LUE models (i.e., rEC-LUE_(T) and other seven LUE models) at p -value < 0.01 and p -value < 0.05, respectively.**

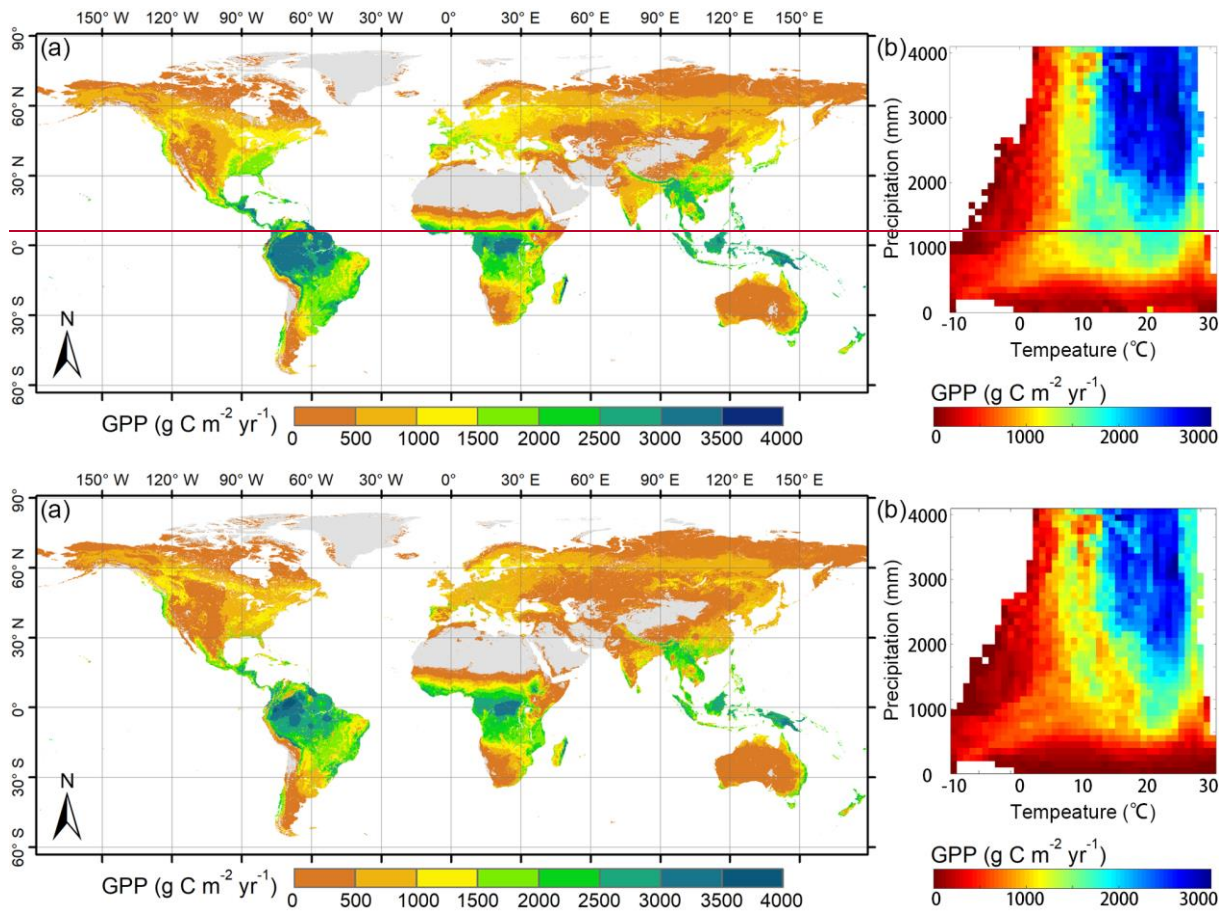
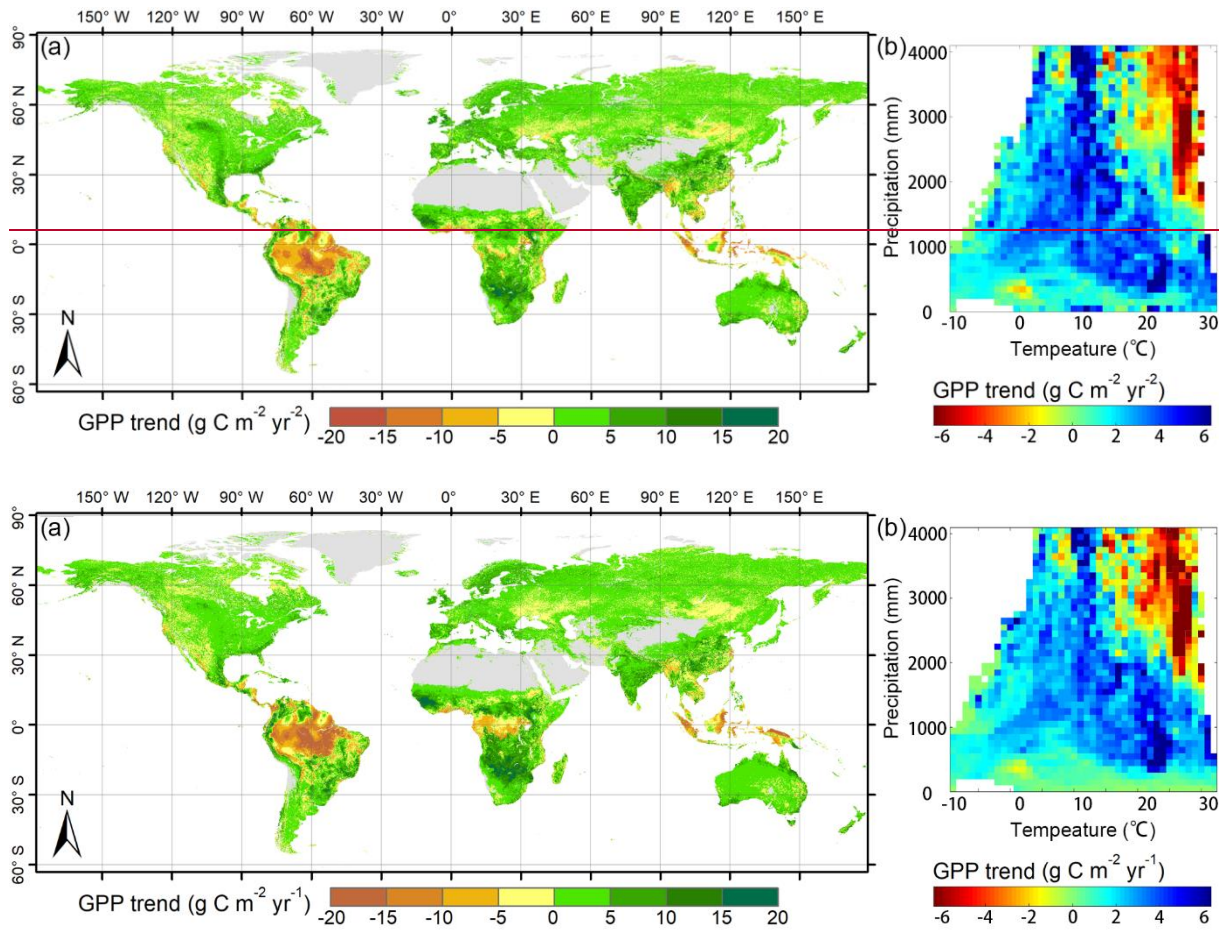
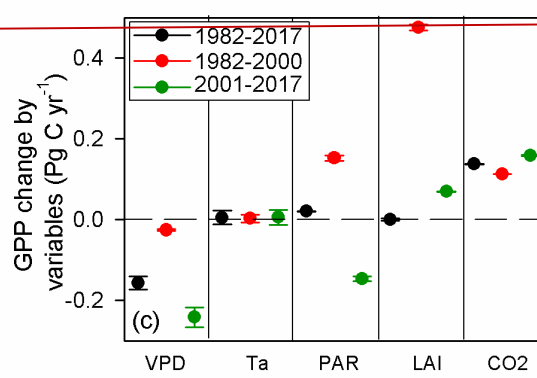
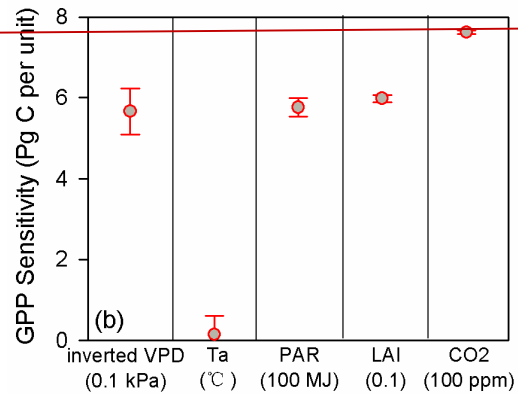
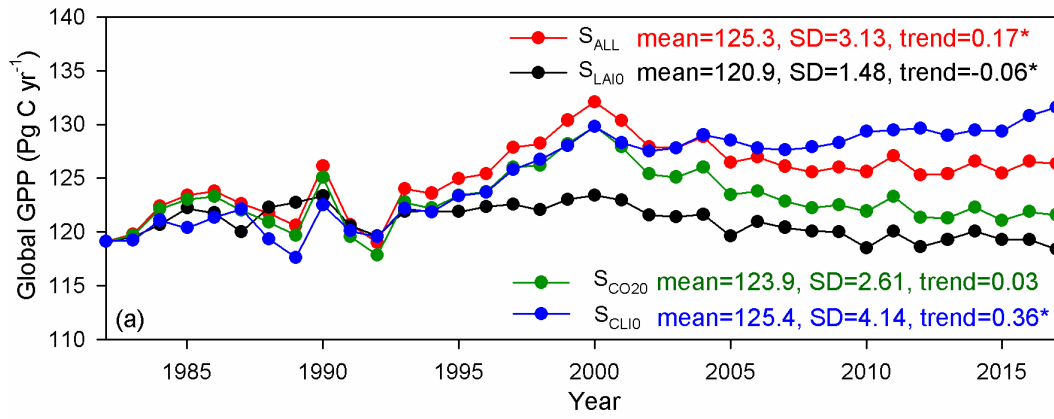


Figure 54: Spatial pattern of global GPP simulated by the revised EC-LUE model during 1982–2017: (a) averaged annual GPP, (b) averaged annual GPP at different temperature and precipitation gradients.



810 **Figure 65:** Spatial pattern of global GPP trend simulated by the revised EC-LUE models during 1982–2017: (a) trend of annual GPP, (b) trend of annual GPP at different temperature and precipitation gradients.



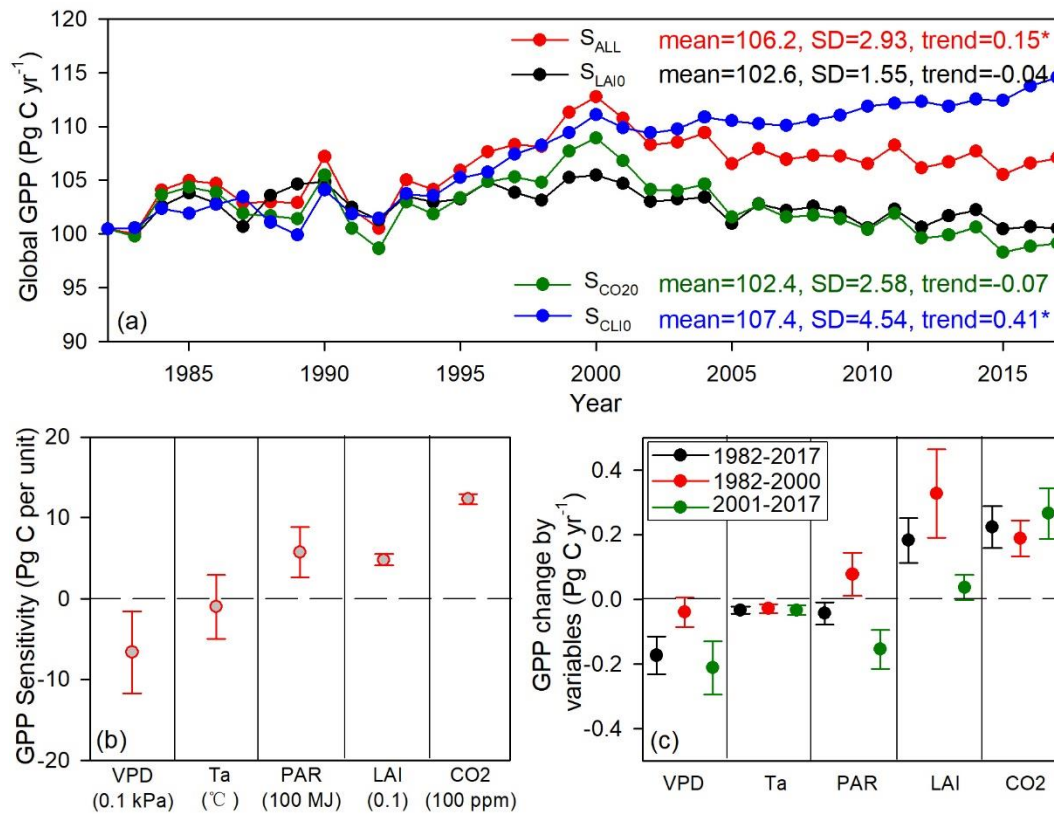
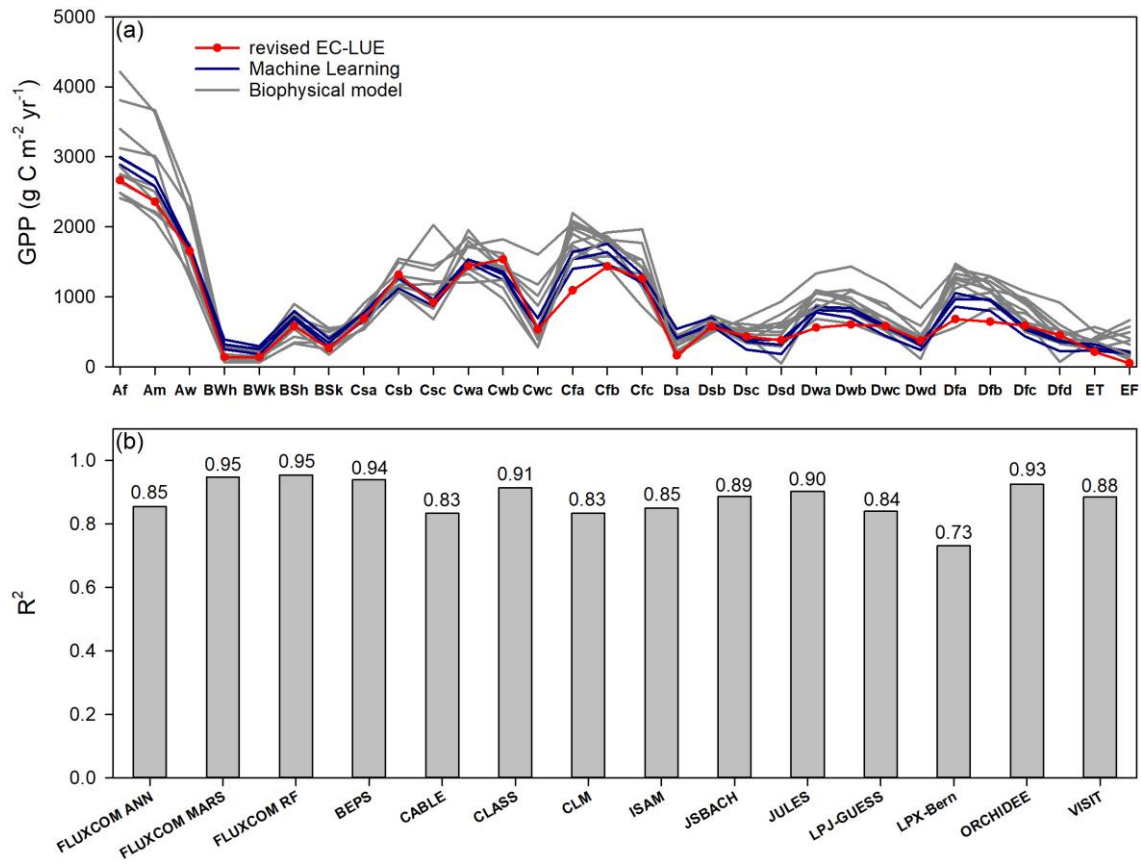


Figure 7: Long-term changes in global GPP and the environmental regulations: (a) Global summed GPP derived from the four experimental simulations in section 2.4.5, (b) GPP sensitivity to climate variables (i.e., VPD, T_a , and PAR), LAI, and atmospheric CO₂, (c) contributions of climate variables (i.e., VPD, T_a , and PAR), LAI, and atmospheric CO₂ to GPP changes over 1982–2017, 1982–2000, and 2001–2017. * indicates the significant level at p -value<0.05.

815



820 **Figure 7: Comparisons of long-term (1982 to 2010s) averaged GPP between the revised EC-LUE model and other models across**
bioclimatic zones in the Köppen-Geiger climate classification map (Beck et al., 2018). (a) the regional averaged value (b) correlation
coefficients (R^2) of GPP across all the bioclimatic zones between the revised EC-LUE model and other models. These models
including machine learning models (FLUXCOM ANN, FLUXCOM MARS, FLUXCOM RF; Jung et al., 2017), biophysical models
BEPS (Ju et al., 2006; Liu et al., 2018), and ten biophysical models in TRENDY (CABLE, CLASS, CLM, ISAM, JSBACH, JULES,
825 **LPJ-GUESS, LPX-Bern, ORCHIDEE, and VISIT). The abbreviations for the bioclimatic zones are as follows: Af, tropical,**
rainforest; Am, tropical, monsoon; Aw, tropical, savannah; BWh, arid, desert, hot; BWk, arid, desert, cold; BSh, arid, steppe, hot;
BSk, arid, steppe, cold; Csa, temperate, dry summer, hot summer; Csb, temperate, dry summer, warm summer; Csc, temperate,
dry summer, cold summer; Cwa, temperate, dry winter, hot summer; Cwb, temperate, dry winter, warm summer; Cwc, temperate,
830 **dry winter, cold summer; Cfa, temperate, no dry season, hot summer; Cfb temperate, no dry season, warm summer; Cfc, temperate,**
no dry season, cold summer; Dsa, cold, dry summer, hot summer; Dsb, cold, dry summer, warm summer; Dsc, cold, dry summer,
cold summer; Dsd, cold, dry summer, very cold winter; Dwa, cold, dry winter, hot summer; Dwb, cold, dry winter, warm summer;
Dwc, cold, dry winter, cold summer; Dwd, cold, dry winter, very cold winter; Dfa, cold, no dry season, hot summer; Dfb, cold, no
dry season, warm summer; Dfc, cold, no dry season, cold summer; Dfd, cold, no dry season, very cold winter; ET, polar, tundra;
EF, polar, frost.

835

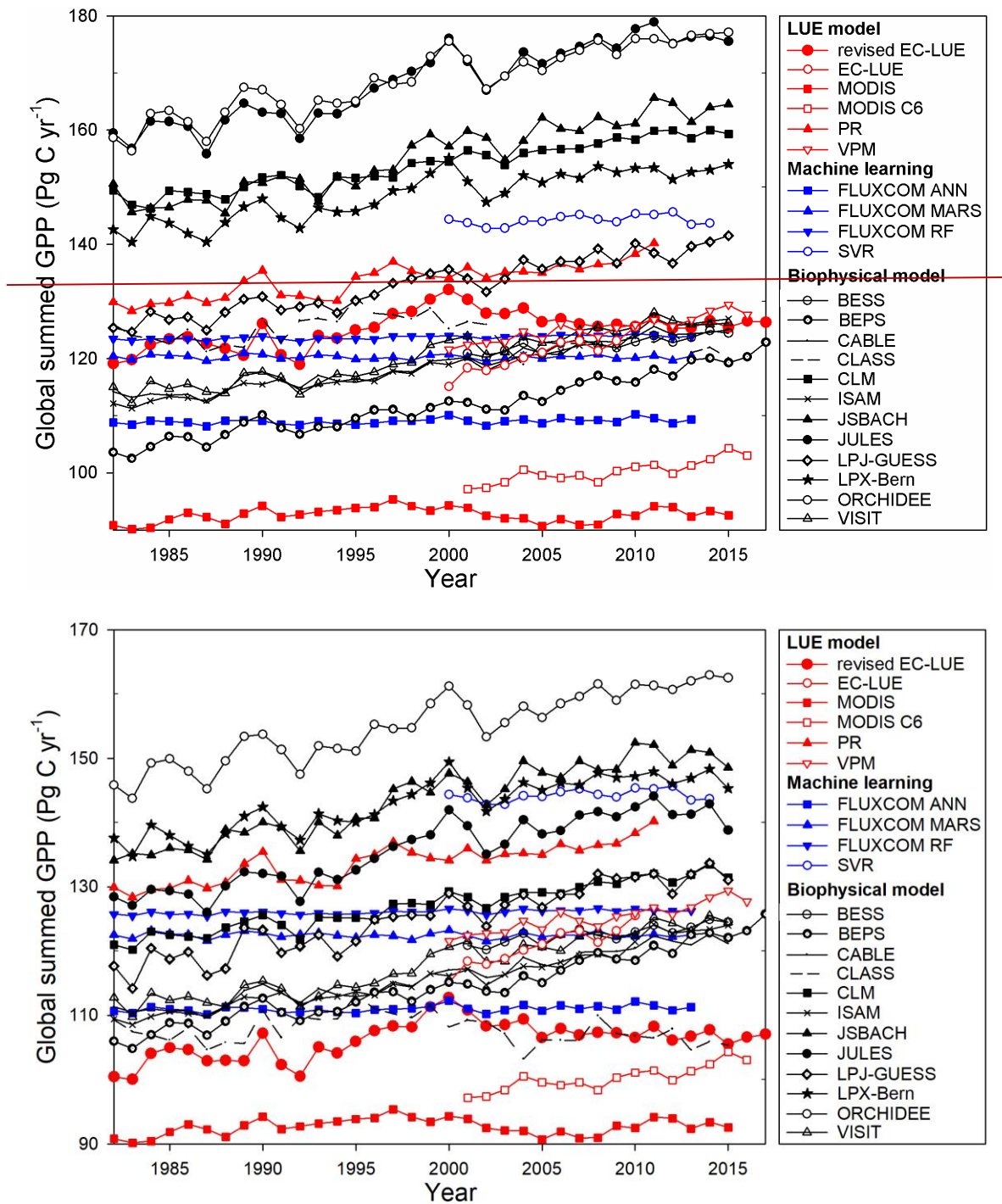
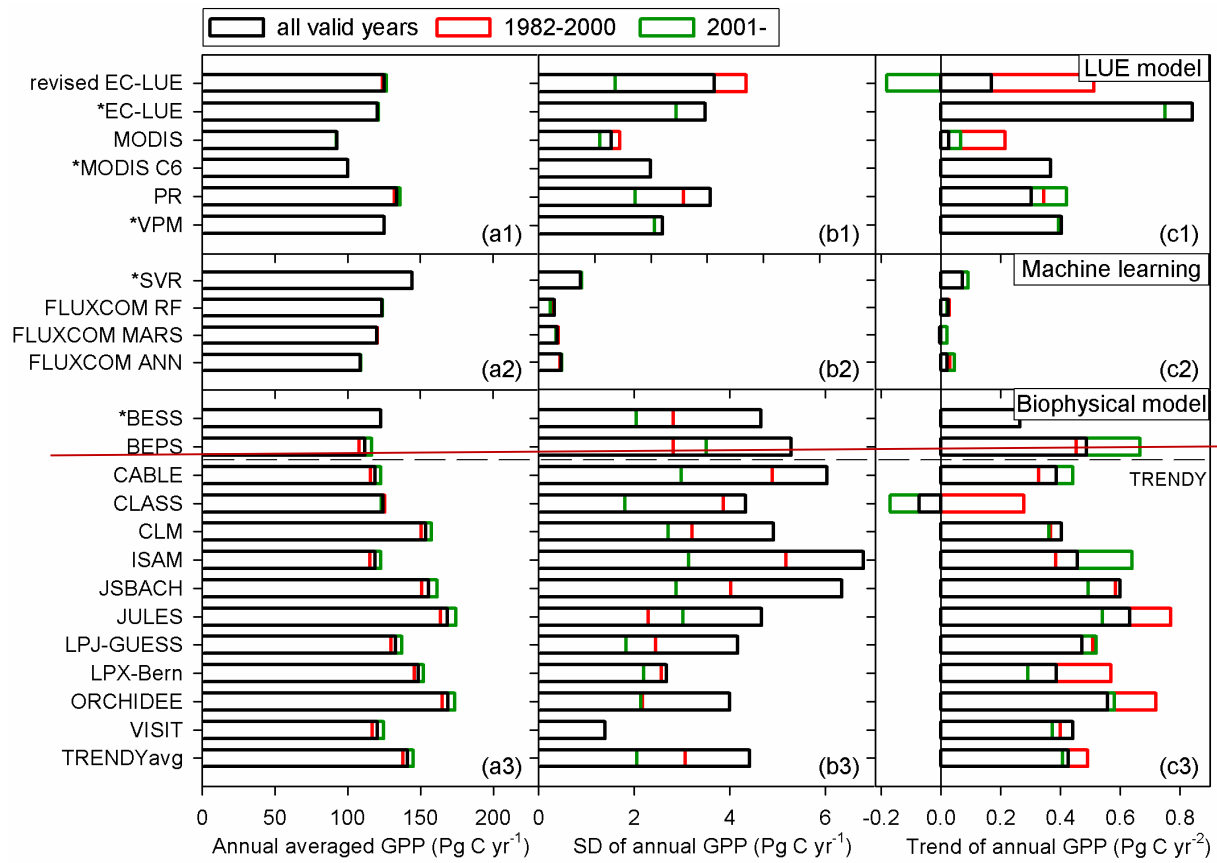


Figure 8: Comparisons of annual global summed GPP estimates from various models. The datasets or model algorithms were obtained from: EC-LUE (Cai et al., 2014), MODIS (Smith et al., 2016), MOD17 C6 (Running et al., 2004), PR (Keenan et al., 2016), VPM (Zhang et al., 2017), FLUXCOM (Jung et al., 2017), SVR (Kondo et al., 2015), BESS (Jiang and Ryu, 2016), BEPS (Ju et al.,

2006; Liu et al., 2018), and **TRENDY**. Ten of the twelve biophysical models (except BESS and BEPS) were the models in TRENDY: (CABLE, CLASS, CLM, ISAM, JSBACH, JULES, LPJ-GUESS, LPX-Bern, ORCHIDEE, and VISIT).



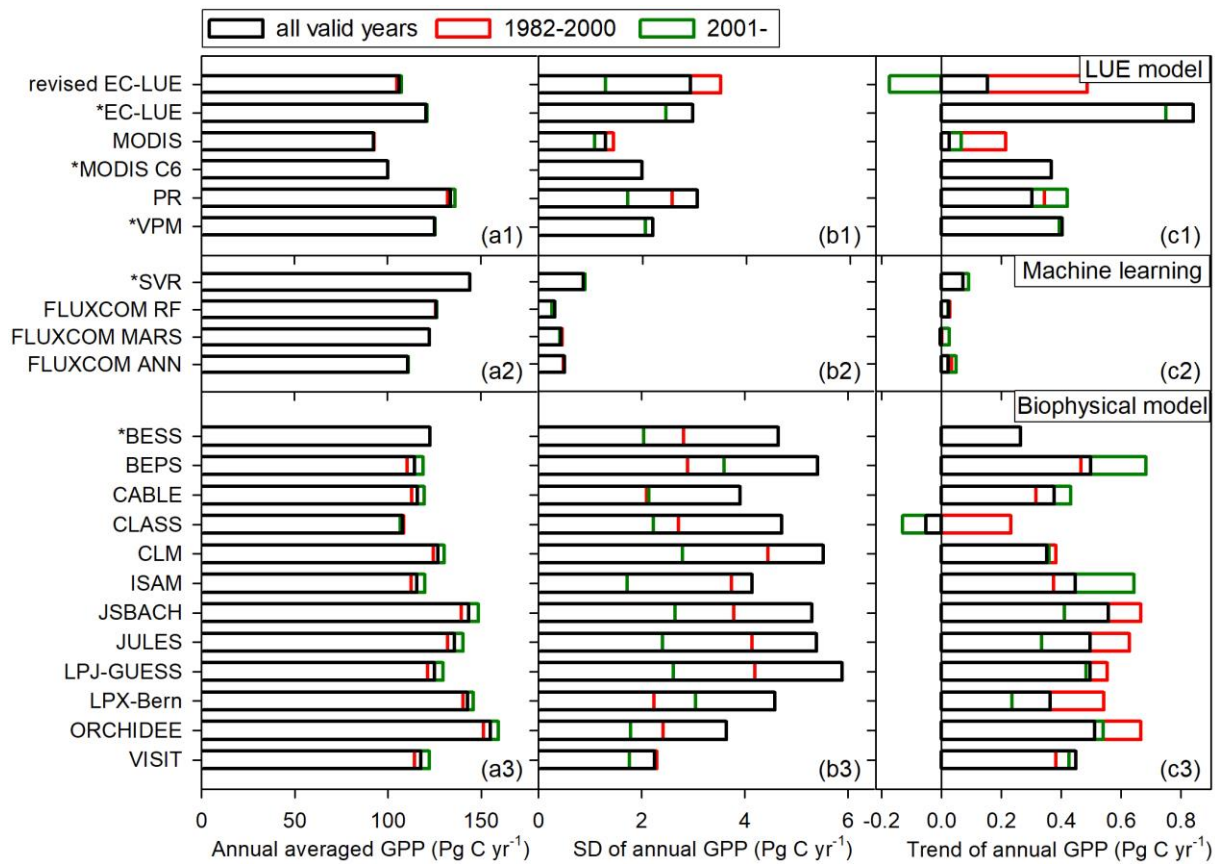


Figure 9: Comparison of (a1)–(a3) averaged annual GPP, (b1)–(b3) interannual variability in annual GPP represented by standard deviation (SD), and (c1)–(c3) annual GPP trend among different GPP datasets or models. The references of these models are the same as in Figure 9. * indicates that the valid period of the dataset is beginning/begins from 2000 or 2001. TRENDYavg is the averaged GPP of the ten TRENDY models.

850